TECHNISCHE UNIVERSITÄT MÜNCHEN

TUM School of Medicine and Health

Evaluation of strategies to increase safety of adoptive T-cell therapy against chronic hepatitis B

Alexandre Klopp

Vollständiger Abdruck der von der TUM School of Medicine and Health der Technischen Universität München zur Erlangung eines

Doktors der Medizin (Dr. med.)

genehmigten Dissertation.

Vorsitz: Prof. Dr. Susanne Kossatz

Prüfende der Dissertation:

1. Prof. Dr. Ulrike Protzer
2. Prof. Dr. Julia Jellusova
3. Prof. Kathrin Schumann, Ph.D.

Die Dissertation wurde am 28.11.2023 bei der Technischen Universität München eingereicht und durch die TUM School of Medicine and Health am 04.06.2024 angenommen.

Table of content

Abstract

Despite a highly effective vaccine, hepatitis B remains a major health problem with 296 million chronically infected patients worldwide that are at high risks of developing secondary diseases like hepatocellular carcinoma or liver cirrhosis. Current treatment options include nucelos(t)ide analogues and pegylated interferon (IFN)-α but they are rarely able to cure the infection. Based on the fact that chronic hepatitis B (CHB) is strongly associated with a defective T-cell response, novel treatment options have been developed to restore the inadequate immune response in patients. They include the administration of genetically modified T cells that are redirected towards hepatitis B virus (HBV)-infected cells by virus-specific receptors. This therapeutic concept, more commonly known as adoptive T-cell therapy (ACT), has shown very promising results in the treatment of several hematological malignancies in recent years. However, treatment-related side effects, including severe cytokine release syndrome (CRS), have tempered enthusiasm. These observed adverse events, that might also hold true for ACT with HBV-specific T cells, have underlined the importance of investigating strategies to increase the safety of ACT by allowing on-demand depletion of adoptively transferred T cells.

In this study, T cells were retrovirally transduced with an HBV-specific chimeric antigen receptor (S-CAR) or T-cell receptor (TCR) and in addition a safeguard molecule, namely inducible caspase 9 (iC9), herpes simplex virus thymidine kinase (HSV-TK), or the CD20-based molecule RQR8. *In vitro,* HBV-specific receptor expression was slightly diminished when the respective safeguard molecule was co-expressed, however T-cell functionality as assessed with real-time cytotoxicity assays using HBV-replicating hepatoma cells as target cells was not affected. Induction of iC9 or HSV-TK by addition of an iC9 dimerizer (chemical inducer of dimerization, CID) or the prodrug ganciclovir (GCV) respectively, halted cytotoxicity of HBV-specific T cells within less than one hour. Induction of RQR8 through ADCC led to a two-fold reduction of IFN-γ secretion by RQR8-S-CAR T cells. *In vivo* in AAV-HBV-infected $Rag2^{-/-}$IL-$2Rgc^{-/-}$ mice, induction of iC9 led to a strong but not complete depletion of adoptively transferred S-CAR T cells within one hour. Three days after CID-injection, S-CAR T cells in both liver and spleen were reduced by $3log_{10}$ compared to mice in which HBV-specific T cells had not been depleted, thereby preventing hepatoxicity and excessive cytokine secretion. Remaining S-CAR T cells were mostly unfunctional as determined by restimulation with HBsAg, thus also haltering their antiviral effect.

In conclusion, HBV-specific T cells that co-express a safeguard mechanism effectively eliminate HBV-replicating cells. Induction of cell death via iC9 is efficient *in vitro* and *in vivo*,

leading to a strong depletion of HBV-specific T cells and thus prevention of cytotoxicity and cytokine release.

Zusammenfassung

Trotz eines hochwirksamen Impfstoffs stellt Hepatitis B nach wie vor ein großes Gesundheitsproblem dar. Weltweit sind schätzungsweise 296 Millionen Patienten chronisch infiziert und haben ein hohes Risiko, Folgeerkrankungen wie Leberzellkarzinom oder Leberzirrhose zu entwickeln. Zu den derzeitigen Behandlungsmöglichkeiten gehören Nukleos(t)id-Analoga und pegyliertes Interferon (IFN)-α die jedoch nur selten zu einer vollständingen Abheilung der Infektion führen. Auf der Grundlage, dass chronische Hepatitis B (CHB) in starkem Maße mit einer defekten T-Zell-Antwort verbunden ist, wurden neue Behandlungsmöglichkeiten entwickelt, um die unzureichende Immunantwort der Patienten wiederherzustellen. Dazu gehört die Verabreichung von gentechnisch veränderten T-Zellen, die durch virusspezifische Rezeptoren auf Hepatitis-B-Virus (HBV) infizierte Zellen umgelenkt werden. Dieses therapeutische Konzept, das allgemein als adoptive T-Zell-Therapie (ACT) bezeichnet wird, hat in den letzten Jahren sehr vielversprechende Ergebnisse bei der Behandlung verschiedener hämatologischer Malignome gezeigt. Allerdings haben behandlungsbedingte Nebenwirkungen, darunter das schwere Zytokinfreisetzungssyndrom (CRS), die Begeisterung gedämpft. Diese beobachteten Nebenwirkungen, die auch auf die ACT mit HBV-spezifischen T-Zellen zutreffen könnten, haben deutlich gemacht, wie wichtig es ist, Strategien zu untersuchen die die Sicherheit der ACT erhöhen, indem sie eine bedarfsgerechte Depletion der adoptiv übertragenen T-Zellen ermöglichen.

In dieser Studie wurden T-Zellen durch retrovirale Transduktion erzeugt, die einen HBV-spezifischen chimären Antigenrezeptor (S-CAR) oder T-Zell-Rezeptor (TCR) und zusätzlich ein sogenanntes Suicide-Gen, nämlich die induzierbare Caspase 9 (iC9), die Herpes-Simplex-Virus-Thymidin-Kinase (HSV-TK) oder das CD20-basierte Molekül RQR8, ko-exprimierten. *In vitro* führte die Ko-Expression des jeweiligen Suicide-Gens zu einer geringfügigen Verringerung der Rezeptorexpression, veränderte jedoch nicht die Funktionalität der T-Zellen, die anhand von Zytotoxizitätstests unter Verwendung von HBV-replizierenden Hepatomazellen als Zielzellen getestet wurde. Die Induktion von iC9 oder HSV-TK durch Zugabe eines iC9-Dimerisierers (chemical inducer of dimerization, CID) bzw. der Prodrug Ganciclovir (GCV) stoppte die Zytotoxizität von HBV-spezifischen T-Zellen innerhalb von weniger als einer Stunde. Die Induktion von RQR8 durch ADCC führte zu einer zweifachen Reduzierung der IFN-γ Sekretion von RQR8-S-CAR T-Zellen. *In vivo* in AAV-HBV-infizierten $Rag2^{-/-}IL\text{-}2Rgc^{-/-}$ Mäusen führte die Induktion von iC9 zu einer starken, aber nicht vollständigen Depletion der adoptiv transferierten S-CAR T-Zellen innerhalb einer Stunde. Drei Tage nach der CID-Verabreichung war die Zahl der S-CAR T-Zellen sowohl in der Leber als auch in der Milz im Vergleich zu Mäusen, bei denen die Depletion HBV-spezifischer T-Zellen nicht

induziert worden war, um $3\log_{10}$ reduziert, wodurch Hepatoxizität und übermäßige Zytokinsekretion verhindert wurden. Die verbleibenden S-CAR T-Zellen waren größtenteils nicht funktionsfähig, wie durch erfolglose Restimulation mit HBsAg festgestellt wurde, wodurch auch ihre antivirale Wirkung aufgehoben wurde.

Zusammenfassend lässt sich sagen, dass HBV-spezifische T-Zellen, die einen Suicide Gen ko-exprimieren, HBV-replizierende Zellen wirksam eliminieren. Die Induktion des Zelltods durch iC9 ist *in vitro* und *in vivo* effizient und führt zu einer starken Depletion der transduzierten T-Zellen und damit zur Verhinderung der Zytotoxizität und der Zytokinfreisetzung.

Abbreviations

AAV	adeno-associated virus
ACT	adoptive T-cell therapy
ALT	alanine amino transferase
APC	antigen presenting cell
B-ALL	acute lymphoblastic B-cell lymphoma
BFA	Brefeldin A
BSA	bovine serum albumin
bp	base pair
CAR	chimeric antigen receptor
cccDNA	covalently closed circular DNA
CEA	carcinoembryonic antigen
CHB	chronic hepatitis B virus infection
CID	chemical inducer of dimerization
CLL	chronic lymphocytic leukemia
CMV	cytomegalovirus
CRISPR	clustered regularly interspaced short palindromic repeats
CRS	cytokine release syndrome
CTLA4	cytotoxic T-lymphocyte-associated protein 4
CTX	cetuximab
DNA	deoxyribonucleic acid
E:T	effector to target ratio
EBV	Eppstein-Barr virus
ELISA	enzyme-linked immunosorbent assay
FACS	fluorescence-activated cell sorting
FCS	fetal calf serum
FDA	Food and Drug Administration
GCV	Ganciclovir
GvHD	graft-versus-host disease
HBc	HBV core protein
HBeAg	hepatitis B e-antigen
HBsAg	hepatitis B surface antigen
HBV	hepatitis B virus
HBV-HCC	HBV-related HCC
HBx	hepatitis B X protein
HCC	hepatocellular carcinoma
HCV	hepatitis C virus
HDV	hepatitis D virus
HIV	human immunodeficiency virus
HLA	human leukocyte antigen
HSCT	hematopoietic stem cell transplantation

HSV-TK	herpes simplex virus thymidine kinase
hTCM	human T cell medium
ICANS	Immune effector cell-Associated Neurotoxicity Syndrome
ICS	intracellular cytokine staining
iC9	inducible caspase 9
IFN	interferon
IgG	immunoglobulin
IL	interleukin
JAK	janus kinase
LAL	liver-associated lymphocyte
L protein	large envelope protein
M protein	medium envelope protein
MACS	magnetic-activated cell sorting
MAGE-A3	melanoma antigen A3
mCD3, mCD8	murine CD3, murine CD8
MFI	mean fluorescence intensity
mg, mL	miligram, mililiter
MHC	major histocompatibility complex
mRNA	messenger RNA
mTCM	mouse T cell medium
NEAA	non-essential amino acids
NK-cell	natural killer cell
NTCP	sodium taurocholate co-transporting polypeptide
NY-ESO-1	New York esophageal squamous cell carcinoma-1
ORF	open reading frame
PBMC	peripheral blood mononuclear cells
PBS	phosphate-buffered saline
PCR	polymerase chain reaction
PD-1	programmed cell death protein 1
pgRNA	pregenomic RNA
rcDNA	relaxed circular DNA
RKI	Robert Koch-Institut
RNA	ribonucleic acid
Rtx	rituximab
S protein	small envelope protein
S-CAR	HBsAg-specific chimeric antigen receptor
scFv	single-chain variable fragment
T_{CM}	central memory T cells
TCR	T-cell receptor
tEGFR	truncated epidermal growth factor receptor
TIL	tumor-infiltrating lymphocyte
TNF	tumor necrosis factor
T_{regs}	regulatory T cells
WHO	World Health Organization

1 Introduction

1.1 The hepatitis B virus

1.1.1 Hepatitis B virus – Structure and life cycle

The hepatitis B virus (HBV) first described in 1970 (Dane et al. 1970) is an enveloped, partially double-stranded DNA virus, which belongs to the family of the *Hepadnaviridae.* The infectious virion, called Dane particle, is composed of an icosahedral capsid that is comprised of the HBV core protein (HBc) and contains the viral DNA molecule and the viral polymerase. The nucleocapsid is surrounded by a lipid envelope which, carries three different sized glycoproteins [L (Large), M (Medium), S (small)] referred to as HBV surface proteins (HBs) (Seeger et al. 2015).

The genome of HBV is organized in the form of a double-stranded, relaxed circular DNA (rcDNA) with four partially overlapping open reading frames (ORFs) known as presurface-surface (preS-S), precore-core (preC-C), P and X. Each gene encodes for different proteins that are necessary for the viral life cycle (Nassal 2015). The viral envelope proteins (L, M and S) are encoded by the preS-S ORF. The capsid proteins (HBc) as well as the hepatitis B e antigen (HBe) which is secreted and promotes viral persistence (Hakami et al. 2013) are encoded by the preC-C OFR. The P OFR encodes for the viral polymerase that has three different functional domains: DNA polymerase, RNaseH and the reverse transcriptase which is similar to retroviruses. The X ORF encodes for a regulatory protein, HBx which has a transcriptional transactivation activity (Tang et al. 2005) and might be involved in the oncogenic potential of HBV (Ringelhan et al. 2015).

The HBV entry into hepatocytes is characterized by an unspecific and low-affinity binding reaction of the glycoproteins (HBs) to heparan sulfate proteoglycans on the cellular surface (Figure 1.1). This step is then followed by a specific and high-affinity binding of the large protein L to the bile acid transporter sodium taurocholate co-transporting polypeptide (NTCP) (Yan et al. 2012). The viral capsid is then released into the cytoplasm and migrates to the nucleus into which the rcDNA associated with the viral polymerase is being released. The rcDNA is then converted into the covalently closed circular DNA (cccDNA) using the host cell's repair mechanisms. The cccDNA serves as template for the transcription of RNAs from which the

viral proteins and the pregenomic RNA (pgRNA) are translated. Following the export from the nucleus into the cytoplasm, the pgRNA is encapsidated together with the viral polymerase (Seeger et al. 2015). The reverse transcriptase activity of the polymerase catalyzes the synthesis of the negative strand of the viral DNA which then serves as a template for the positive strand of the genome. The newly generated and encapsidated rcDNA can then be recycled and take its way back to the nucleus to increase the pool of cccDNA that serves as reservoir for the viral replication (Seeger et al. 2015). In this form, the viral DNA can persist in the nucleus of infected cells. The matured capsid can however also be enveloped in the endoplasmic reticulum and be secreted within a Dane particle. Further, non-infectious virions being composed of the viral envelope proteins but without the capsid (spherical or filamentous subviral particles) or the viral envelope proteins and the capsid but without the genome (empty virions) can be secreted by the host cell and be detected as HBsAg in the serum of infected patients (Hu et al. 2017). HBV enveloped proteins incorporated into the endoplasmatic reticulum can also reach the surface of the hepatocytes by physiological membrane exchange (Chu et al. 1995).

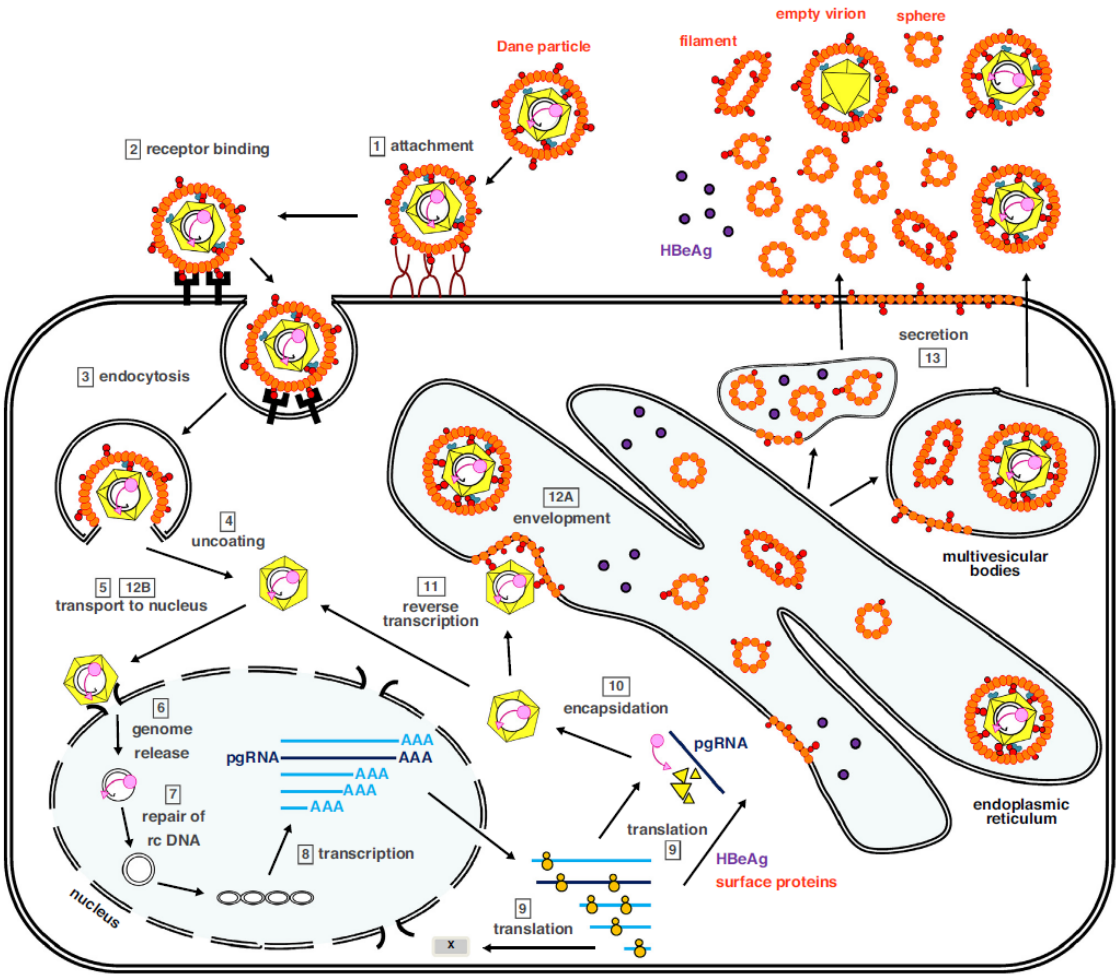

Figure 1.1 Hepatits B virus life cycle

(1) unspecific binding to heparin sulfate proteoglycans followed by, (2) specific binding to the cellular receptor sodium taurocholate cotransporting polypeptide (NTCP), (3) endocytosis, (4) uncoating and (5) transport of the viral capsid to the nucleus, (6) release of the viral genome into the nucleus, (7) conversion of rcDNA to cccDNA by host cell proteins, (8) transcription of viral RNA, (9) translation of viral proteins, (10) encapsidation of the pregenomic RNA (pgRNA) and (11) reverse transcription of the pRNA, (12A) envelopment of the capsid by the envelope proteins S, M and L or (12B) recycle and re-import of mature capsid into the nucleus, (13) secretion of progeny virions. Scheme was adopted from Ko et al. (Ko et al. 2017)

1.1.2 Epidemiology of HBV infection

Worldwide, around 296 million people are suffering from chronic hepatitis B virus. Around one third of those will develop secondary diseases like liver cirrhosis or hepatocellular carcinoma (HCC) being the main cause of the estimated 820 000 HBV-related deaths in 2019. The prevalence of Hepatitis B shows remarkable geographical differences with around 6% of the adult population infected in the Western Pacific Region and the African Region, 1,6% in the European Region and 0,7% the Region of the Americas (WHO, Hepatitis B fact sheet 2021). The most common transmission route also varies depending on the region. In highly endemic

areas, the infection route is mainly vertical (from mother to child) or horizontal (from contaminated blood products) whereas in Europe the infections is most commonly spread via sexual contact (WHO, Hepatitis B fact sheet 2021). In Germany, the prevalence of an active HBV infection (detectable HBsAg in the serum) in the population is around 0,3%. In 2018, 4507 new HBV infections have been reported to the Robert-Koch Institute with an increase of 885 infections compared to 2017. This confirms a tendency of increasing cases of HBV infections since 2015 (Epidemiologisches Bulletin 2018, Robert Koch-Institut).

1.1.3 Hepatitis B Virus – Infection

HBV largely infects and replicates in hepatocytes. Following an HBV infection, it takes an incubation period of 4-7 weeks before HBV DNA and HBsAg becomes detectable in the patient's serum (Yuen et al. 2018). In 95% of adults, the infection with HBV results in an acute self-limiting infection leading to the induction of protective immunity and finally to viral clearance. In 95% of infants and young children however, the virus persists, leading to a chronic infection with high risks of developing hepatocellular carcinoma (HCC) or liver cirrhosis (WHO, Hepatitis B fact sheet 2021). The likelihood of developing a chronic infection is mostly determined by the immune response of the host (Tillmann et al. 2014).

In most cases, HBV infection results in an acute HBV infection. This infection is mostly asymptomatic whereas 14-30% of infected individuals develop symptoms such as jaundice or gastrointestinal complaints. In very rare cases, HBV can cause a fulminant hepatitis with a high morbidity and mortality rate (Peeridogaheh et al. 2018). During acute, resolving hepatitis B a strong immune response is mounted, in which strong and polyclonal T cells that target multiple viral antigens are key to clear the virus (Thimme et al. 2003). These patients show a drop of HBsAg in their serum within 6 months of infection and production of HBs-specific antibodies (Peeridogaheh et al. 2018).

In 5% of the adults and in most infants and young children HBV infection results in a chronic infection (Peeridogaheh et al. 2018). It is characterized by viral persistence and the presence of HBsAg in the serum of infected patients for more than six months. No HBs-specific antibodies can be detected in chronically infected patients. The T cell response is inefficient because it is weak and oligoclonal (Rehermann et al. 1995).
Four different phases can be observed in the natural process of the chronic HBV infection (Dandri et al. 2012). The immune tolerant phase is defined by rapid viral replication, HBeAg positivity in the serum and a low immune response. These patients are asymptomatic and

usually show normal liver values, as the immune system is mainly responsible for the appearance of symptoms and the damage to the liver. The immune active phase is defined by an enhanced activation of the immune system leading to an increase of liver enzymes, a drop of viral DNA and eventually to an HBe-anti-HBe seroconversion. The immune control phase is defined by an important drop or even loss of the viral replication. Most patients show an HBeAg seroconversion and normalization of the liver values. In some patients an HBsAg seroconversion can occur and the infection can be considered as healed. Reactivation, mostly occurring in immunosuppressed patients, defines the fourth phase and is characterized by the increase of HBV replication in a patient with a previously inactive or resolved hepatitis B.

1.1.4 Mechanisms promoting HBV chronicity

As mentioned above, the immune system of the host plays the key role in preventing chronicity and clearing the viral infection. The subviral particles which can be detected as HBsAg in excessive amount in chronically infected patients are considered to play an important role in maintaining a persistent infection. By down-regulating IFN-α production in plasmacytoid dendritic cells, HBsAg indirectly inhibits the T-cell response (Shi et al. 2012). The Toll-like receptor-induced antiviral activity of both, Kupffer cells (KCs) and liver sinusoidal endothelial cells (LSECs) is suppressed in presence of HBsAg. This indirectly suppresses the KCs- or LSECs mediated T cell response (Wu et al. 2009, Jiang et al. 2014). HBsAg was also shown to inhibit IL12-production in monocytes by blocking the JNK-MAPK pathway (Wang et al. 2013). Also, other HBV-specific antigens have regulatory effects on the immune system. HBx can reduce the HBV antigen presentation by inhibiting the degradation of viral proteins by cellular proteases (Tang et al. 2006). The HBV polymerase downregulates MyD88 expression which plays an important role for the activation of the innate immune system (Wu et al. 2007). HBeAg negatively affects the activation of $CD8^+$ T cells by downregulating the co-stimulatory domain CD28 (Li et al. 2014). Furthermore, HBeAg interacts with the innate immune system by downregulating Toll-like receptors on hepatocytes and Kupffer cells (Visvanathan et al. 2007).

The T-cell response in chronically infected patients is narrow and scarce while it is strong and polyspecific during an acute infection (Bertoletti et al. 1994, Rehermann et al. 1995, Maini et al. 1999). The viral load and thereby the antigen levels seem to be a driving force in the exhaustion of T cells (Asabe et al. 2009). A high antigen level is directly associated with functional impairment (loss of cytotoxicity and secretion of cytokines) and deletion of $CD8^+$ T cells (Wherry et al. 2003). Furthermore, during chronic HBV infection patients show very high expressions of exhaustion markers such as PD1 and CTLA4 on $CD8^+$ T cells which strongly

reduces their functionality (Boni et al. 2007, Schurich et al. 2011). Higher number of regulatory T cells (Tregs), that have an inhibitory effect on effector T cells, can also be observed in CHB (Li et al. 2016). Thus, promoting the disease progression and the development of HCC. But also $CD4^+$ T cells play an important role in the outcome of HBV infection as they seem to be responsible for the induction of a strong $CD8^+$ T-cell response (Schmidt et al. 2013). In fact, experiments in chimpanzees showed that $CD4^+$ T-cell depletion prior to HBV infection led to a weak $CD8^+$ T cell response and thus to persistence of the virus (Asabe et al. 2009). Also it has been shown, that $CD4^+$ T cells can promote the production of antibodies of B-cells from the identic antigen specificity (Zhu et al. 2019). While it was widely known that a lack of HBV-specific $CD4^+$ T cells is associated with HBV persistence (Urbani et al. 2005, Boni et al. 2007), Zhu et al. found that a high frequency of HBV-specific $CD4^+$ T cells positively correlated with high levels of viral clearance in HBV-infected patients (Wang et al. 2020). One possible other important element, why especially children get chronically affected while adults predominantly develop an acute infection might be the OX40 expression on $CD4^+$ T cells. Publicover and al. have in fact shown that adults have a higher expression of OX40 than children, which are less likely to clear an HBV infection (Publicover et al. 2018).
B cell mediated immunity also plays a substantial role regarding the course of the HBV infection while the exact mechanisms remain largely unknown. Patients with a resolved chronic HBV infection receiving an immunosuppressive therapy that targets B cells (e.g. rituximab) are for example at a much higher risk of viral reactivation. This risk is even higher than in patients that are treated with drugs that primarily target T cells (Shouval et al. 2013, Yuen et al. 2018). Burton et al. recently discovered that even though HBsAg-specific B cells persisted in many patients with CHB, they did not produce any antibodies. In-depth analyses showed that these HBs-Ag specific B cells had developed a particular phenotype of atypical memory B cells (atMBC) with high expressions of PD-1 (Burton et al. 2018).

1.1.5 Prevention and treatment of HBV infection

As the most common transmission routes of HBV are known, general prevention measures include preventing unprotected sexual intercourse and contact to contaminated blood products and injection equipment as well as appropriate hygiene practices in the surrounding of an infected patient

The most effective way of preventing HBV infection however is a prophylactic vaccine with recombinant HBsAg that induces anti-HBsAg antibodies. The Standing Committee on Vaccination at the Robert Koch Institute (STIKO) recommends two vaccine doses at an interval

of 8 weeks for all infants that have reached the age of 2 months and a third vaccine dose at the age of 11-4 months. Newborns from HBsAg-positive mothers should start with the immunization against hepatitis B within 12 hours after birth. This includes a first dose of the HBV vaccine as well as passive immunization with HBs-specific immunoglobulins. Vaccination should be repeated after 1, 2 and 12 months (Epidemiologisches Bulletin 2022, Robert Koch-Institut). The WHO estimated that in 2015, 84% of all children around the world had been vaccinated against hepatitis B which significantly reduced HBV transmission and thus the HBV prevalence among children to 1.3% (WHO, Global Hepatitis Report 2017). The vaccine induces a protective immunity in 95% of all individuals that are vaccinated. 5% of vaccinated individuals are so-called non responder, in which no protective antibody titer of > 10IU/L can be observed (Jacques et al. 2002).

While in most cases an acute infection with HBV does not require any specific treatment measures because of its self-limiting character, people with CHB are more likely to require a medical therapy. The factors that define if a medical treatment is required include: viral load (serum HBV DNA), liver damage (ALT values) and hepatic impairment. Other parameters such as the age, comorbidities and genetic risk factors might also be considered. Treatment options for CHB include immunomodulatory agents, especially interferon alpha (IFN-α) and pegylated interferon alpha (peg-IFNα), and antiviral drugs such as lamivudine, telbivudine, entecavir, adefovir and tenofovir (Tang et al. 2018).

Beside their immunomodulatory effect, IFN-α also has virostatical and antiproliferative properties leading to degradation of the nuclear viral DNA (Lucifora et al. 2014). As a cytokine, IFN-α is physiologically secreted by activated leukocytes. It stimulates the synthesis of translation inhibitory proteins in HBV-infected hepatocytes, which inhibit the translation of viral mRNAs. Thus, the viral protein synthesis and logically the viral replication process is blocked (Robek et al. 2004). Furthermore, IFN-α stimulates the antigen expression by up-regulating HLA class I molecules on infected cells and promotes the maturation of T- and NK-cells (Korenman et al. 1991, Niederau et al. 1996). The systemic administration of IFN-α is associated with a lot of side effects that include flu-like symptoms, gastrointestinal or/and neurological disorders (Cooksley 2004). This and the modest response rate observed in most patients is why its use is mostly restricted to aggressive and severe forms of CHB (EASL Guidelines 2017).

Nucleos(t)ide analogs, in particular entecavir and tenovofir are recommended as first line agents in the treatment of chronic hepatitis B disease (Pol et al. 2012). They exhibit their antiviral effect by inhibiting the HBV polymerase through incorporation in the DNA and thus resulting in chain termination. Most of these drugs, also widely used in HIV-infected patients,

inhibit the reverse transcriptase activity of the HBV polymerase which highlights the similarities of the enzymes of both viruses. The side effects being less prominent than for IFN-α, nucleos(t)ide analogs might become ineffective through the development of viral resistance. After 5 years of treatment, lamivudine is associated with a resistance rate of 74%. The resistance rate of newer nucleos(t)ide analogs such as entecavir and tenovofir however is extremely low while their capacity of suppressing viral replication remains unaffected (Fung et al. 2011).

Although all of the mentioned therapeutic measures are able to suppress the viral replication and thus lower the viral load and normalize ALT-levels, they cannot eradicate the virus because they do not target the cccDNA. The cccDNA is stably maintained in CHB and is the molecular basis of viral persistence. It serves as a template for the viral proteins and can cause a relapse as soon as the antiviral treatment is withdrawn (Zoulim et al. 2015). This highlights the need of therapies that target and eliminate cccDNA and thus induce functional cure.

One plausible way is an immunotherapy that modulates the patient's T-cell response. This can on one hand be achieved through therapeutic vaccination, in which the administration of DNA or peptide vaccines, vector or cell-based vaccines increases the antigen presentation on antigen-presenting cells. This would then restore the effector T cell response (Kosinska et al. 2017). On the other hand, adoptive T cell therapy in which T cells are genetically modified in order to express an HBV-specific T cell receptor on their surface can help to overcome the immune tolerance observed in CHB (Tan et al. 2020).

A newer approach of targeting cccDNA is gene-editing. The CRISPR/Cas9 system or the zinc finger nucleases can target very specific DNA sequences and induce a DNA double-strand break in the cccDNA (Dong et al. 2015). Other methods, include epigenetic modification of cccDNA, which can regulate the transcription of cccDNA but does not eliminate it (Zhu et al. 2019).

1.2 Adoptive T-cell therapy

The idea of adoptive T-cell therapy (ACT) comprises administration of *ex-vivo* expanded tumor resident or genetically modified T cells that specifically target the desired antigens in order to achieve a therapeutic effect. The first insights of ACT were gained in patients suffering from leukemia who received an allogeneic hematopoietic stem cell transplantation (HSCT). In these patients, the graft's immunocompetent T cells, were not only responsible for severe side effects such as a graft versus host disease (GvHD) but also had a beneficial effect by targeting allogenic antigens on leukemic cells thus reducing the tumor load and relapses. This is known as graft-versus-leukemia effect (GvL) (Perica et al. 2015). A similar observation was made in

patients with a chronic HBV infection, in which, after receving a bone-marrow transplant from an HBV-immune donor, a rise of a strong and specific $CD4^+$ and $CD8^+$ T-cell response was detected which finally led to viral clearance (Ilan et al. 1993, Lau et al. 1997).

In recent years, immunotherapy including adoptive T-cell therapy has made substantial progress and has evolved in being a very promising therapeutic strategy for malignancies or viral infections. The first ACT has been approved by the US federal drug agency (FDA) in 2017 using T cells that specifically target the surface marker CD19 on B cells (Tisagenlecleucel). The therapy was first reserved to children and youths under the age of 25 who were suffering from relapsed and refractive acute lymphatic leukemia (ALL). A clinical study showed that three months after treatment, 82% of children were in remission. After six months, 75% of the children were relapse free. Under the current therapeutic standard which involves chemotherapy or targeted therapy the remission rates were only 20% or 33%, respectively (Buechner et al. 2017, Heymach et al. 2018). In 2018, the indication for Tisagenlecleucel has been expanded. It has been approved for adults suffering from relapsed and progredient diffuse large B-cell lymphoma (Schuster et al. 2017). Further indications for B cell malignancies might follow in the foreseeable future.

The second ACT that had been approved by the FDA in 2017 is axicabtagene ciloleucel which similar to Tisagenlecleucel comprises genetically modified T-cells expressing a CD19-specific CAR. It is approved for adults with relapsed large B-cell lymphoma and since then shown promising results with response rates of around 74%. (Locke et al. 2019, Neelapu et al. 2019) Numerousness other T cell therapies with T cells that target different antigens are currently in development or already facing clinical trials. Since then, further CD19-specific CAR T-cell therapies have been approved by the FDA including brexucabtagene autoleucel for the treatment of mantle cell lymphoma and lisocabtagene maraleucel for the treatment of large B-cell lymphoma (Han et al. 2021). Recently the FDA has approved a CAR T-cell therapy (idecabtagene vicleucel) for adult patients with relapsed or refractory multiple myeloma which targets the B-cell maturation antigen (BCMA) (Munshi et al. 2021).

Currently, three different strategies have been developed for ACT including ACT with tumor-infiltrating lymphocytes (TILs) or ACT with genetically modified T cells that either express an antigen-specific T cell receptor (TCR) or chimeric antigen receptor (CAR) (Figure 1.2).

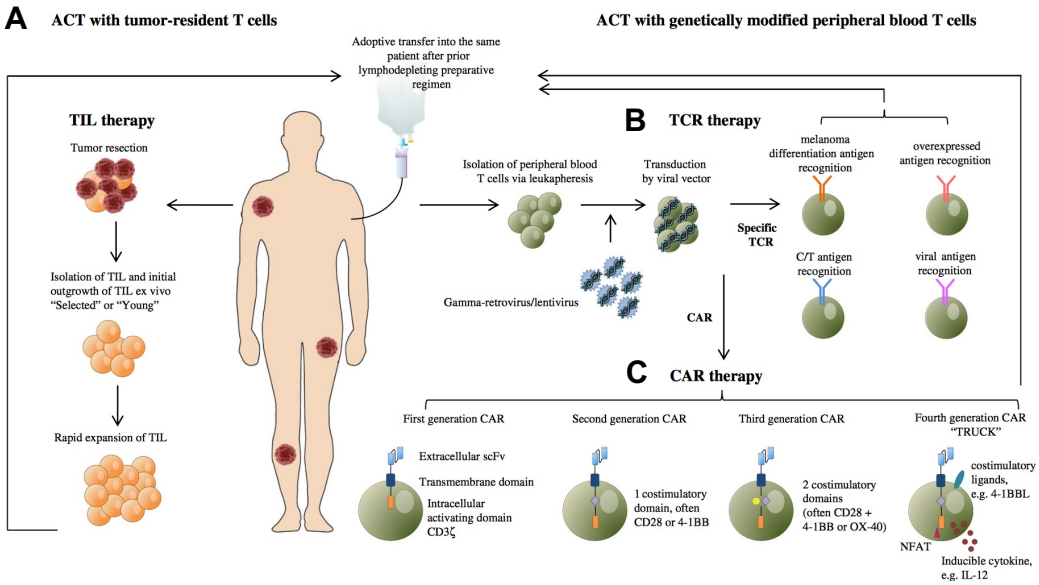

Figure 1.2 Schematic overview of the different strategies for adoptive T-cell therapy

(A) In ACT with tumor-resident T cells, tumor-infiltrating T cells (TILs) are isolated from a resected tumor and then expanded *ex vivo*. After successful proliferation of TILs, they are re-infused into the patient which is treated with a lymphodepleting conditioning regimen prior to the T-cell transfer. **(B, C)** In ACT with genetically modified peripheral blood T cells, T cells are isolated from the patient and (retrovirally) transduced in order to express a (B) TCR or (A) CAR, specific for the desired antigen. The transduced T cells are then expanded ex-vivo and re-infused into the patient. Scheme was derived from Rohaan et al. (Rohaan et al. 2019).

1.2.1 Adoptive T-cell therapy with tumor infiltrating lymphocytes (TILs)

The presence of tumor infiltrating lymphocytes in neoplastic diseases is associated with a better prognosis (Clemente et al. 1996, Yao et al. 2017). After the discovery of IL-2 in 1976 which allows the expansion of T lymphocytes *ex vivo*, first promising studies regarding the adoptive transfer of tumor infiltrating lymphocytes have been performed by Rosenberg et al. in the 1980s. He could in fact show an anti-tumor effect in mice with metastases of different tumor types which were treated with TILs that had previously been isolated from the mice and expanded with IL-2 (Rosenberg et al. 1986). The established protocol in these murine studies still represents the basis for today's TIL treatment protocol in patients. It comprises the isolation of TILs from a collected tumor biopsy, the *ex vivo* proliferation of the TILs with IL-2 and an anti-CD3 antibody and the reinfusion of an increased TILs number to the patient (Dudley et al. 2003). Nowadays, ACT with TILs is especially used in patients with metastatic melanoma where promising clinical results have been observed (Chandran et al. 2017). The isolation of TILs from other tumors such as breast cancer, ovarian cancer or renal cell carcinoma has also

been achieved, however, the antitumor reactivity of these TILs was very limited (Rohaan et al. 2019).

1.2.2 Adoptive T-cell therapy with TCR-engineered T cells

The idea of TCR-based ACT is to genetically modify T cells to express a new T cell receptor that allows recognition of an additional and defined antigen.
A T cell receptor is composed of an α- and a β-chain and forms a complex with the subunits of the CD3 complex, which is involved in the transmission of the signal after binding of the respective antigen. Based on the co-receptor of the T cells, a distinction is made between $CD8^+$ and $CD4^+$ T cells. Only antigens that are presented on cellular surfaces by major histocompatibility complexes (MHC) can be recognized by the TCR complex and the respective co-receptor. Depending on whether the antigenic peptides are presented on MHC-I or MHC-II molecules, a specific subset of T cells is addressed and activated: MHC-I-bound peptides are essentially derived from the cytosol (proteasomal degradation) of any nucleated cells and can activate $CD8^+$ (cytotoxic) lymphocytes. MHC-II-bound peptides are mostly degradation products of endocytosed (extracellular) antigens, originate from the lysosomal degradation pathway of antigen-processing cells and activate $CD4^+$ (helper) cells.
Upon activation, T cells produce cytokines such as IL-2 which simulates their proliferation and differentiation (Janas et al. 2005). The secretion of TNF-α and IFN-γ activates macrophages but also has direct anti-tumor or antiviral effects (Ruby et al. 1991). The specific cytotoxic function of $CD8^+$ T cells is ensured by the secretion of perforin or granzymes or by the interaction of Fas-receptor (FasR) on the target cell and the Fas-ligand (FasL) on the cytotoxic T cell. Both mechanisms lead to the induction of apoptosis of the target cell (Andersen et al. 2006).

In order, to genetically modify T cells, a T cell clone that shows a high affinity to the desired antigen can for example be isolated from a patient in remission from the targetable disease. The genetic information of the α- and β-chains of this specific TCR is then isolated and cloned into retroviral or lentiviral vectors which allow the transduction of T cells to obtain antigen specific T cells. The genetically modified T cells can then however express both, their endogenous TCR as well as the transgenic TCR with a high risk of miss-matched α- and a β-chains of both TCRs. This creates new receptors with unknown specificity increasing the risk of possible side effects and reduces the expression of the transgenic TCR. Numerous strategies have been developed to prevent this problem, like the insertion of cysteines into the constant region of α- and β-chains (Kuball et al. 2007).

First successful clinical trials with transgenic T cells have been made with T cells expressing a TCR that targets the melanoma differentiation antigen MART-1 present in the majority of melanomas (Morgan et al. 2006). Further antigens that can be targeted by TCR gene therapy include MAGE (Kageyama et al. 2015), carcinoembryonic antigen (CEA) (Parkhurst et al. 2011) or NY-ESO-1 (Robbins et al. 2015). NY-ESO-1 is prominently expressed in different tumors such as melanomas, neuroblastomas, synovial sarcomas, and liposarcomas. The fact that it is nearly not expressed in healthy tissues makes it a perfect target for genetically modified T cells. Tumor regression was observed in 4 out of 6 people suffering from synovial sarcoma which were treated with genetically engineered T cells reactive with NY-ESO-1 (Robbins et al. 2011). But also, several other high affinity transgenic TCRs with specificity for viral antigens such as HBV have been described. Wisskirchen et al. have identified high affinity TCRs that recognize peptides from HBV surface protein or core protein on infected hepatocytes and that showed promising results *in vitro* and *in vivo.* Co-culture of T cells grafted with HBV-specific TCRs with HBV-infected target cells led to the complete elimination of infected cells (Wisskirchen et al. 2017). The transfer of the T cells in HBV-infected humanized mice, controlled HBV infection (Wisskirchen et al. 2017, Wisskirchen et al. 2019). Bertoletti and colleagues have also identified T-cell receptors capable of recognizing HCC cell lines expressing viral antigen from integrated HBV DNA (Gehring et al. 2011). They further reported that the adoptive transfer of HBsAg-specific T cells into a patient suffering from HCC metastases was safe and mediated a reduction of HBsAg levels (Qasim et al. 2015).

1.2.3 Adoptive T-cell therapy with CAR-engineered T cells

CAR T-cell therapy is based on the genetic modification of T-cells in order to express a chimeric antigen receptor (CAR) which targets a specific antigen on the cell surface. Similar to transgenic TCRs, CARs are expressed on T cells via retroviral or lentiviral transduction. Other, non-viral methods, such as CRISPR-Cas9 (Doudna et al. 2014) or Sleeping Beauty (Monjezi et al. 2017) are currently in development.

Generally a CAR is composed of three different domains. The extracellular domain is responsible for the specificity of the CAR and comprises a single-chain variable fragment (scFv) derived from a specific monoclonal antibody against the targetable antigen. It is linked via a spacer to the transmembrane domain which anchors the receptor into the cellular membrane. The intracellular domain contains the signaling domain which resembles the signaling domains of the TCR complex and co-stimulatory domains.

Compared to transgenic TCR T cells, CAR T cells can recognize antigens independently of MHC antigen presentation. Since the development of the first CAR in 1993 (Eshhar et al.

1993), commonly referred to as first generation CAR, further generations have followed. The first generation CAR only contained one signaling domain, CD3ζ and showed a low proliferation rate and limited persistence *in vivo* (Hwu et al. 1995). This low clinical response was due to a lack of activation of the CAR T cells. Thus co-stimulatory domains, including CD28, 4-1BB or OX40 have been introduced into CARs which activate the T cells in a different manner and lead to a higher persistence *in vivo* (Kowolik et al. 2006). Whereas second generation CARs only contain one co-stimulatory domain in addition to CD3ζ, third generation CARs are equipped with two different co-stimulatory domains (Sadelain et al. 2013). Most CAR T cells nowadays are directed towards tumor antigens but their usage has also been successful in the treatment of viral infections. In fact, the functionality of a CAR that is specific for the HBV envelope protein (S-CAR) has been demonstrated in both, *in vitro* and *in vivo* models. The co-culture of S-CAR T cells with HBV-replicating hepatoma cells, resulted in the induction of cytokines and effective cell lysis (Bohne et al. 2008). *In vivo,* the adoptive transfer of S-CAR T cells into transgenic mice resulted in a strong antiviral effect with the viral load in the serum being reduced by $2\log_{10}$ 12 days after T-cell transfer (Krebs et al. 2013).

1.2.4 Side effects of adoptive T-cell therapy

Historically, side effects have already been observed in the early days of adoptive cell therapy. Patients suffering from leukemia who received an allogeneic hematopoietic stem cell transplantation (HSCT) developed a graft versus host disease (GvHD). This is typically caused by an HLA-mismatch between the donor and the host, that engenders that the graft's immunocompetent T cells recognize the host tissues as foreign (Maraninchi et al. 1987). The risk of GvHD in HSCT is nowadays however reduced because of the HLA-match between the donor and the recipient. In adoptive T-cell therapy only autologous T cell products are currently approved as they reduce the likelihood that the transferred cells might be recognized as foreign by the recipient's immune system. However, the risk of side effects with ACT still remains. Several trials have in fact reported a substantial morbidity and occasionally mortality resulting from the toxicity of adoptive T-cell therapy (Santomasso et al. 2019). They include, on-target, off-tumor toxicity, cytokine release syndrome and off-target effects (Tey 2014).

On-target, off-tumor toxicity results from the fact that some antigens that are targeted with adoptive T-cell therapy are not only expressed on the tumor cells but also on healthy tissues. One example is the treatment of B cell malignancies with CD19 CAR T-cell therapy. This CAR does not only target malignant B cells but also normal B cells resulting in B-cell depletion and

hypogammaglobulinemia with a high risk of reactivation of a latent infection (Wudhikarn et al. 2020). Morgan et al. reported the death of a patient with colorectal cancer which was treated with CAR T cells recognizing Her2neu. This antigen is in fact also expressed on healthy lung tissues and lead to severe pulmonary infiltrates with lethal consequences five days after transfer of the cells (Morgan et al. 2010).

Cytokine release syndrome (CRS) being the most frequent side effect of CAR T-cell therapy is caused by an excessive activation and expansion of CAR T-cells. In fact, the activation of CAR T-cells leads to the secretion of IFN-γ, activating bystander cells like monocytes and macrophages which then secrete high levels of pro-inflammatory cytokines such as IL6 (Shimabukuro-Vornhagen et al. 2018). Very high levels of IL6 correlate with the severity of CRS and mainly contribute to the key symptoms which range from flu-like symptoms to hypotonic shock, neurotoxicity and multi-organ system failure (Winkler et al. 1999, Teachey et al. 2013). In a trial in which children and young adults suffering from acute lymphoblastic leukemia (ALL) were treated with an anti-CD19 CAR T-cell therapy, 88% developed a CRS (Maude et al. 2018). Whereas most CRS are rather mild and can effectively be managed with anti-cytokine therapy like interleukin-6 receptor antagonist (Tocilizumab), some patients can present life-threatening manifestations with fatal outcome (Shimabukuro-Vornhagen et al. 2018).

Off-target effects of adoptive T-cell therapy have been observed when mutations are deliberately inserted in the sequence of a particular TCR or CAR in order to increase their specificity and potency. For example, patients suffering from melanoma were treated with T cells that were transduced with a MAGE-A3 TCR. This TCR, was isolated from a previous patient and mutations in the α-chain were introduced to increase TCR affinity. A few days after treatment the patients died from a cardiogenic schock because this TCR, after affinity maturation, did not only recognize the tumor cells but also the cardiac protein titin. Previously conducted *in vitro* and *in vivo* studies in mice did not reveal this off-target effect (Linette et al. 2013). Another potential concern is the miss-match between the α- and β-chains of both the endogenous and the transgenic TCR creating different receptors with potentially harmful specificity (van Loenen et al. 2010).

The second most common side effect observed in patients treated with CAR T-cells is an Immune effector cell-Associated Neurotoxicity Syndrome (ICANS). In fact, in patients receiving CD19- or CD22-specific CAR T cells, a high incidence of neurological disorders including confusion, delirium, aphasia and seizure have been reported. While the exact

pathophysiological reason remains mainly unknown, high cytokine levels are believed to play a major role in the development of neurological toxicity (Bonifant et al. 2016, Sheth et al. 2021).

Bertoletti et al. reported that the transfer of autologous HBsAg-specific TCR-redirected T cells into a patient suffering from HBV HCC metastases and who had previously undergone a mismtached liver transplant was safe (Qasim et al. 2015). However, when treating chronic HBV infection with HBV-specific T cells, one could assume that in a clinical setting, targeting a healthy organ might increase the risk of developing a fulminant hepatitis. A consequence would be acute liver failure that is associated with a very high mortality rate. The use of the S-CAR which does not only recognize cell-bounded HBsAg but also soluble HBsAg could theoretically lead to an on-target off-organ activation of T cells and thus lead to excessive secretion of cytokines. With the idea to limit potential side-effects, Kah et al. have generated T cells via mRNA electroporation that only transiently express HBV-specific TCRs and transferred them into HBV-infected, humanized mice. However in this experimental setting only a limited antiviral effect was observed with an HBV rebound occurring 10 days after the last T-cell injection (Kah et al. 2017).

1.2.5 Increasing safety of adoptive T-cell therapy

All these described concerns have demonstrated the necessity to develop and investigate strategies to increase safety of adoptively transferred T cells. The co-expression of a safeguard mechanism, whose induction leads to a selective elimination of transferred T cells on demand, is thus a promising technique to increase safety of T-cell therapy. The most commonly used mechanisms in the clinics are an inducible caspase 9 (iC9) (Di Stasi et al. 2011), a thymidine kinase of herpes simplex virus (HSV-TK) (Bonini et al. 1997) and the antibody-based, truncated EGFR (EGFRt) (Wang et al. 2011) (Figure 1.3).

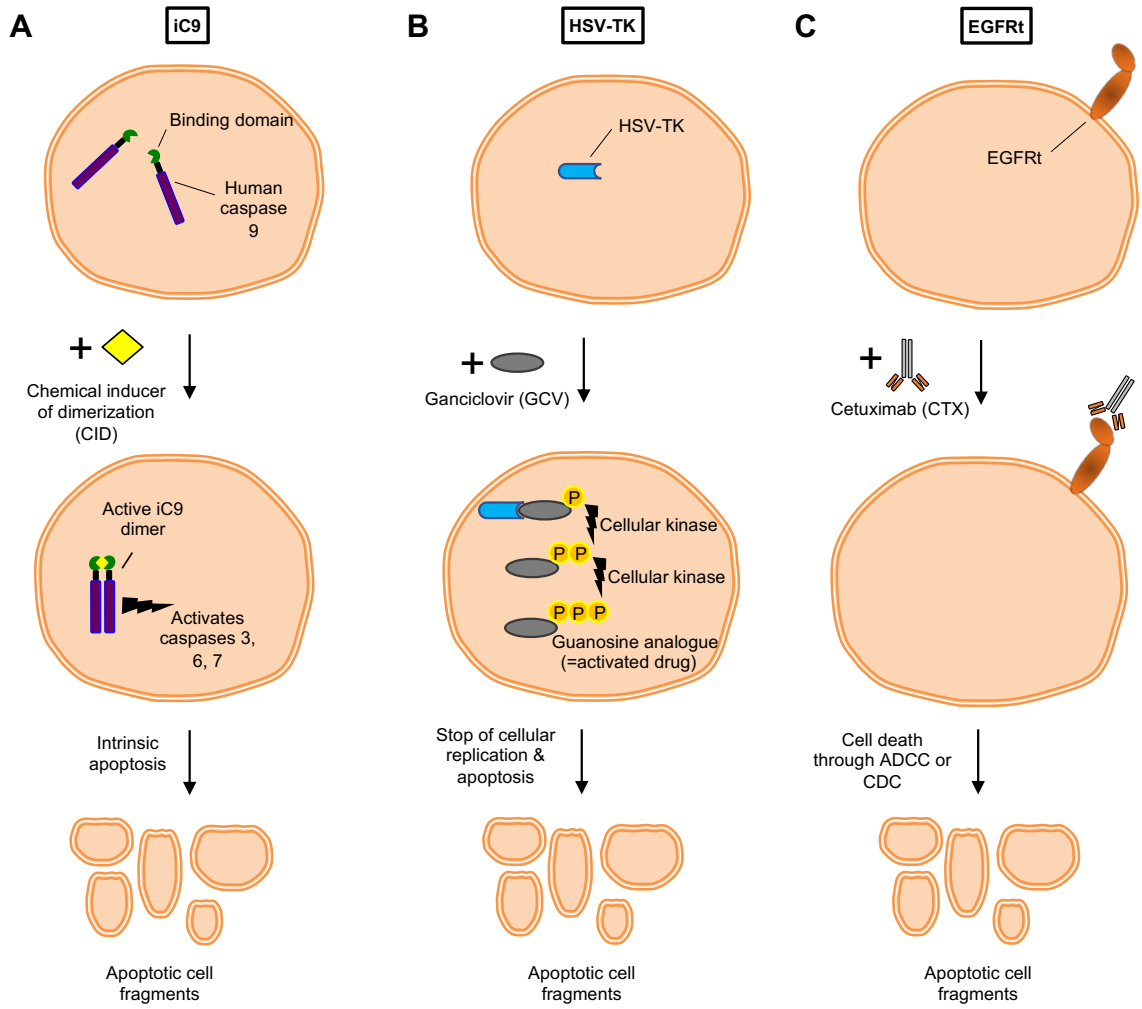

Figure 1.3 Mechanism of action of different safeguard mechanisms

(A) The binding domain of the iC9 molecule can bind small molecules that act as chemical inducer of dimerization (CID), resulting in dimerization of two iC9-molecules and activating the intrinstic apoptotic pathway through activation of downstream executing caspases. **(B)** HSV-TK phosphorylates the non-toxic prodrug ganciclovir (GCV) which is then further phosphorylated by host cellular kinases. The GCV-triphosphate, as guanine analogue, leads to cell death by halting DNA replication. **(C)** Targetable surface antigens expressed on transduced T cells (e.g. truncated EGFR) lead to cell death through antibody or complement dependent cellular cytotoxicity after administration of the associated antibody (e.g. Cetuximab)

iC9 is composed of an inducible human caspase 9 fused to a human binding protein that allows dimerization using a small molecule (AP1903 or AP20187) that acts as chemical inducer of dimerization (CID). Addition of CID brings two iC9-molecules into close proximity which as a dimer then rapidly activates executioner caspases (caspases 3, 6 and 7) leading to the apoptosis of $iC9^{+}$ T cells (Figure 1.3A). In a phase I clinical study, iC9-expressing T cells were administrated to ten children with refractive leukemia after HSCT. Four patients developed a GvHD and were treated with an unique dose of CID (0,4mg/kg) which lead to the elimination of >90% of transduced T cells in the blood within 30 minutes and the complete abrogation of GvHD (Zhou et al. 2014).

HSV-TK works upon administration of ganciclovir (GCV). In fact, after addition of GCV, the drug is monophosphorylated by the HSV-TK and then gets further phosphorylated by host cell kinases. This triphosphate form of GCV acts as analogue of guanosine which is then incorporated into the DNA and stops the cell replication and induces cell death (Bonini et al. 1997) (Figure 1.3B). HSV-TK also emerged as being very effective in the prevention of GvHD. In a clinical study, the induction of the safeguard mechanism in ten patients which received donor T cells after HSCT, led to a total control of GvHD (Ciceri et al. 2009).

Antibody-based safeguard mechanisms induce cell-death through antibody-dependent cell-mediated cytotoxicity (ADCC) or complement dependent cytotoxicity (CDC) after binding of a specific monoclonal antibody. In fact, the expression of CD20 (Introna et al. 2000) or a truncated EGFR (tEGFR) (Wang et al. 2011) on T cells lead to the efficient elimination of transduced T cells *in vitro* after administration of rituximab or cetuximab respectively (Figure 1.3C). Philip et al. have developed a new molecule (RQR8) which combines both epitopes from CD20 and from CD34. This allows, on one hand the selection and tracking of RQR8-transduced T cells with an anti-CD34 antibody and on the other hand the specific deletion of the T cells after rituximab administration (Philip et al. 2014). Kieback et al. introduced a 10-amino-acid tag into TCR sequences, which allowed them to deplete the transduced T cells with a tag-specific antibody (Kieback et al. 2008).

Other strategies of increasing the safety of adoptive T-cell therapy include the generation of CARs recognizing two antigens (TanCARs) (Hegde et al. 2016) or the transduction of T cells with two distinctive CARs which must both bind their respective antigen in order to induce a T-cell activation (Wilkie et al. 2012, Kloss et al. 2013). This would increase the specificity of T-cell therapy or impede possible on target, off tumor effects.

Also, unspecific means can be utilized to counteract side effects in adoptive T-cell therapy. For example, clinical experience has demonstrated that the interleukin-6 receptor-blocking antibody tocilizumab is an effective treatment for CAR T-cell induced CRS (Grupp et al. 2013, Maude et al. 2014). The same goes for the administration of corticosteroids which was shown to be effective in the management of CRS that occurred after T cell therapy (Lee et al. 2014, Maude et al. 2014, Brudno et al. 2016). Recently, Mestermann et al. revealed that the tyrosine kinase inhibitor Dasatinib allows a strong and reversible inhibition of CAR-mediated T cell activation (Mestermann et al. 2019).

1.3 Aim of this thesis

The outcome of HBV infection is strongly determined by the infected patient's T-cell response. Whereas in an acute HBV infection a strong immune response is developed, the T-cell response in chronically infected patients is deficient. Current antiviral treatment options for chronic hepatitis B reduce viral replication but in most of the cases do not cure the infection. Hence, adoptive T-cell therapy with HBV-specific T cells is considered as an encouraging therapeutic strategy to promote viral clearance and eventually lead to functional cure.

HBV-specific CARs and TCRs have previously been generated in our lab and showed promising results both *in vitro* and *in vivo*. In fact, *in vitro,* T cells expressing one of the HBV-specific receptors killed 100% of HBV-replicating target cells and secreted high amounts of cytokines such as IFN-γ. *In vivo*, T-cell transfer into HBV-infected mice led to a transient increase of alanine amino transferase (ALT) levels through specific elimination of HBV-infected hepatocytes. In a clinical setting however, the administration of T cells targeting infected hepatocytes might increase the risk of developing a hepatic flare. Furthermore, adverse side effects including cytokine release syndrome which has been observed in several clinical trials of adoptive T-cell therapy might also hold true for HBV-targeting adoptive T-cell therapy. Thus, strategies to increase safety of adoptively transferred HBV-specific T cells are needed to counteract the described concerns. The aim of the present project was the evaluation, *in vitro* and *in vivo*, of different strategies to deplete adoptively transferred HBV-specific T cells and thus increase their safety.

In the first part of this thesis, I aimed to compare different intra- and extracellularly expressed safeguard molecules *in vitro* to evaluate which mechanism would represent the most promising means to deplete transduced T cells. To do so, new retroviral vectors containing a safeguard mechanism together with an HBV-specific receptor were cloned. T cells were transduced with the newly generated retroviral vectors and quantitative assays to assess their efficiency and sensitivity were performed.

In the second part and as a confirmation of the *in vitro* results obtained, I compared the same safeguard molecules in an immunocompetent mouse model. Based on the results of this experiment and the *in vitro* results, I selected iC9 as most promising safeguard mechanism in HBV-specific cells and further evaluated the effect and the kinetics of iC9-mediated depletion on adverse effects of T-cell therapy, the absolute T-cell count and the antiviral effect in an immunocompromised mouse model.

2 Results

In order to determine the most suitable safeguard mechanism in the context of an HBV-specific T-cell therapy, the most prominent and clinically approved safeguard molecules were first evaluated in different *in vitro* and *in vivo* experiments. The most suitable safeguard mechanism, determined through both, *in vitro* and *in vivo* experiments, was then further evaluated *in vivo*. A part of the results shown in the following section (i.e., Figures 2.1, 2.5, 2.6, 2.9, 2.19, 2.20, 2.21, 2.22, 2.23, 2.24, 2.25 and 2.26) have been published in Frontiers in Immunology (Klopp et al. 2021).

2.1 In vitro comparison of safeguard mechanisms

The different safeguard mechanisms were first cloned into a retroviral vector encoding for HBV-specific receptors. After retroviral transduction of T cells with the newly generated constructs, various experiments were performed. These included functionality assessments of both the HBV-specific receptors and the safeguard molecules as well as titration experiments of the effector T cells and the molecules inducing the different safeguard-mechanisms.

2.1.1 in vitro assessment of HBV-specific T cells co-expressing iC9

The first safeguard mechanism tested was the inducible caspase 9 (iC9). For this purpose, iC9 was cloned into a retroviral vector encoding for HBV-specific receptors. The new constructs contained iC9 linked to the S-CAR (env-specific), the TCR $4G_{S20}$ (S-specific) or TCR $6K_{C18}$ (core-specific) via a 2A element guaranteeing equimolar expression of both proteins (Figure 2.1A). Receptor expression was quantified by flow cytometry analysis after retroviral transduction of $CD8^+$ T cells with the new retroviral vectors or with retroviral vectors not containing iC9. As shown on Figure 2.1B, all the receptors were successfully expressed on $CD8^+$ T cells. However, the transduction rate was reduced by 10-40% when iC9 was co-expressed (Figure 2.1B).

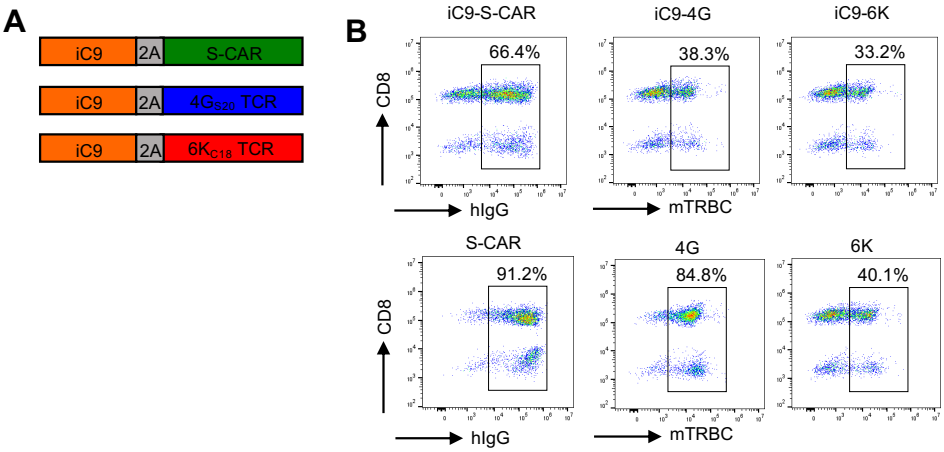

Figure 2.1 iC9-S-CAR/TCR expression in T cells

(A) Scheme of the safeguard molecule inducible caspase 9 (iC9) linked to HBV-specific receptors via a 2A element allowing both proteins to be equimolarly expressed. The S-CAR is based on a single-chain antibody fragment specific for the viral envelope protein on HBV-infected cells, a human IgG1 spacer (hIgG) and CD28/CD3 signaling domains. The TCR $4G_{S20}$ is specific for the envelope peptide S20 and TCR $6K_{C18}$ is specific for the core peptide C18. They both contain murine constant domains (mTRBC) that allow better pairing of TCR chains. **(B)** T cells were transduced either with a retroviral vector encoding for an HBV-specific receptor alone or with the retroviral vectors that comprise iC9 linked to HBV-specific receptors. On day 10, cells were stained for hIgG (CAR) or mTRBC (TCRs) and the respective receptor expression was quantified by flow cytometry. Figure was adapted from Klopp et al., (Klopp et al. 2021).

Having observed that HBV-specific receptor expression on T cells was slightly reduced when iC9 was co-expressed, we next investigated in a co-culture experiment with HBV^+ HepG2.2.15 cells if the killing efficiency by HBV-specific T cells was impacted when iC9 was co-expressed. Viability of the HBV-replicating target cell line was measured using a real-time cytotoxicity assay. While target cell killing by iC9-S-CAR T cells was a little bit slower than by S-CAR T cells (Figure 2.2A), the effector functions of TCR-expressing T cells were not affected by iC9 co-expression (Figure 2.2C, E). HBV-specific cytokine production was also not affected by iC9 co-expression (Figure 2.2B, D, F).

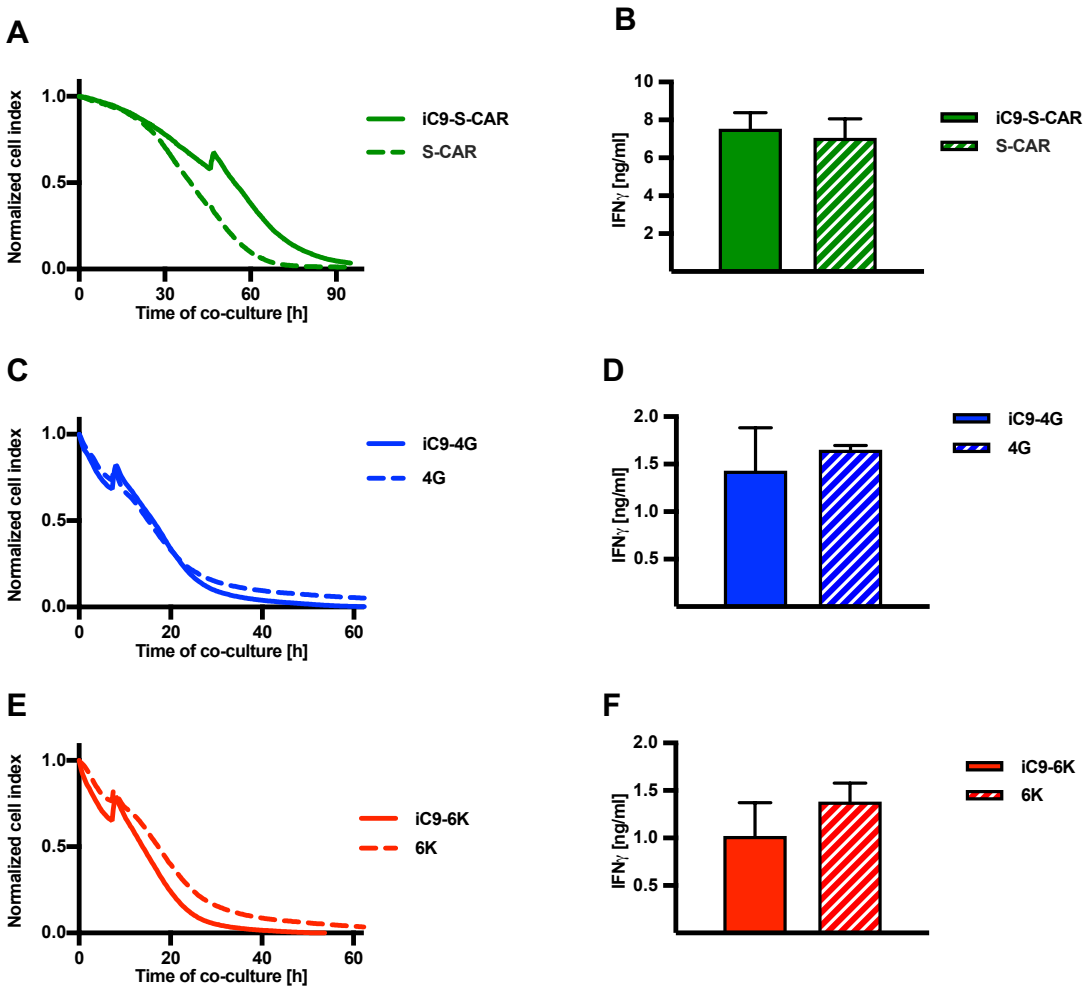

Figure 2.2 Comparison of the functionality of HBV-specific T cells with- or without iC9 co-expression

A co-culture was performed with 1.25 x 10^4 HBV-specific T cells that co-expressed or did not co-express iC9 and HBV$^+$ HepG2.2.15 target cells at an effector-to-target ratio of 1:4. **(A, C, E)** The viability of target cells was measured using an xCELLigence Real-Time Cell Analysis (RTCA) and is displayed as normalized cell index (normalized to the start of co-culture). **(B, D, F)** IFN-γ determined in cell culture medium on day four of the co-culture. This experiment was repeated three times and one representative example is shown. Co-cultures were done in technical triplicates and mean, or mean +/- SEM are shown, respectively.

In the previous co-culture experiment (Figure 2.2), an effector to target (E:T) ratio of 1:4 was used to investigate the killing by iC9-expressing HBV-specific T cells. In a next co-culture experiment, we analyzed how the increase or decrease of the effector to target ratio would influence the killing by HBV-specific T cells. As an example, only the killing by iC9-S-CAR T cells was assessed, and the viability of target cells was measured using a real-time cytotoxicity assay. The more S-CAR T cells were added to the assay, the greater and faster was the extent of specific target cell lysis (Figure 2.3A). The concentration of IFN-γ, measured on day five,

was however lower for the 2:1 E:T ratio than for the 1:1 or 1:2 E:T ratio (Figure 2.3B). A possible reason could be that with the highest E:T, nearly 100% of the target cells were already killed after 30 hours. As the supernatant for the IFN-γ was only collected on day five, and because of the short half-life IFNγ (Ando et al. 2014) it might be that at the day of measurement most of the IFNγ in the supernatant was already degraded. Addition of mock transduced T cells in the highest E:T ration did not affect the viability of the target cell line (Figure 2.3A).

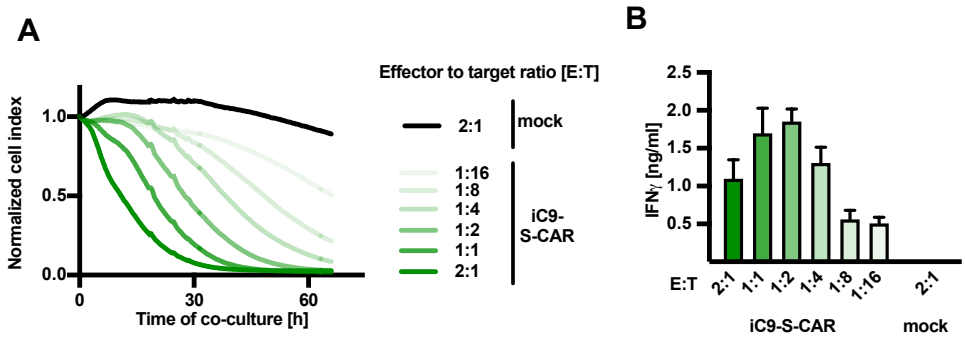

Figure 2.3 iC9-S-CAR T-cell functionality in different effector to target ratios

Retrovirally transduced iC9-S-CAR T-cells were co-cultured with 5 x 10^4 S-protein expressing Huh7S target cells at different effector-to-target ratios (E:T) ranging from of 2:1 to 1:16. **(A)** Killing of target cells was measured using an xCELLigence RTCA and is reported as normalized cell index (normalized to the start of co-culture). **(B)** IFN-γ measured in cell culture medium on day five of the co-culture. This experiment was repeated three times and one representative example is shown. Co-cultures were done in technical triplicates and mean, or mean +/- SEM are shown, respectively.

Next, we investigated the effect of inducing the safeguard mechanism iC9 in HBV-specific T cells. For this purpose, iC9-expressing HBV-specific T cells were co-cultured with HBV^+ HepG2.2.15 cells or HBV^- HepG2 cells. Target cell viability was measured using an XTT viability assay (measuring end-point viability of target cells; Figure 2.4A, B) or an xCELLigence assay (measuring real-time viability of target cells; Figure 2.4C-F). After one day, the chemical inducer of dimerization (CID; 500 ng/ml) was added to the co-culture to activate iC9. When co-cultured with S-CAR T cells, the viability of HBV-replicating HepG2.2.15 cells was reduced (filled bars, Figure 2.4A) while the viability of HBV^- HepG2 cells remained nearly unaffected (filled bars, Figure 2.4B). When CID was added to iC9-S-CAR T cells, the viability of HBV-replicating HepG2.2.15 cells was similar to the mock group (hatched bars, Figure 2.4A). No difference was observed when CID was added to S-CAR T cells that did not co-express iC9 (hatched bars, Figure 2.4A). Likewise, cytotoxicity of iC9-TCR T cells was rapidly halted after iC9 induction, while killing efficiency of TCR T cells not co-expressing iC9 remained unaltered (Figure 2.4C, E).

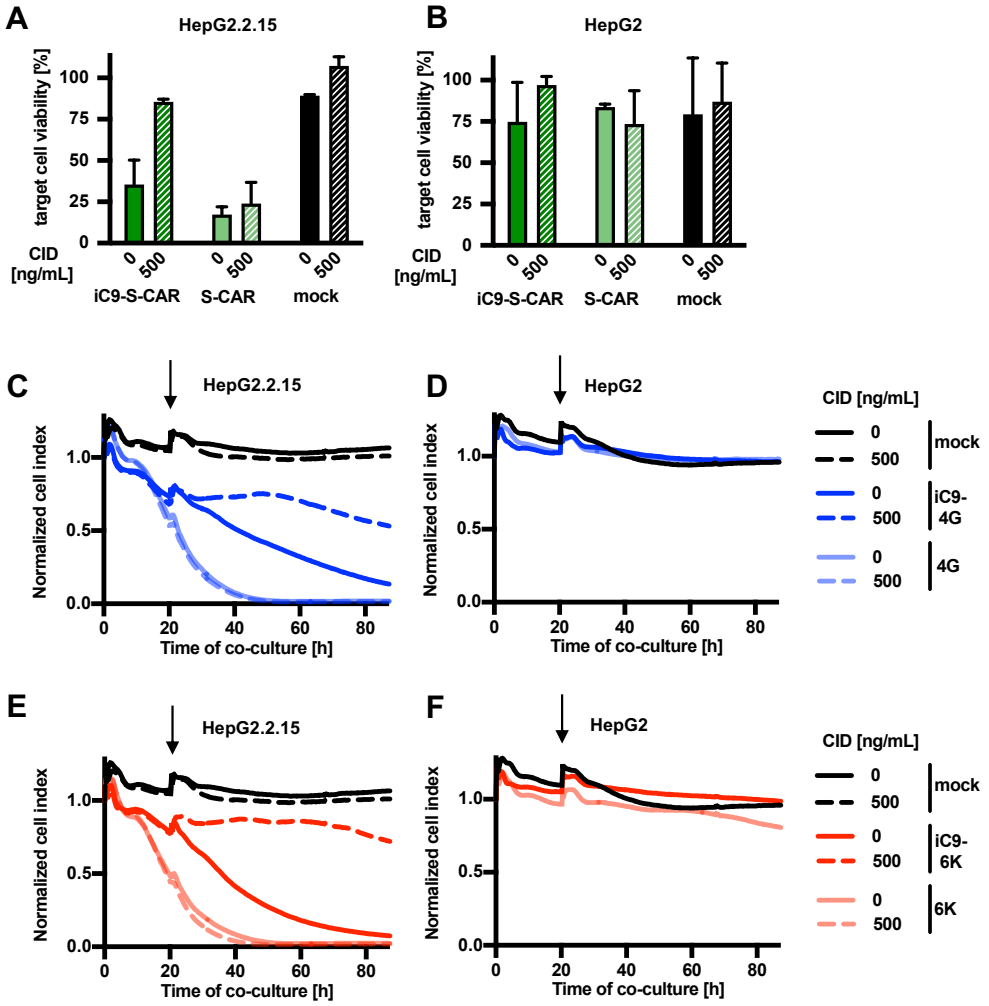

Figure 2.4 iC9-mediated depletion of HBV-specific T cells

Retrovirally transduced HBV-specific T-cells co-expressing iC9 were co-cultured with 5 x 10^4 HBV^+ HepG2.2.15 or HBV^- HepG2 target cells at an effector-to-target ratio of 1:4. Activation of the inducible caspase 9 was achieved by adding CID (highlighted by an arrow in C-F) the first day of co-culture in a concentration of 500 ng/ml (according to the manufacture's recommendations) leading to apoptosis of iC9-expressing T cells. **(A,B)** End-point viability of target cells was measured using an XTT assay. Due to capacity constraints an xCELLigence assay could not be performed for this experimental group. **(C-F)** Target cell viability was measured using an xCELLigence RTCA and is displayed as normalized cell index (normalized to the start of co-culture). This experiment was repeated three times and one representative example is shown. Co-cultures were done in technical triplicates and mean, or mean +/- SEM are shown, respectively.

After observing that induction of iC9 was very effective in HBV-specific T cells, we wondered if lowering the concentration of CID could still induce iC9 in a similar way and if very high doses of CID might have toxic side effects to either target or effector cells. A co-culture was performed with iC9-expressing HBV-specific T cells and HBV^+ HepG2.2.15 target cells. CID was added in different concentrations ranging from 1 ng/ml to 1000 ng/ml when around 40% of target cells

were killed as assessed by a real-time cytotoxicity assay. Addition of CID strongly reduced the killing by HBV-specific T cells within one hour independently of the respective concentration (Figure 2.5A, C, E). The lowest concentration of CID was as effective as the highest concentration. Furthermore, the HBV-specific IFN-γ production of T cells measured four days after CID addition was significantly reduced (Figure 2.5B, D, F).

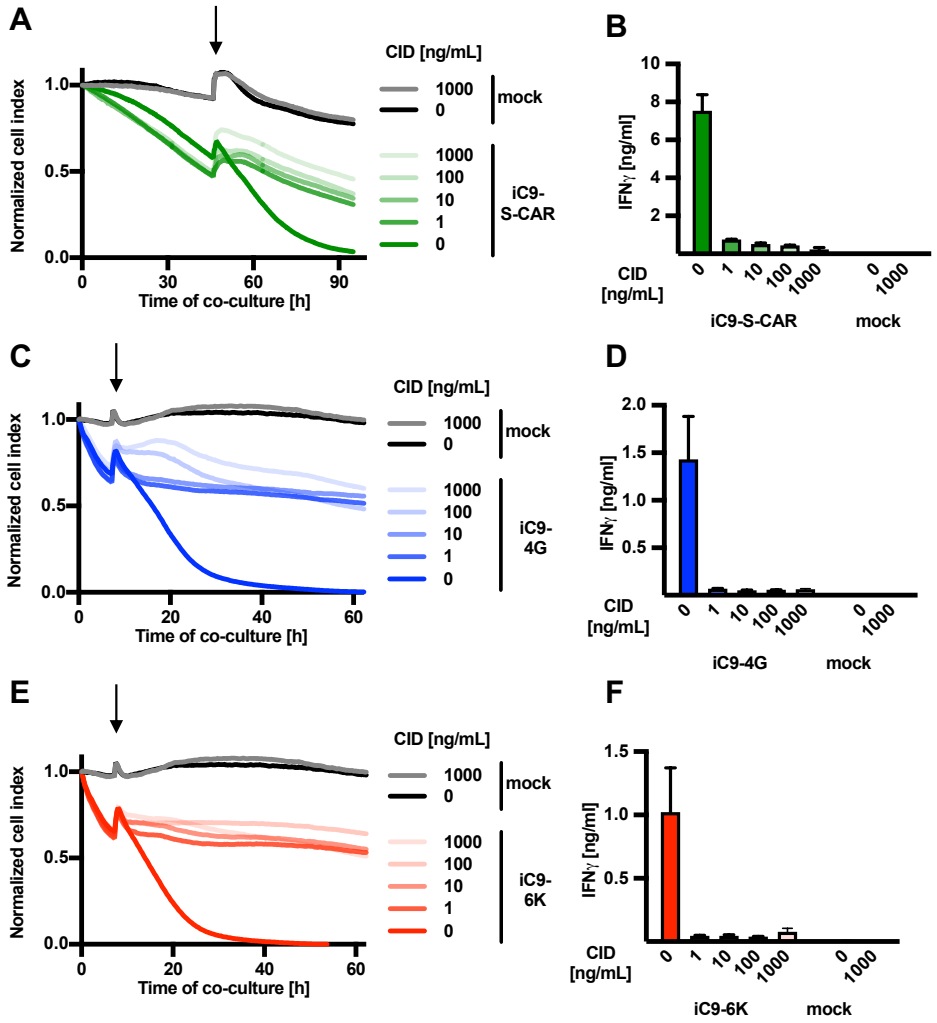

Figure 2.5 Titration of CID

A co-culture was performed with 1.25 x 10^4 HBV-specific T cells co-expressing iC9 and HBV$^+$ HepG2.2.15 target cells at an effector-to-target ratio of 1:4. Different concentrations (ranging from 1 ng/ml to 1000 ng/mL) of CID were added (highlighted by an arrow) the first (C,E) or second (A) day of co-culture in order to activate iC9. **(A,C,E)** The viability of target cells was measured using an xCELLigence RTCA and is displayed as normalized cell index (normalized to the start of co-culture). **(B, D, F)** IFN-γ determined in cell culture medium on day four of the co-culture. This experiment was repeated twice and one representative example is shown. Co-cultures were done in technical triplicates and mean are shown. Figure was adapted from Klopp et al., (Klopp et al. 2021).

Overall, we concluded that after co-expression of iC9, HBV-specific T cells were still effective killers and that effector functions of the T cells could rapidly be stopped after induction of the iC9 safeguard mechanism.

2.1.2 in vitro assessment of HBV-specific T cells co-expressing HSV-TK

The second safeguard mechanism tested was HSV-TK. Similar to iC9, HSV-TK was first cloned into retroviral vectors encoding for HBV-specific receptors. The new constructs contained HSV-TK linked to the S-CAR (env-specific), the TCR $4G_{S20}$ (S-specific) or the TCR $6K_{C18}$ (core-specific) (Figure 2.6A) via a 2A element. Receptor expression was determined by flow cytometry analysis after retroviral transduction of T cells and was around 60-90% for the three constructs (Figure 2.6B). In contrast to iC9, co-expression of HSV-TK on the T cells did not generally lead to a lower receptor expression rate.

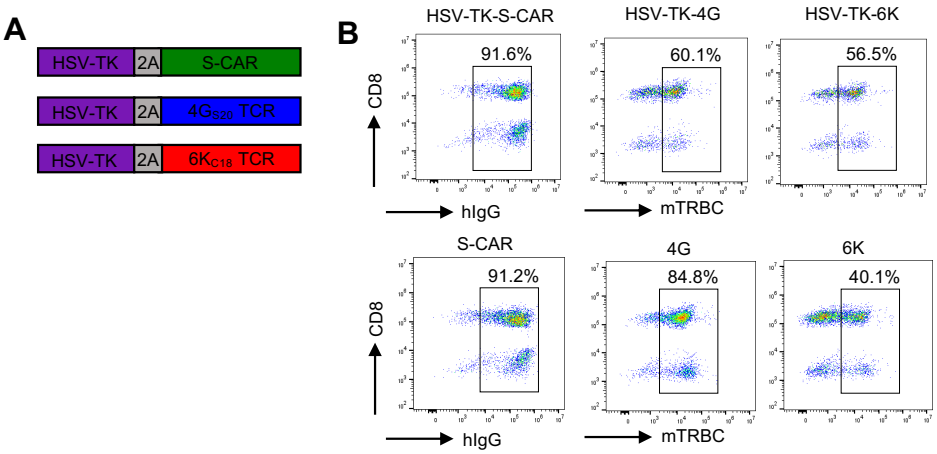

Figure 2.6 HSV-TK-S-CAR/TCR expression in T cells

(A) Scheme of the safeguard molecule herpes simplex virus thymidine kinase (HSV-TK) linked to HBV-specific receptors through a 2A element. **(B)** T cells were transduced either with a retroviral vector encoding for an HBV-specific receptor alone or with the retroviral vectors that comprise HSV-TK linked to HBV-specific receptors. On day 10, cells were stained for hIgG (CAR) or mTRBC (TCRs) and the respective receptor expression was quantified by flow cytometry. Figure was adapted from Klopp et al., (Klopp et al. 2021).

In a co-culture experiment with HBV^+ HepG2.2.15 cells, we assessed the killing efficiency of HSV-TK expressing HBV-specific T cells in comparison to HBV-specific T cells not co-expressing HSV-TK. Even though co-expression of HSV-TK did not impact the receptor expression rates of the S-CAR or the TCRs (Figure 2.6B), the killing was slightly detained (Figure 2.7A, C E). Also, the HBV-specific cytokine production by HSV-TK-4G T cells was

diminished whereas no striking difference was observed for HSV-TK-6K and HSV-TK-S-CAR T cells (Figure 2.7, B, D, F).

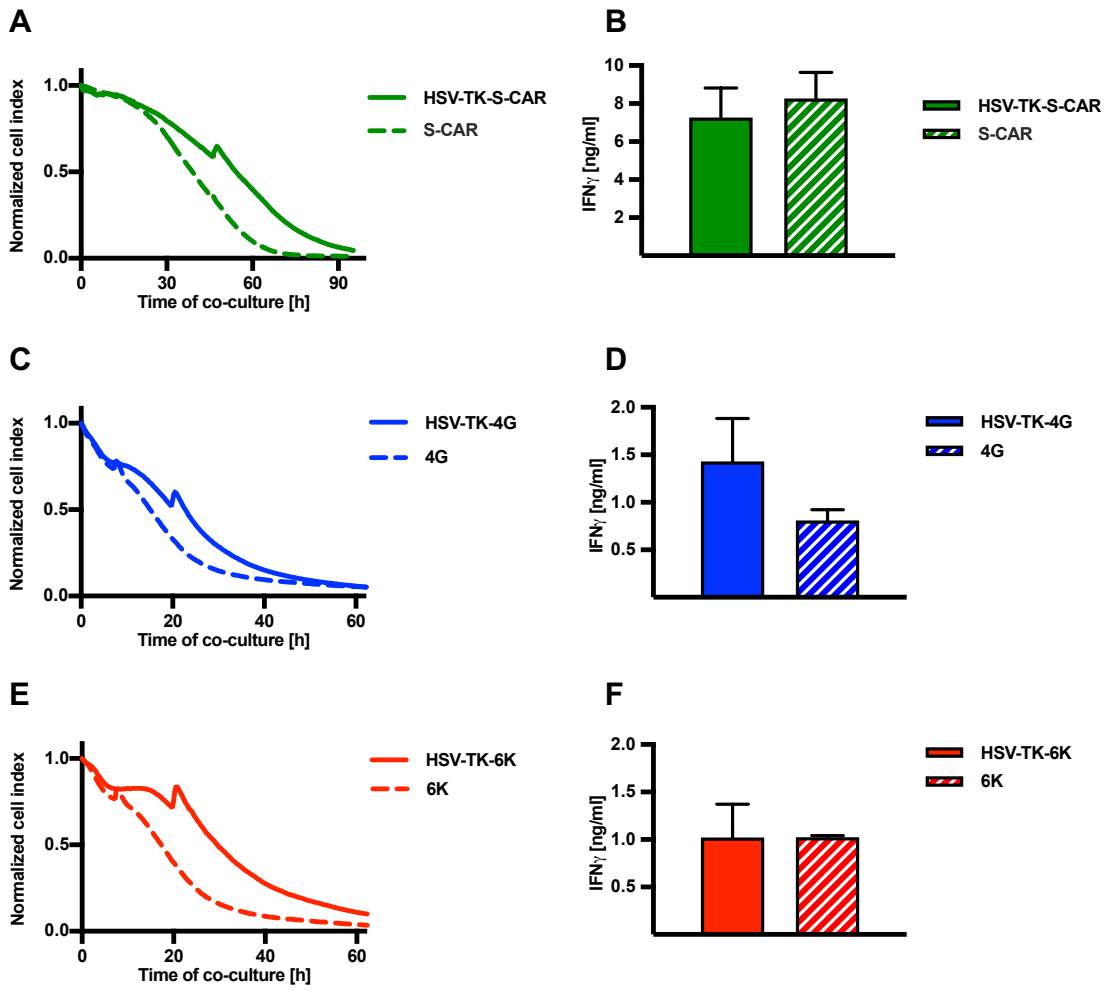

Figure 2.7 Comparison of the functionality of HBV-specific T cells with- or without HSV-TK co-expression

A co-culture was performed with 1.25 x 10^4 HBV-specific T cells that co-expressed or did not co-express HSV-TK and HBV^+ HepG2.2.15 target cells at an effector-to-target ratio of 1:4. **(A,C,E)** The viability of target cells was measured using an xCELLigence RTCA and is displayed as normalized cell index (normalized to the start of co-culture). **(B, D, F)** IFN-γ determined in cell culture medium on day four of the co-culture. This experiment was repeated three times and one representative example is shown. Co-cultures were done in technical triplicates and mean, or mean +/- SEM are shown, respectively.

Having observed that HSV-TK^+ HBV-specific T cells efficiently killed HBV-replicating target cells (Figure 2.6), we investigated the efficiency of effector cell death via HSV-TK. To this end, transduced T cells were co-cultured with HBV^+ HepG2.2.15 cells or HBV^- HepG2 cells and real-time target cell viability was measured. GCV (10 mg/ml) was added to the co-culture after one day to induce effector cell death via HSV-TK. After administration of GCV, cytotoxicity of HSV-TK-expressing T cells was halted within less than one hour (Figure 2.8A, C, E). HBV^-

HepG2 cells were not killed by the transduced T cells nor were they affected by the GCV addition (Figure 2.8B, D, F).

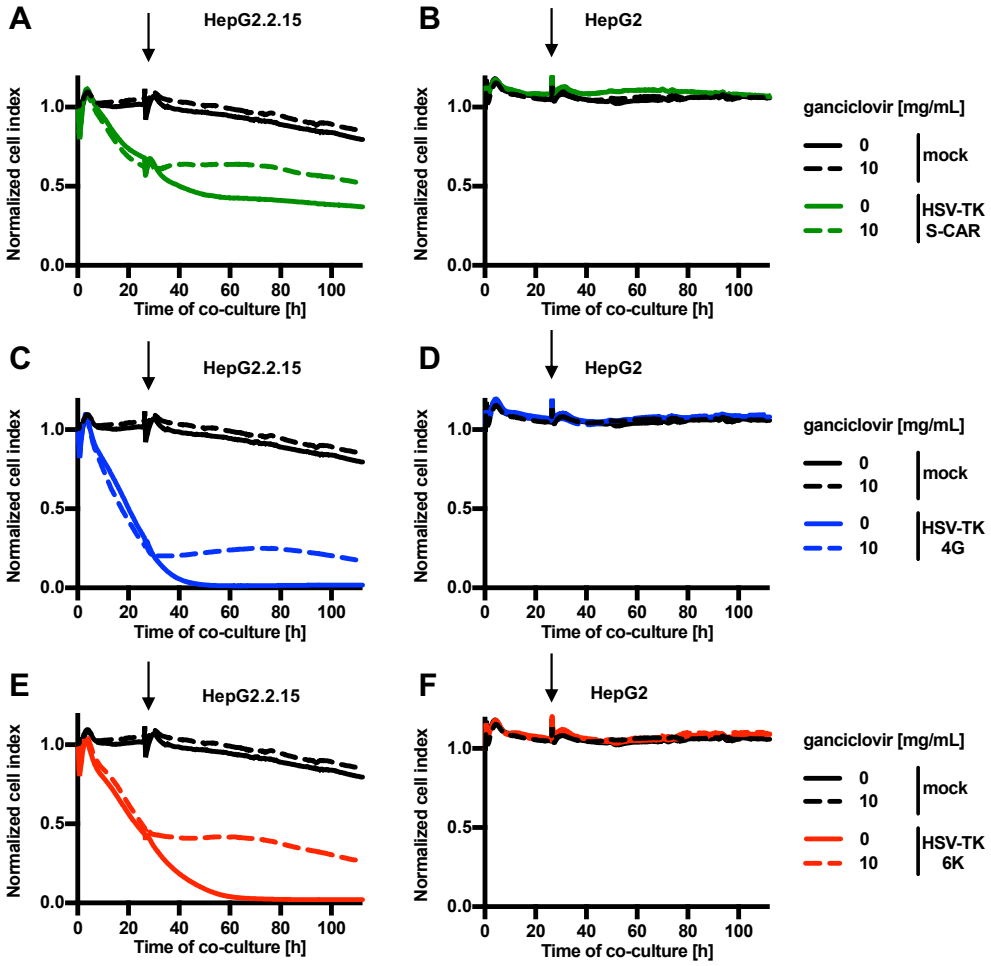

Figure 2.8 HSV-TK-mediated depletion of HBV-specific T cells

Retrovirally transduced HBV-specific T-cells co-expressing HSV-TK were co-cultured with 5 x 10^4 HBV^+ HepG2.2.15 or HBV^- HepG2 target cells at an effector-to-target ratio of 1:4. Activation of the herpes-simplex-thymidine kinase was achieved by adding GCV (highlighted by an arrow) after the first day of co-culture in a concentration of 10 mg/ml stopping cell-replication and leading to T-cell death. **(A-F)** Target cell viability was measured using an xCELLigence RTCA and is displayed as normalized cell index (normalized to the start of co-culture). This experiment was repeated three times and one representative example is shown. Co-cultures were done in technical triplicates and mean are shown.

In the previous experiment (Figure 2.8), GCV was used in a concentration of 10 mg/ml following the manufacture's recommendations. GCV is a common drug used for the treatment of CMV infection. Its side effects go from diarrhea and stomach pain to severe pancytopenia (Matsumoto et al. 2015). Furthermore, GCV solutions are very alkaline (pH approximately 11) resulting in severe tissue irritation when given via intramuscular or subcutaneous injection in a clinical setting (El-Samaligy et al. 1996). Thus, it is necessary that the concentration of GCV

is kept as high as necessary to be effective, but as low as possible to avoid possible side effects. A titration experiment of GCV was performed on this purpose. HSV-TK-expressing HBV-specific T cells were co-cultured with HBV$^+$ target cells and GCV was added in different concentrations ranging from 1000 mg/ml to 1 mg/ml. Although a concentration of 1 mg/ml was still enough to stop the cytotoxicity of transduced T cells, it occurred later than with higher concentrations (Figure 2.9A, C, E). Also, the suppression of IFN-γ production was less pronounced when GCV was added in a concentration of 1 mg/ml in comparison to the other concentrations (Figure 2.9B, D, F).

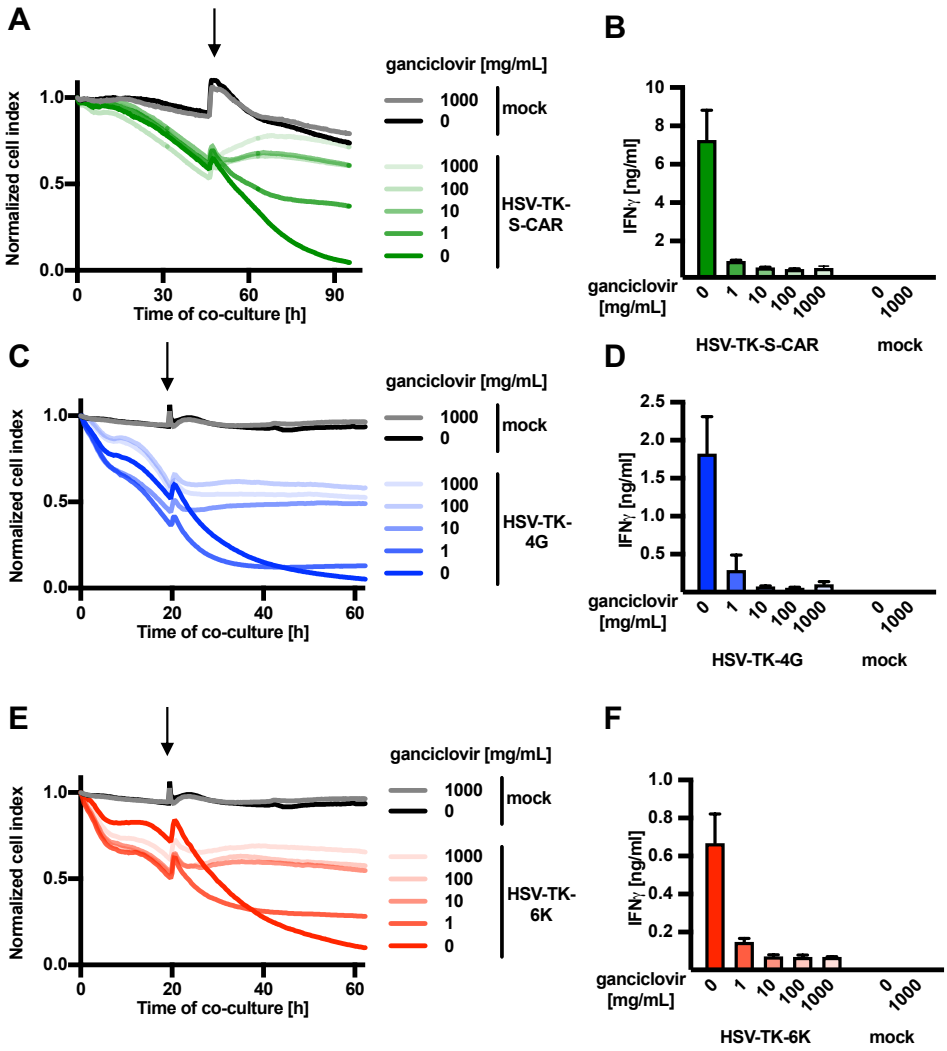

Figure 2.9 Titration of GCV

A co-culture was performed with 1.25 x 10^4 HBV-specific T cells co-expressing HSV-TK and HBV$^+$ HepG2.2.15 target cells at an effector-to-target ratio of 1:4. Different concentrations (ranging from 1 mg/mL to 1000 ng/ml) of GCV were added (highlighted by an arrow) the first (C,E) or second (A) day of co-culture in order to induce cell death **(A,C,E)** The viability of target cells was measured using an xCELLigence RTCA and is displayed as normalized cell index (normalized to the start of co-culture). **(B, D, F)** IFN-γ determined in cell culture medium on day four of the co-culture. This experiment was repeated twice and one representative example is shown. Co-cultures were done in technical triplicates

and mean, or mean +/- SEM are shown, respectively. Figure was adapted from Klopp et al., (Klopp et al. 2021).

Taken together, we saw that co-expression of HSV-TK did not alter the effector function of HBV-specific T cells and that induction of HSV-TK efficiently stopped the killing by HBV-specific T cells *in vitro.*

2.1.3 in vitro assessment of HBV-specific T cells co-expressing RQR8

The third and last safeguard mechanism tested was RQR8. In analogy to iC9 and HSV-TK, RQR8 was first cloned into the retroviral vectors encoding for the HBV-specific receptors (Figure 2.10A). The receptor expression rate was determined by flow cytometry analysis after retroviral transduction of T cells. Whereas co-expression of RQR8 did not have an impact on the expression rate of S-CAR and TCR 6K, the transduction rate for TCR 4G was reduced by 50% when RQR8 was co-expressed (Figure 2.10B).

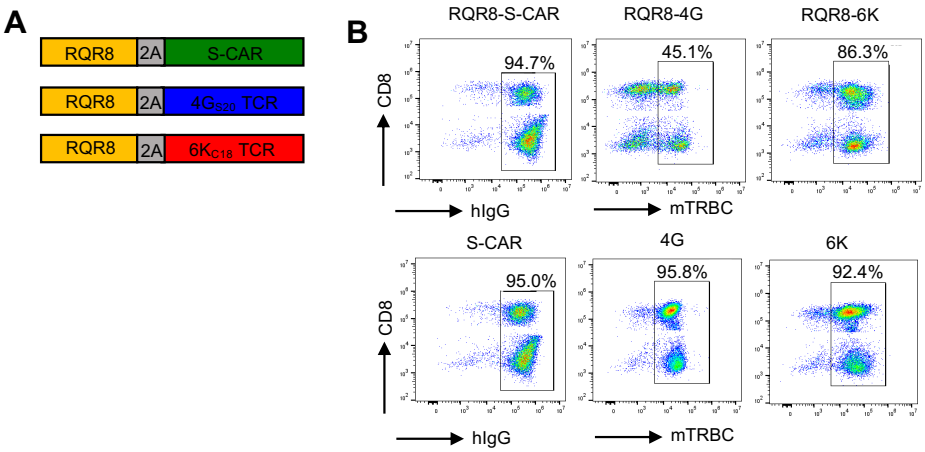

Figure 2.10 RQR8-S-CAR/TCR expression in T cells

(A) Scheme of the safeguard molecule RQR8 linked to HBV-specific receptors through a 2A element. **(B)** T cells were transduced either with a retroviral vector encoding for an HBV-specific receptor alone or with the retroviral vectors that comprise HSV-TK linked to HBV-specific receptors. On day ten, cells were stained for hIgG (CAR) or mTRBC (TCRs) and the respective receptor expression was quantified by flow cytometry.

As a next step, we investigated if HBV-specific T cells that co-express RQR8 were still functional. Hence, we co-cultured RQR8$^+$ HBV-specific T cells with HBV$^+$ HepG2.2.15 cells or HBV$^-$ HepG2 cells. Target cell viability was measured using an XTT viability assay (measuring the end-point viability of target cells; Figure 2.11A) or an xCELLigence assay (measuring the

real-time viability of target cells; Figure 2.11C, E). When co-cultured with RQR8-S-CAR T cells, the viability of HBV$^+$ target cells was reduced. However not to the same extent than with RQR8$^-$-S-CAR T cells (hatched bars, Figure 2.11A). The viability of HepG2 cells was not affected (filled bars, Figure 2.11A). Also, the IFN-γ production by RQR8$^+$-S-CAR T cells was slightly reduced in comparison to RQR8$^-$-S-CAR T cells (hatched bars, Figure 2.11B). Similar results were observed for RQR8$^+$-6K T cells (Figure 2.11E, F), whereas effector functions of TCR 4G T cells remained unaltered when RQR8 was co-expressed (Figure 2.11C, D).

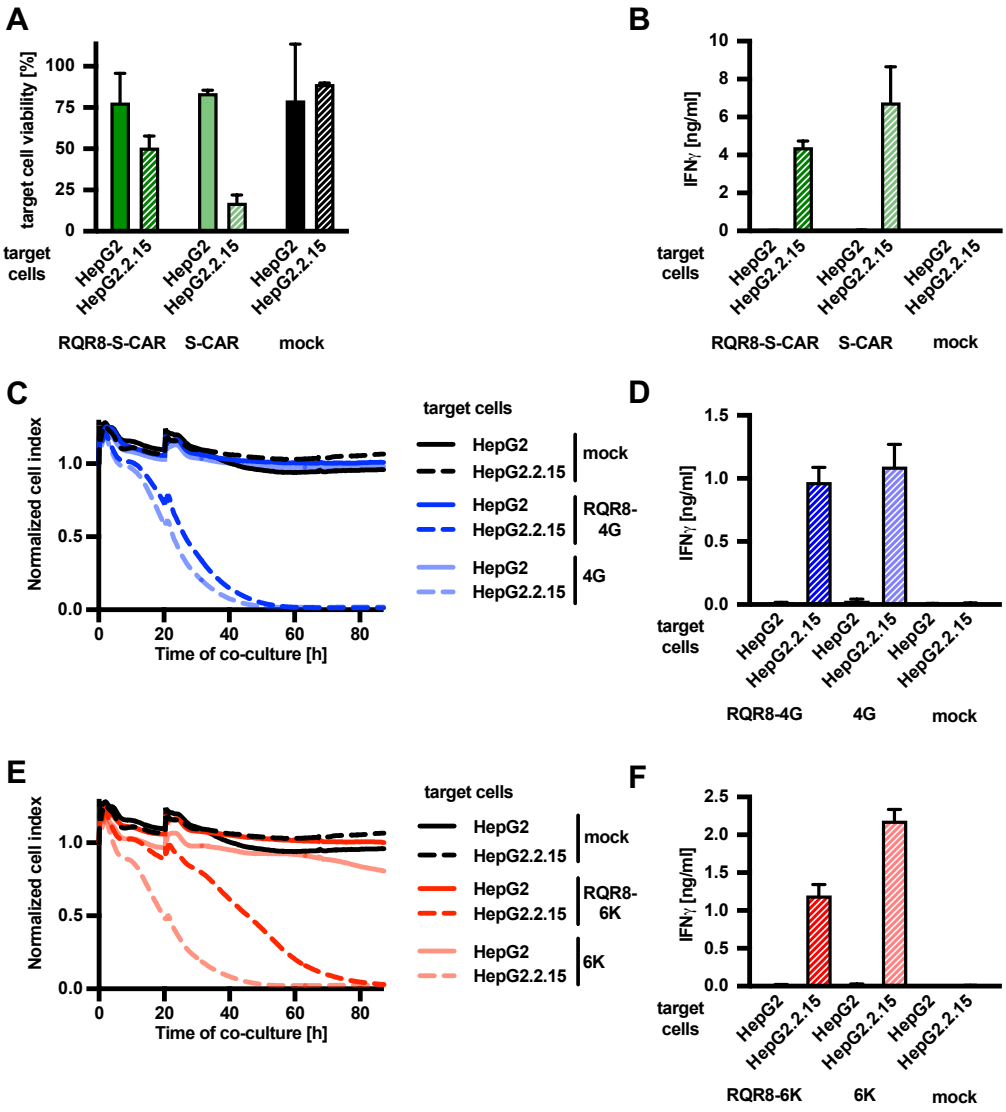

Figure 2.11 Comparison of the functionality of HBV-specific T cells with- or without RQR8 co-expression

Retrovirally transduced HBV-specific T-cells that co-expressed or did not co-express RQR8 were co-cultured with 5 x 10^4 HBV$^+$ HepG2.2.15 or HBV$^-$ HepG2 target cells at an effector-to-target ratio of 1:4. (**A)** End-point viability of target cells (filled bars for HepG2; hatched bars for HepG2.2.15) was measured using an XTT assay **(C,E)** Target cell viability (solid lines for HepG2; dashed lines for HepG2.2.15) was measured using an xCELLigence RTCA and is displayed as normalized cell index (normalized to the

start of co-culture). **(B, D, F)** IFN-γ determined in cell culture medium on day four of the co-culture. This experiment was repeated twice and one representative example is shown. Co-cultures were done in technical triplicates and mean, or mean +/- SEM are shown, respectively.

After successfully showing that co-expression of RQR8 had no impact on the functionality of S-CAR T cells, the next step was to investigate the induction of RQR8. Due to the complexity and costs of the assay this was done exemplarily with RQR8-S-CAR T cells. One way of inducing RQR8 is via antibody dependent cell-mediated cytotoxicity (ADCC). ADCC is usually performed by an NK cell that recognizes IgG (in this case rituximab) bound on a cell (in this case RQR8-expressing T cell) leading to cell lysis (Figure 2.12A). Two days after start of the co-culture of RQR8-S-CAR T cells with target cells (Huh7 or S-protein expressing Huh7S cells), NK-cells and rituximab (Rtx) were added to the co-culture. The NK-cells were added in different ratios (16x to 2x) to the RQR8-S-CAR T cells. To test the selectivity of RQR8-induction via Rtx, cetuximab (Ctx) was added to different co-culture wells instead of Rtx as a negative control (Figure 2.12B). NK cells were expanded from freshly isolated PBMCs using an expansion protocol established by Nina Kallin. The NK-cell population frequency increased from 10% to 50% within two days and a nearly pure NK-cell population could then be generated by magnetic cell separation with CD56 MicroBeads (Figure 2.12C). The INF-γ ELISA performed on day three, showed that IFN-γ secretion was highest when only S-CAR T cells were added to the target cells. The addition of NK cells and cetuximab did not reduce IFNγ-production as cetuximab does not bind RQR8. The addition of NK cells and rituximab however led to a reduction of IFN-γ secretion which was even more prominent the more NK cells were added (Figure 2.12D).

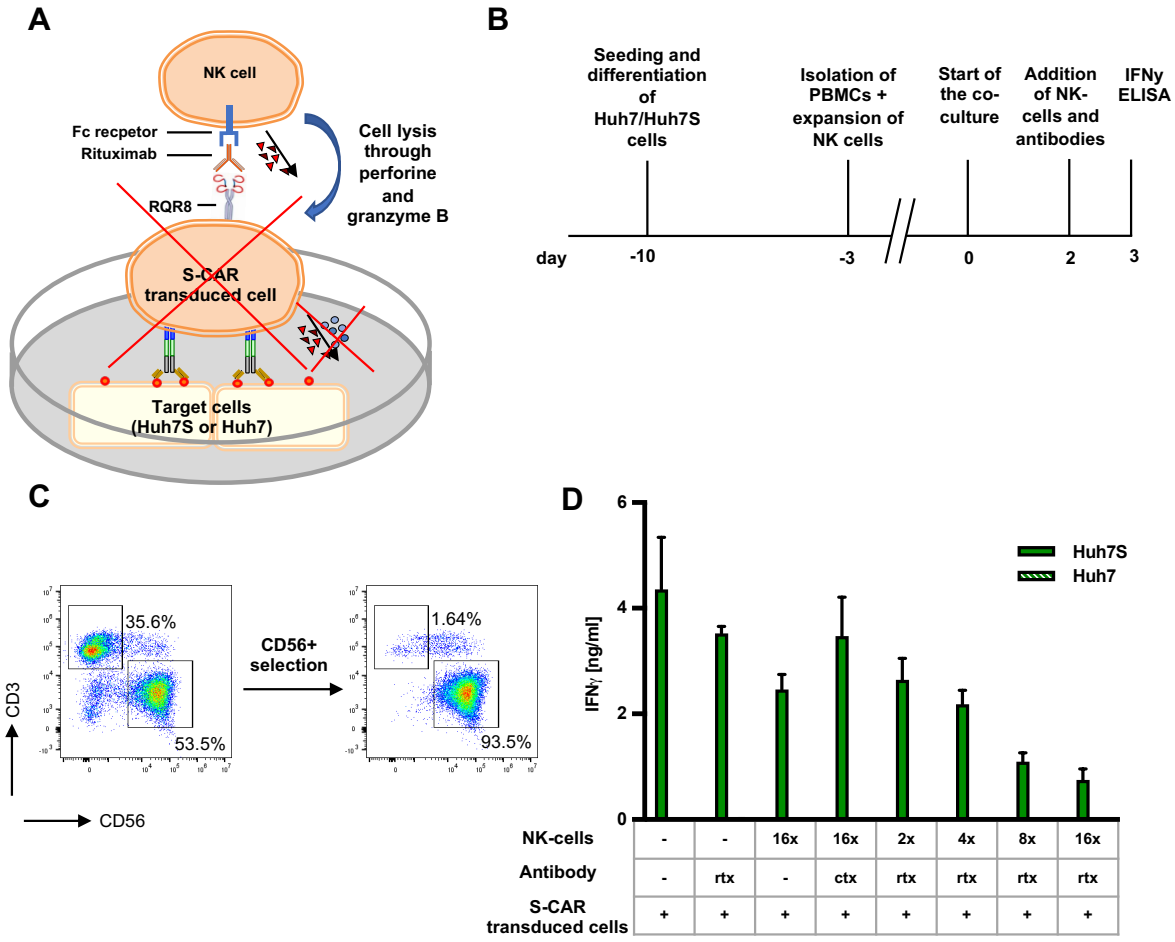

Figure 2.12 ADCC assay for functional evaluation of RQR8

(A) Schematic representation of RQR8-mediated cell death through antibody dependent cell-mediated cytotoxicity (ADCC). **(B)** Scheme of the experimental procedure. Ten days prior to start of the co-culture with RQR8-S-CAR T cells, the target cells (Huh7 and S-protein expressing Huh7S cells) were seeded and differentiated. Three days prior to start of the co-culture, PBMCs were isolated and NK cells were expanded. The NK cells and the respective antibodies [rituximab (Rtx) or cetuximab (Ctx)] were added on day two after start of the co-culture. An IFN-γ ELISA was performed on day three. **(C)** Flow cytometry analysis shows the ratio of $CD56^+$ cells before and after positive selection of $CD56^+$ cells. PBMCs were isolated and $CD56^+$ NK cells were selected (positive selection) using magnetic cell separation with CD56 MicroBeads. **(D)** IFN-γ determined in cell culture medium on day three of the co-culture. This experiment was performed once and the representative example is shown. Co-cultures were done in technical triplicates and mean +/- SEM are shown, respectively.

Another way of inducing RQR8 is via complement depended cytotoxicity (CDC). CDC is activated after binding of an antibody (in this case rituximab) to a target cell (in this case RQR8-expressing T cell) which leads to the recruitment and activation of components of the complement cascade which ultimately leads to pores called Membrane Attack Complex (MAC) and to cell lysis (Figure 2.13A). RQR8-S-CAR T cells were co-cultured with target cells (Huh7 or Huh7S cells) and two days after start of the co-culture the respective antibodies (rituximab

or cetuximab) in different concentrations and rabbit serum as source of complement factors were added to the assay (Figure 2.13B). An IFN-γ ELISA performed on day three, showed high IFNγ-secretion when only effector cells were added to the target cells. Nearly no IFNγ-secretion was observed when the transduced T cells were co-cultured with Huh7 cells. Addition of cetuximab in the highest concentration did not lead to a reduction of IFN-γ secretion. Addition of rituximab seemed to slightly reduce IFN-γ secretion in a concentration-depended manner (Figure 2.13C).

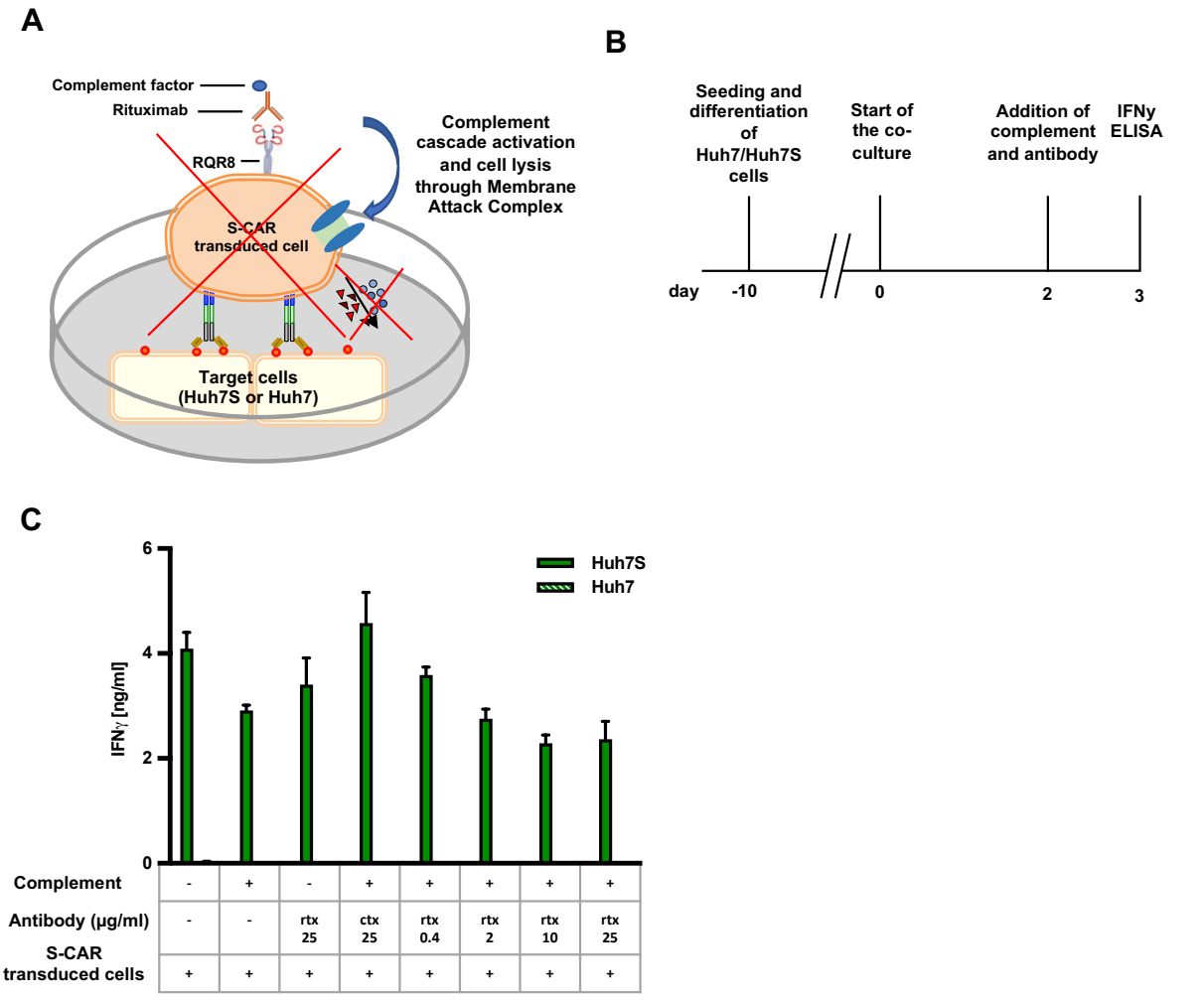

Figure 2.13 CDC assay for functional evaluation of RQR8

(A) Schematic representation of RQR8-mediated cell death via complement dependent cytotoxicity (CDC). **(B)** Scheme of the experimental procedure. Ten days prior to start of the co-culture with RQR8-S-CAR T cells, the target cells (Huh7 and S-protein expressing Huh7S cells) were seeded and differentiated. Complement factors and the respective antibodies (Rtx or Ctx) were added on day two after start of the co-culture. An IFN-γ ELISA was performed on day three. **(C)** IFNγ determined in cell culture medium on day three of the co-culture. This experiment was performed once and the representative example is shown. Co-cultures were done in technical triplicates and mean +/- SEM are shown, respectively.

We concluded that HBV-specific T cells co-expressing RQR8 were still specifically activated by HBV^+ target cells and that induction of RQR8 through ADCC led to the elimination of RQR8-S-CAR T cells and thus to a two-fold reduction of IFN-γ secretion. Despite the tendency to reduce S-CAR function, no clear statement about RQR8-induction through CDC was possible at that stage and needed further evaluation.

2.2 *In vivo* assessment of safeguard mechanisms

In vitro, both HSV-TK and iC9 showed promising results as possible safeguard molecules in HBV-specific T cells. In fact, HBV-specific-TCR and S-CAR T cells co-expressing iC9 or HSV-TK were activated by HBV^+ target cells (HepG2.2.15 or Huh7S) and showed efficient killing. The killing by these cells could be reduced or stopped in presence of the CID or GCV, respectively. RQR8, as extracellular, antibody-dependent safeguard mechanism, could not reliably be tested *in vitro*. As a next step, we aimed to further evaluate the different safeguard mechanisms *in vivo*. A first experiment was conducted in immunocompetent mice in order to compare the three safeguard mechanisms against each other. Only the S-CAR was tested in the *in vivo* experiments as it functions independently of human MHC molecules and is thus easier to apply. Based on this experiment and the *in vitro* results, iC9 was selected as most promising strategy to increase safety of adoptive T cell therapy against CHB and it was further evaluated in an immunocompromised mouse model.

2.2.1 Comparison of safeguard-mechanisms in an immunocompetent mouse model

As a preparation of the on-coming *in vivo* experiments, we first wanted to control if murine splenocytes could also be transduced with the newly generated S-CAR constructs and if transduced murine splenocytes were also activated *in vitro.* Exemplary only the iC9-S-CAR construct was tested in this experiment, presuming that same or similar results would have been achieved with the other constructs. We retrovirally transduced freshly isolated murine splenocytes with the iC9-S-CAR construct and determined its expression by FACS analysis which showed a receptor expression rate of nearly 90% (Figure 2.14A). For functional assessment of the transduced splenocytes, they were cultured on an HBs-coated plate and an mIFNγ ELISA was performed. On day five, iC9-SCAR transduced splenocytes showed a high secretion in presence of HBsAg in comparison to mock transduced T cells but nearly no secretion in presence of PBS (Figure 2.14B). We concluded, that murine splenocytes could effectively be transduced with the iC9-S-CAR construct and that the transduced cells showed specific activation in presence of HBsAg.

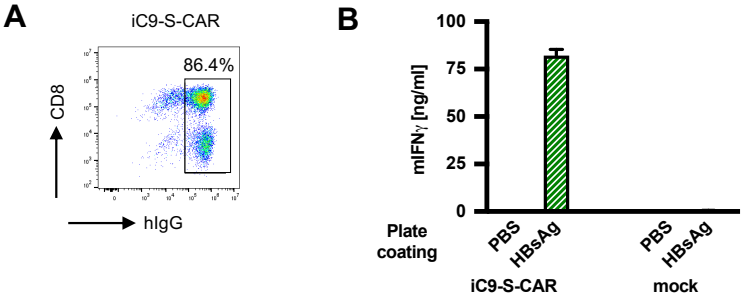

Figure 2.14 iC9-S-CAR expression and functionality assessment in murine splenocytes

(A) Murine T cells were transduced with a retroviral vector that comprises iC9 linked to the S-CAR. On day 10, cells were stained for hIgG (CAR) and the respective receptor expression was quantified by flow cytometry. **(B)** The retrovirally transduced iC9-S-CAR T-cells (1 x 10^4 cells per well) were cultured on plate-bound HBsAg or PBS as a negative control to determine their functionality. mIFN-γ was measured in cell culture medium on day five of the culture. Cultures were done in triplicates and mean +/- SEM are shown.

In a first *in vivo* experiment, iC9, HSV-TK and RQR8 safeguard mechanisms were compared in an immunocompetent mouse model. First, we hereby wanted to confirm the *in vitro* results and second select the most promising mechanisms for further *in vivo* evaluation. As in previous *in vivo* experiments in our lab, we had observed a rejection of S-CAR T cells due to an immune response against the human domains of the S-CAR, a mouse model had been established which allows specific tolerization of immunocompetent mice against allogenic receptor- and safeguard domains (Festag et al. 2019). Three weeks after establishing a stable HBV infection in CD45.2$^+$ mice (=d-105), they were irradiated to deplete their endogenous immune cells (Figure 2.15A). One day after irradiation (=d-104), T cells expressing an unfunctional CAR (SΔ-CAR; same extracellular domain than the S-CAR but different intracellular domains rendering it unfunctional) and T cells expressing one of the three safeguard mechanism (iC9-aGD2-CAR-, RQR8-aGD2-CAR- or HSV-TK-CD34-T cells) were transferred into the mice in order to tolerize them against human domains of the respective molecules (Figure 2.15B). GD2 is a surface glycolipid mostly expressed on neuroblastoma tumor cells and a common targeted antigen for immunotherapy. CD34 is a transmembrane protein usually located on the surface hematopoietic stem cells and often used as a marker/selection gene. These constructs were kindly provided to us from Martin Pulé and allowed us to tolerize the mice against the different safeguard mechanisms without having to generate new constructs expressing one of the three safeguard mechanisms and SΔ-CAR. Three months after tolerization (=d0), T cells co-expressing a functional S-CAR and one of the three safeguard mechanisms were injected into the mice (Figure 2.15C). The respective safeguard mechanism was then triggered at day four. CID was administered intraperitoneally, whereas Rtx (murine immunoglobulin G2a rituximab

provided by Martin Pule) and GCV were injected intravenously. The mice were sacrificed at day seven (Figure 2.15A).

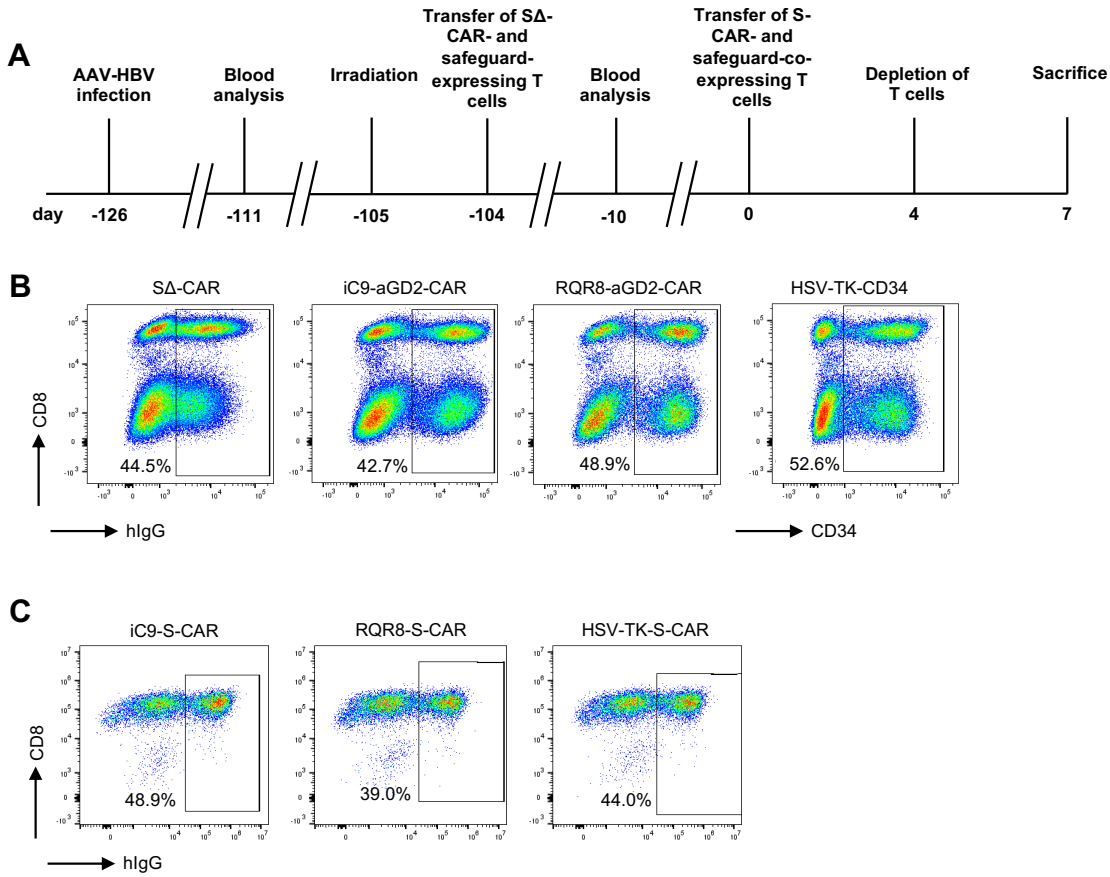

Figure 2.15 Evaluation of safeguard-expressing S-CAR T cells in immunocompetent mice

(A) Scheme of the experimental procedure. An adeno-associated virus vector (AAV-HBV) was used to infect CD45.2^{+} mice with HBV. 2 x 10^{10} viral particles were injected intravenously per mouse. To induce tolerization against allogenic domains of the CAR- and safeguard-molecules, 2 x 10^{6} SΔ-CAR T cells and 2 x 10^{6} of iC9-, RQR8- or HSV-TK-expressing T cells (iC9-aGD2-CAR-, RQR8-aGD2-CAR- or HSV-TK-CD34-T cells) were injected intraperitonially per animal one day after sublethal irradiation of the mice with 5 gray (day -104). The extracellular domain of the SΔ-CAR is identical to the S-CAR, however it is rendered unfunctional by exchanging its intracellular domains. 104 days later (day zero), 2.5 x 10^{6} S-CAR T cells (n=2), iC9- (n=6), RQR8- (n=5) or HSV-TK-S-CAR T cells (n=4) were transferred per mouse. On day four, the respective depleting substance (CID for iC9 and SΔ-CAR (i.p.), Rtx (i.v.) for RQR8 and GCV (i.v.) for HSV-TK) or a negative control (identical preparation to the respective substance but without the active molecule) was injected. Mice were sacrificed on day seven. **(B)** Flow cytometry analysis showing the receptor expression of the retrovirally transduced T cells injected on day -104. **(C)** Flow cytometry analysis showing the receptor expression of the retrovirally transduced T cells injected on day zero. (iC9-S-CAR n=3 per group, HSV-TK-S-CAR n=2 per group, RQR8-S-CAR + Rtx n=3, RQR8-S-CAR - Rtx n=2, SΔ-CAR n=1 per group)

As mentioned before, a sublethal irradiation of the mice was performed one day before administration of SΔ-CAR T cells and iC9-, RQR8- or HSV-TK-expressing T cells in order to allow specific tolerization of the immunocompetent mice against allogenic domains of the respective molecules. Over the course of the experiment, the concentration of endogenous immune cells was monitored by flow cytometry analysis (Figure 2.16A). The concentration of endogenous $CD4^+$, $CD8^+$ and $CD19^+$ cells in the blood was strongly decreased one day upon irradiation (d-104). They had however regained physiological concentrations on day of the transfer of functional S-CAR T cells (d0) (Figure 2.16B, C, D).

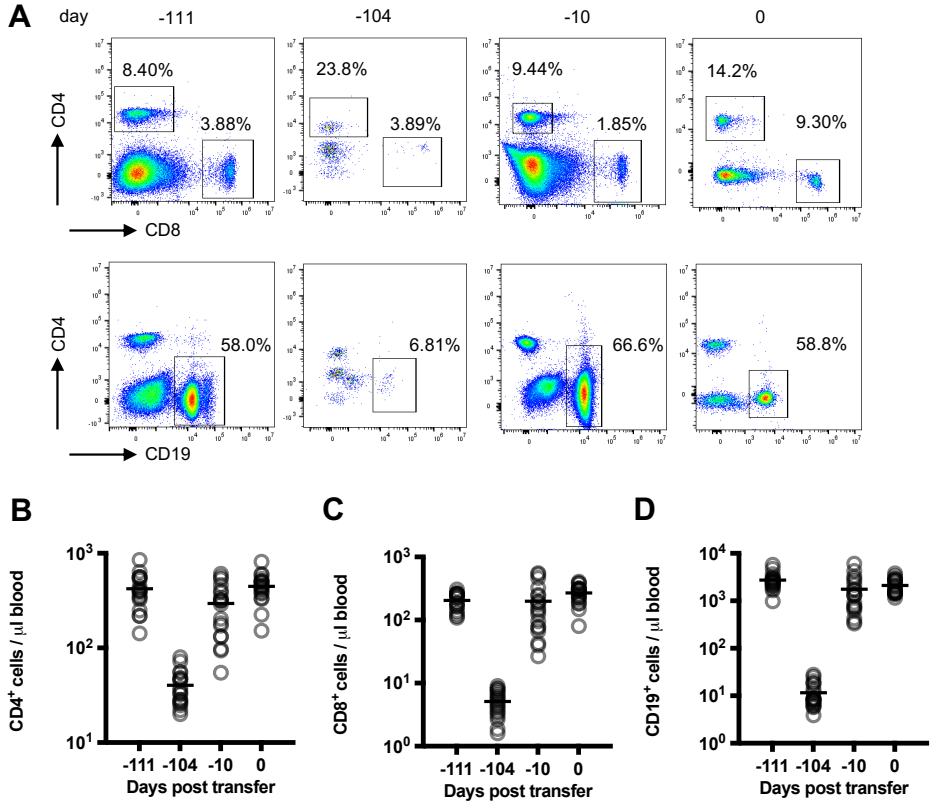

Figure 2.16 Monitoring of the endogenous immune system in irradiated mice

To induce tolerization against allogenic domains of the CAR- and safeguard-molecules, mice were irradiated one day before injection of the transduced T cells on day -104. The concentration of endogenous immune cells ($CD4^+$- (A), $CD8^+$- (C) and $CD19^+$-cells (E)) was assessed before irradiation on day -111, one day after irradiation on day -104 as wells as on day -10 and on day zero. **(A)** Exemplary flow cytometry plots assessing $CD4^+$-, $CD8^+$- and $CD19^+$-cells of a single mouse on days -111, -104, -10 and zero. **(B, C, D)** Count of endogenous immune cells isolated from the blood on day -111, -104, -10 and zero. Absolute cell counting was accomplished by adding counting beads to the respective flow cytometric sample and the result was extrapolated to the concentration in blood considering the volume of blood used for the analysis. Data points represent individual animals and mean values are indicated. (n = 17)

In order to determine if and to what extent induction of the respective safeguard mechanism on day four was successful, mice were scarified on day seven and number of transferred cells in blood, spleen and the liver was determined by flow cytometry analysis. Differentiation between transferred ($CD45.1^+/CD45.2^+$) and endogenous ($CD45.2^+$) cells was achieved using the congenic marker CD45.1/2. In the iC9-group, a $0.5\log_{10}$ reduction of transferred cells in the blood and a $1\log_{10}$ reduction of transferred cells in the spleen and the liver in comparison to the mice which did not receive CID was observed (Figure 2.17A). However, the results were not statistically significant. In the RQR8-group, administration of Rtx led to no reduction of transferred cells in the spleen and only to a slight reduction of transferred cells in the blood ($0.1\log_{10}$ reduction) and the liver ($0.5\log_{10}$ reduction) in comparison to the mice which did not receive Rtx (Figure 2.17A). In the HSV-TK group the difference between the mice having received GCV and those where HSV-TK had not been induced was even smaller, with a $0.1\log_{10}$ reduction of transferred cells observed in the blood and the liver and a $0.1\log_{10}$ increase of transferred cells in the spleen (Figure 2.17A). To further assess the functionality of the transferred T cells, the isolated liver associated lymphocytes (LALs) and splenocytes were incubated on HBsAg-coated plates and afterwards intracellular cytokine production (IFN-γ, TNF-α and IL-2) was analyzed by flow cytometry. In one mouse from the iC9-group that was not depleted, the isolated $CD45.1^+/CD45.2^+$ T cells from the spleen still showed HBsAg-specific production of cytokines. This expression was completely absent in all the mice that had received CID (Figure 2.17B). A similar observation (however less pronounced) was observed in the HSV-TK-group. In the RQR8-group however HBsAg-specific production of cytokines was detected in both, a mouse which did receive Rtx and a mouse which did not receive Rtx (Figure 2.17B). The functional profile of LALs was comparable to that of splenocytes (Figure 2.17C). As a negative control the isolated LALs and splenocytes were also cultured on PBS. Here no specific cytokine secretion was observed (Data not shown).

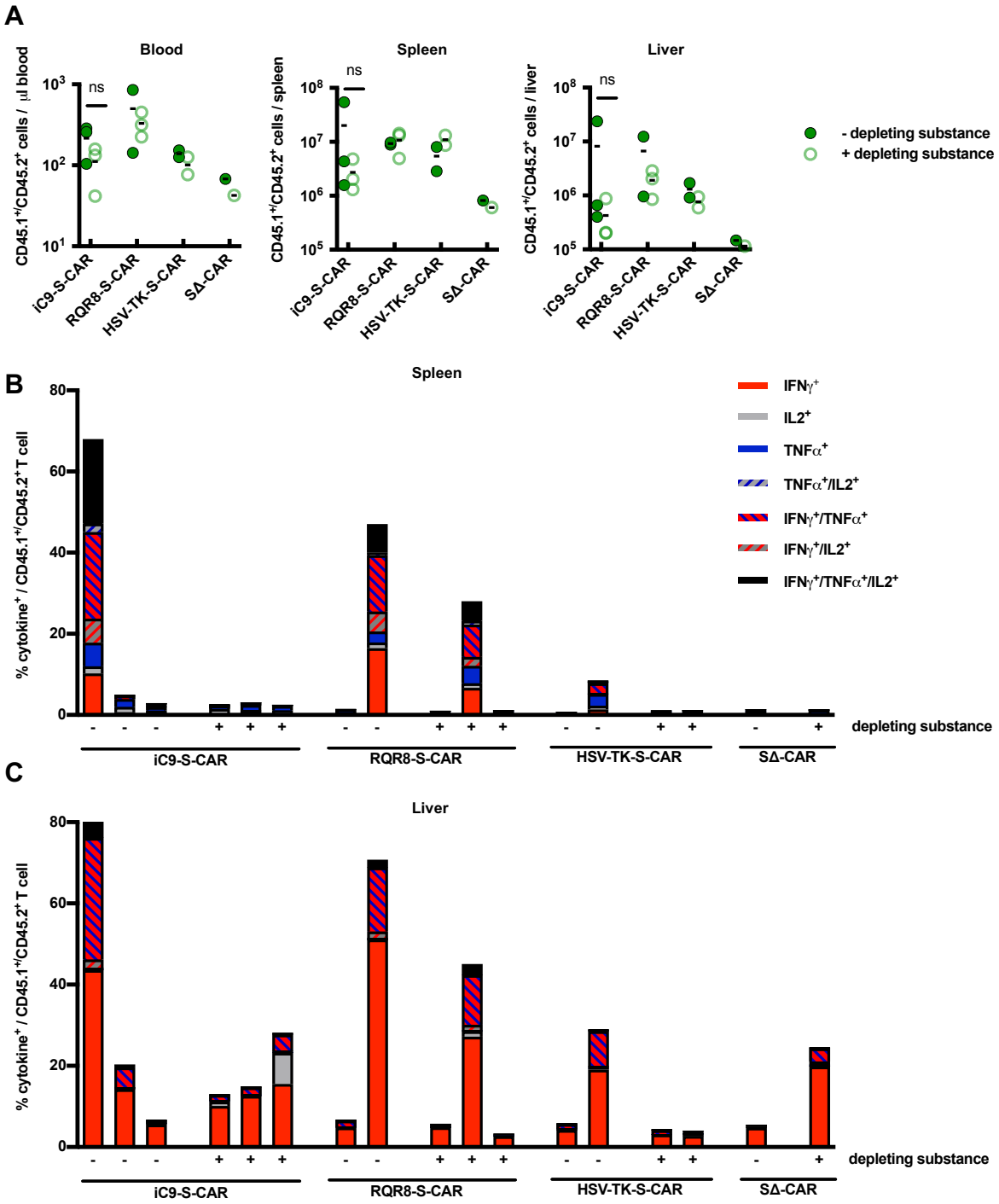

Figure 2.17 Depletion of transduced T cells via iC9, RQR8 or HSV-TK in immunocompetent mice

(A) Count of transferred CD45.1$^+$/CD45.2$^+$ T cells isolated from the blood, the spleen and the liver on day seven. Absolute cell counting was accomplished by adding counting beads to the respective flow cytometric sample and the result was extrapolated to the concentration in blood or to the whole organ considering the proportion that was used to isolate splenocytes or LALs. **(B, C)** Isolated splenocytes and LALs were cultured overnight on plate-bound HBsAg to determine the *ex vivo* functionality of the transferred CD45.1$^+$/CD45.2$^+$ T cells. On the next day, intracellular cytokine expression (IFN-γ, TNF-α and IL-2) of the cultured splenocytes (B) and LALs (C) was determined by flow cytometry. The isolated splenocytes and LALs were also cultured on PBS as negative control (Data not shown). (A) Data points represent individual animals and mean values are indicated. (B, C) Each column represents an

individual animal. (iC9-S-CAR n=3 per group, HSV-TK-S-CAR n=2 per group, RQR8-S-CAR + Rtx n=3, RQR8-S-CAR - Rtx n=2, SΔ-CAR n=1 per group)

Although the depletion of transferred T cells via the different safeguard mechanisms not being evident throughout this experiment, we still wondered if induction of the safeguard mechanisms had an impact on the antiviral effect of the S-CAR T cells. For this purpose, HBs-, HBe-, and ALT-levels were determined in the sera of the mice on day zero, four and seven. Whereas in the iC9-group, induction of the safeguard mechanism seemed to halt the effect of S-CAR T cells on circulating HBsAg, in the RQR8- and HSV-TK-group S-CAR T cells continued their antiviral effect even though the respective safeguard mechanism had been induced (Figure 2.18A). Considering the ALT levels, liver damage was only observed in mice of the iC9- and RQR8-group in which T cells had not been depleted assuming that induction of those safeguard mechanisms prevented excessive hepatotoxicity. The opposite was however observed in the HSV-TK group (Figure 2.18C).

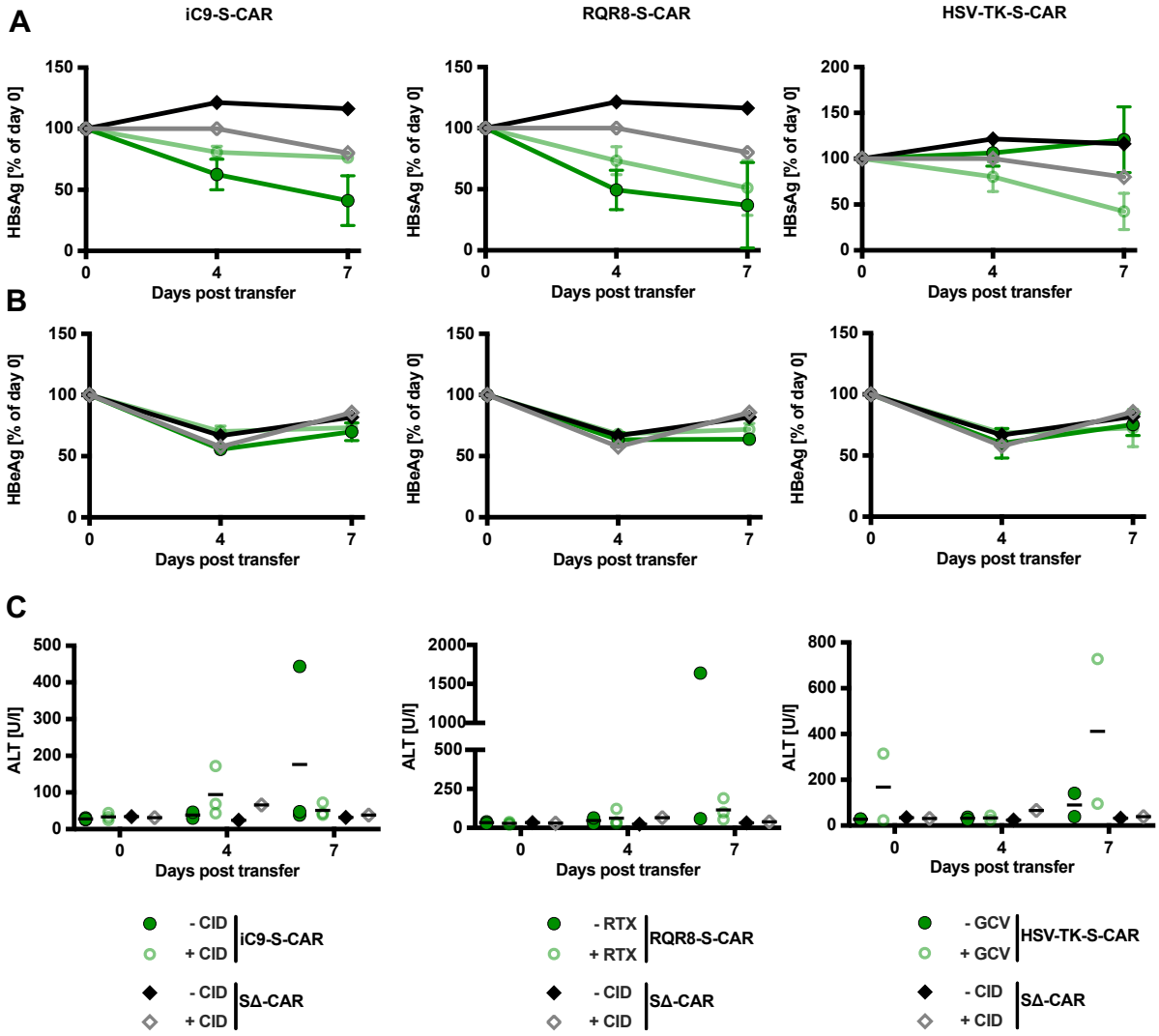

Figure 2.18 Antiviral effect of safeguard-expressing S-CAR T cells in immunocompetent mice

(A-C) Sera of the mice were analyzed for HBsAg, HBeAg and ALT by diagnostic assays on day zero, four and seven after T-cell transfer. (A, B) Data are given as mean values +/- SD. (C) Data points represent individual animals and mean values are indicated. The SΔ-CAR group is identical throughout the experiment and is only shown in each graph for better reference. (iC9-S-CAR n=3 per group, HSV-TK-S-CAR n=2 per group, RQR8-S-CAR + Rtx n=3, RQR8-S-CAR - Rtx n=2, SΔ-CAR n=1 per group)

In consideration of these results, we concluded that there was a tendency of specific deletion when iC9 was induced whereas no striking difference was observed in the other groups. Furthermore, induction of iC9 seem to reduce the antiviral effect of S-CAR T cells. Due to the low number of mice per group (n=3), analysis and interpretation of data was however difficult. Furthermore the injection of the very alkaline GCV solution proved to be technically difficult and caused distress to the animals. Considering all these described concerns we decided against a further in-depth evaluation of HSV-TK *in vivo*.

2.2.2 Assessment of iC9 in an immunocompromised mouse model

Based on the results of the first mouse experiment and the *in vitro* results, we selected iC9 as most promising safeguard mechanism in HBV-specific T cells and further evaluated it *in vivo*. As induction of iC9 and the following specific depletion of iC9-expressing cells works independently of the endogenous immune system, an immunocompromised mouse model was chosen for further investigation. To allow a more excessive S-CAR T cell activation and thus making the testing of iC9 easier the mouse model was optimized using a high-titer HBV infection and higher concentration of T cells. Nearly six weeks after establishing a stable, high-titer HBV infection in Rag2$^{-/-}$IL-2Rgc$^{-/-}$ mice, retrovirally transduced murine CD45.1^{+} T cells that co-expressed iC9 and the S-CAR were administered intraperitoneally. Four and 13 days after T-cell transfer, CID was applied. One part of the mice was sacrificed on day seven when we expected hepatotoxicity to peak (Krebs et al. 2013, Festag et al. 2019) and the other part on day 14 (Figure 2.19A). Like the previous *in vivo* experiment, one group of mice received T cells expressing an unfunctional CAR (SΔ-CAR; same extracellular domain as the S-CAR but different intracellular domains rendering it unfunctional) serving as control (Figure 2.19B).

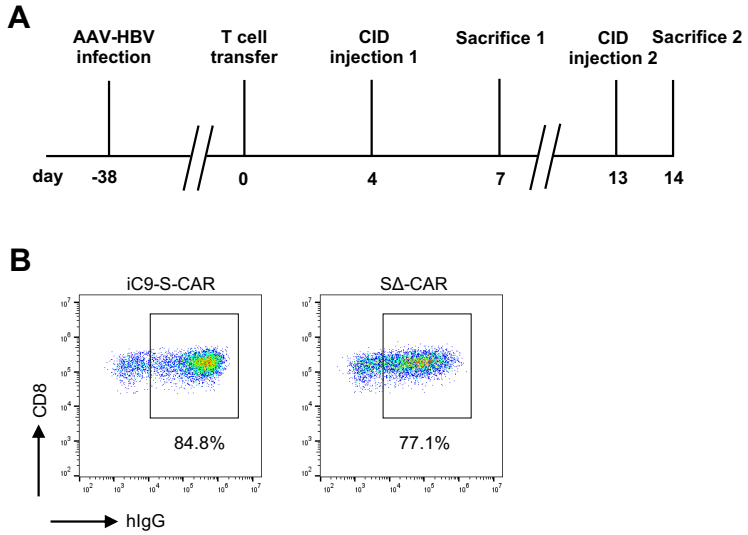

Figure 2.19 Evaluation of iC9-expressing S-CAR T cells in immunodeficient mice

(A) Scheme of the experimental procedure. HBV infection of Rag2$^{-/-}$IL-2Rgc$^{-/-}$ mice was established using an AAV-HBV vector. 1 x 10^{10} viral particles for male and 3 x 10^{10} viral particles for female mice were injected intravenously per mouse. After five weeks (day zero) 2 x 10^{6} SΔ-CAR T cells (n=6) or iC9-S-CAR T cells (n=17) were transferred per mouse. The extracellular domain of the SΔ-CAR is identical to the S-CAR, but it is rendered unfunctional by exchanging its intracellular domains. On day four and 13, CID or a negative control (identical preparation to the respective substance but without the active molecule) was injected intraperitoneally. Nine mice of the iC9-S-CAR group were sacrificed on day seven, the remaining mice were sacrifice a week later (day 14). **(B)** Flow cytometry analysis showing the receptor expression of the retrovirally transduced T cells injected on day zero. (iC9-S-CAR + CID n=8, iC9-S-CAR - CID n=9, SΔ-CAR n=3 per group, n=4 from iC9-S-CAR + CID and n=5 iC9-S-CAR – CID were sacrificed on day seven). Figure was adapted from Klopp et al., (Klopp et al. 2021).

First, we investigated the impact of iC9 induction on adverse effects of adoptive T-cell therapy. The survival analysis in Figure 2.20A shows that between day eight and twelve, all mice of the group that had received S-CAR T cells, but no CID, died, while those mice, in which S-CAR T cells were depleted, survived. No weight loss was however observed prior to death of the animals (Figure 2.20B). Also, on day seven only a moderate liver damage (average ALT level 150 UI/l) was observed in this group (Figure 2.20C), suggesting that death of the animals was probably not caused by a liver-directed but by a general immune reaction. No hepatotoxicity but a weight loss of around 15% by day 14 was observed in the group of mice in which T cells had been depleted (Figure 2.20B, C).

A cytokine release syndrome is a very common and potentially life threatening side effect of adoptive T-cell therapy (Teachey et al. 2013). To assess this potential concern in context of adoptive T-cell therapy against chronic hepatitis B, serum levels of inflammatory cytokines were measured over the course of the experiment. Whereas in mice which received HBV-specific T cells, the cytokines IFN-γ, TNF-α, IL-6, and MCP-1 were slightly increased four days after T-cell transfer, they stayed steady in mice which received SΔ-CAR T cells (Figure 2.20D-G). From day four to day seven, the cytokines IFN-γ, TNF-α, IL-6 continued to rise in the mice in which T cells had not been depleted. However, in mice in which T cells had been depleted, all cytokines returned to initial levels (Fig. 2.20D-G). However, this effect was transient, with cytokine levels rising again seven days after CID administration. The second CID injection led to an IFN-γ and IL-6 reduction within one day (Fig. 2.20D, F), whereas TNF-α and MCP-1 remained at high levels (Fig. 2.20E, G).

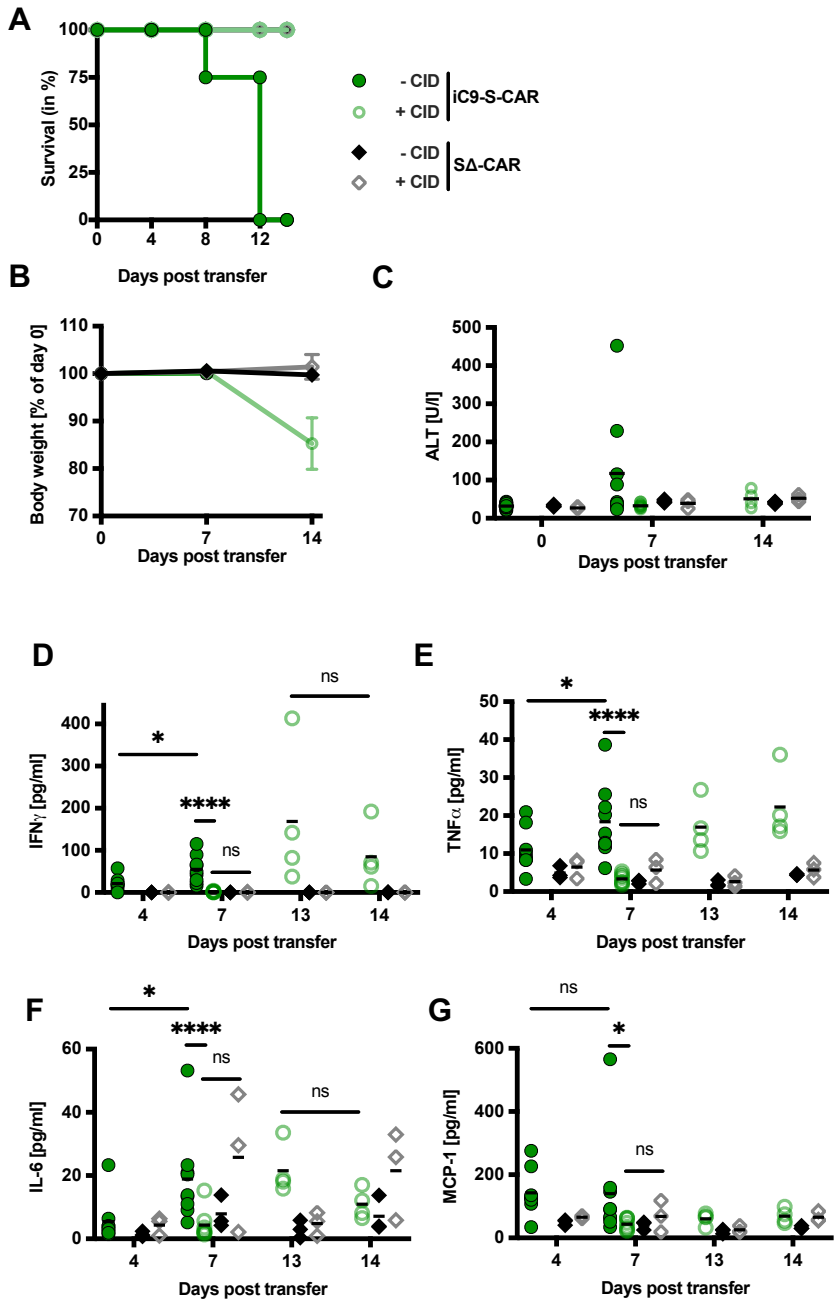

Figure 2.20 Effect of iC9 induction on adverse effects of adoptive T-cell therapy in immunodeficient mice

(A) Survival curve of the mice between day zero (T-cell transfer) and day 14 (sacrifice). **(B)** Course of the body weight in the different groups. Individual weights for each mouse on day zero were set to 100 %. **(C)** Sera of the mice were analyzed for ALT on day zero, seven and 14 after T-cell transfer **(D-G)** Sera of the mice were analyzed for cytokines by cytometric bead array and flow cytometry on day four, seven, 13 and 14 after T-cell. Sera on day four and 13 was isolated just before CID injection. (C) Data points represent individual animals and mean values are indicated. (D-I) Data points represent individual animals and mean values are indicated. (iC9-S-CAR + CID n=8, iC9-S-CAR - CID n=9, SΔ-CAR n=3 per group, n=4 from iC9-S-CAR + CID and n=5 iC9-S-CAR – CID were sacrificed on day seven, Mann-Whitney test: ns not significant, * $p < 0.05$, **** $p < 0.0001$). Figure was adapted from Klopp et al., (Klopp et al. 2021).

Next, we wanted to determine if the depletion of transferred T cells in the blood, the spleen and the liver via iC9 was more pronounced than in the previous, immunocompetent mouse model. To do so mice were sacrificed on day 7 and 14. The congenic marker CD45.1/2 facilitated differentiation between transferred CD45.1$^+$ cells and endogenous CD45.2$^+$ cells immune cells (Figure2.21A, B). Flow cytometry analysis showed that not all transferred CD45.1$^+$ cells were eliminated after CID administration (Figure 2.21A, bottom row). Additional staining for the S-CAR however revealed that mainly T cells with a high S-CAR expression (S-CAR^{hi}) were depleted as they had completely disappeared from the examined blood-, spleen, or liver sample (Figure 2.21B, bottom row). Absolute cell counts revealed that three days after CID injection, the number of transferred T cells in the blood and spleen was reduced by 1.5 log10 and in the liver by 2log10 compared to mice which did not receive CID. The second CID injection on day 13 led to strong cell number reduction in the liver, however not all transferred cells were eliminated (Figure 2.21C).

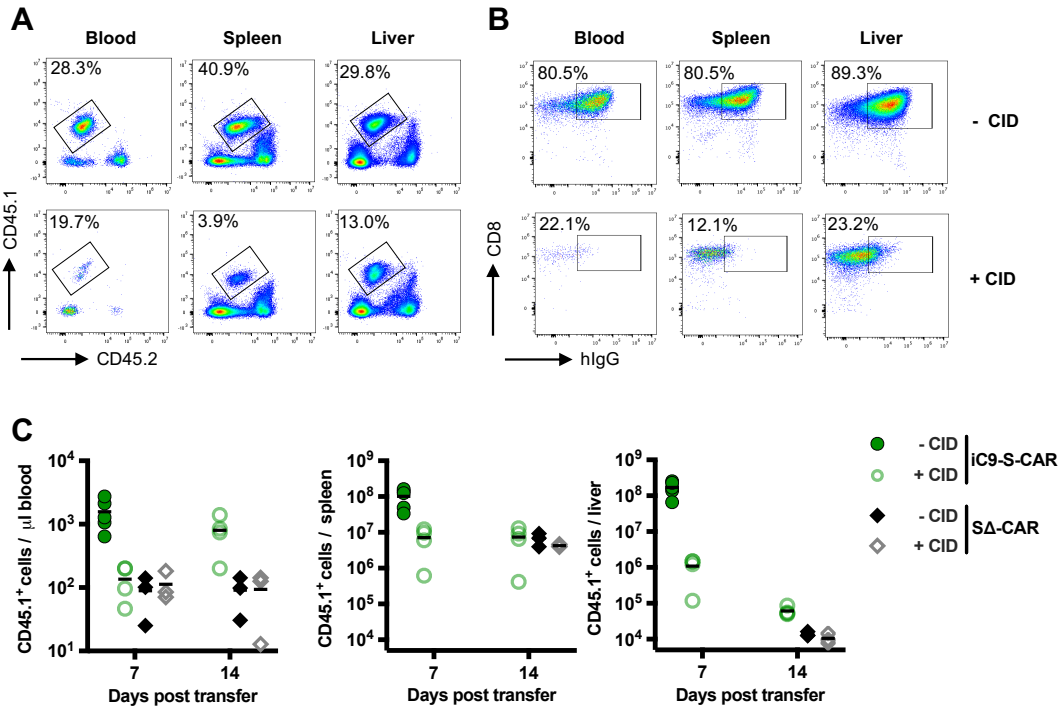

Figure 2.21 Depletion of transduced T cells via iC9 in immunodeficient mice

(A, B) Example of the flow cytometry analysis of transferred T cells isolated from blood, the spleen or the liver on day seven gated on transferred CD45$^+$ T cells (A) or S-CAR expressing transferred cells (B). The upper row shows a mouse which did not get CID and the lower row a mouse which got CID. **(C)** Count of transferred CD45.1$^+$ T cells isolated from the blood, the spleen and the liver on day seven or day 14. Absolute cell counting was accomplished by adding counting beads to the respective flow cytometric sample and the result was extrapolated to the concentration in blood or to the whole organ considering the proportion that was used to isolate splenocytes or LALs. (C) Data points represent individual animals and mean values are indicated (iC9-S-CAR + CID n=8, iC9-S-CAR - CID n=9, SΔ-

CAR n=3 per group, n=4 from iC9-S-CAR + CID and n=5 iC9-S-CAR - CID were sacrificed on day seven). Figure was adapted from Klopp et al., (Klopp et al. 2021).

To determine their *ex-vivo* functionality, the transferred CD45.1$^+$ T cells isolated from the spleen and the liver on day seven or day 14 were cultured overnight on plate-bound HBsAg (specific restimulation), anti-CD3/anti-CD28-antibodies (unspecific restimulation) and on PBS (negative control) and then stained for intracellular cytokine expression (IFN-γ, TNF-α and IL-2, Figure 2.22A). It was observed that on day seven, 60% of the CD45.1$^+$ T cells obtained from the spleen, exhibited HBsAg-specific cytokine production, with IFN-γ being the most prominent (Figure 2.22B). Notably, this expression was significantly reduced in three out of four mice that received CID, which correlates with the observed depletion primarily affecting T cells with a high S-CAR expression (Figure 2.21B). The fact that in the group of mice that received CID, CD45.1$^+$ T cells still secreted cytokines upon unspecific anti-CD3/anti-CD28 stimulation, shows that only the transduced HBV-specific T cells were depleted (Figure 2.22D). After the second CID injection, low HBsAg-specific cytokine production by CD45.1$^+$ T cells extracted from the spleen could still be measured (Figure 2.22E)

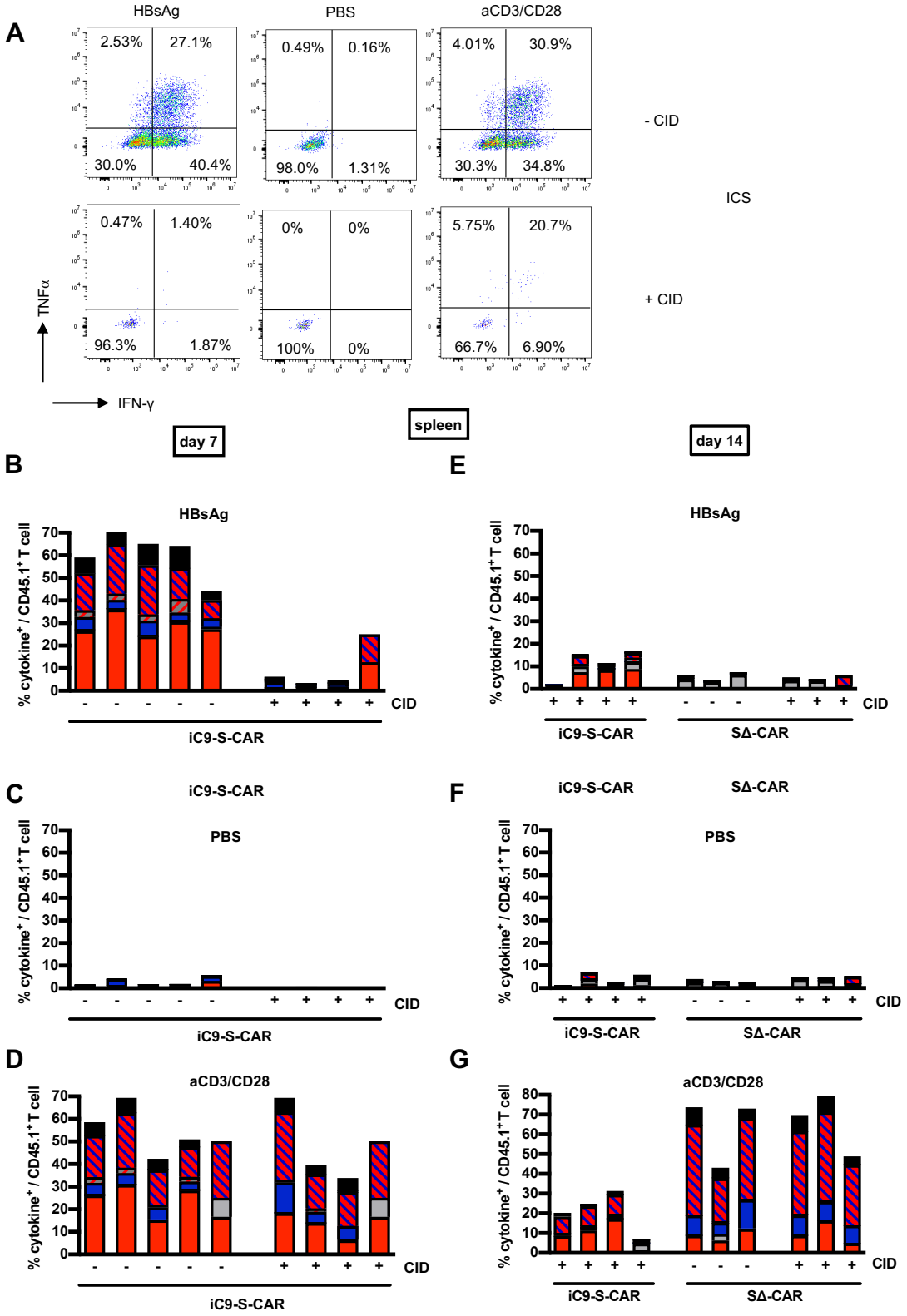

Figure 2.22 *Ex-vivo* functionality of transferred CD45.1$^+$ T cells in the spleen

Isolated splenocytes on day seven or day 14 were cultured overnight on plate-bound HBsAg for specific restimulation, plate-bound anti-CD3/anti-CD28-antibodies for unspecific restimulation and on PBS as negative control to determine the *ex-vivo* functionality of the transferred CD45.1$^+$/CD45.2$^+$ T cells. On

the next day, intracellular cytokine expression (IFN-γ, TNF-α and IL-2) of the cultured cells was determined by flow cytometry **(A)** Exemplary gating strategy of the flow cytometry analysis. The upper row shows a mouse which did not get CID and the lower row a mouse which got CID. Expression of IFN-γ and TNF-α is shown on transferred CD45.1+ T cells. **(B-G)** Intracellular cytokine expression (IFN-γ, TNF-α and IL-2) of the cultured splenocytes as determined by flow cytometry analysis. Each column represents an individual animal. (iC9-S-CAR + CID n=4 and iC9-S-CAR - CID n=5 on day seven, iC9-S-CAR + CID n=4 on day 14, SΔ-CAR n=3 per group). Figure was adapted from Klopp et al., (Klopp et al. 2021).

Interestingly, the functional profile of LALs differed from that of splenocytes in this experiment. Despite the high expression of S-CAR in the non-depleted group (Figure 2.21B), only an average of 15% of cells secreted cytokines upon restimulation with HBsAg (Figure 2.23A). CID administration successfully depleted HBV-specific cells in half of the mice, and even with a subsequent CID injection, still a small number of HBV-specific T cells remained detectable in the liver (Figure 2.23D).

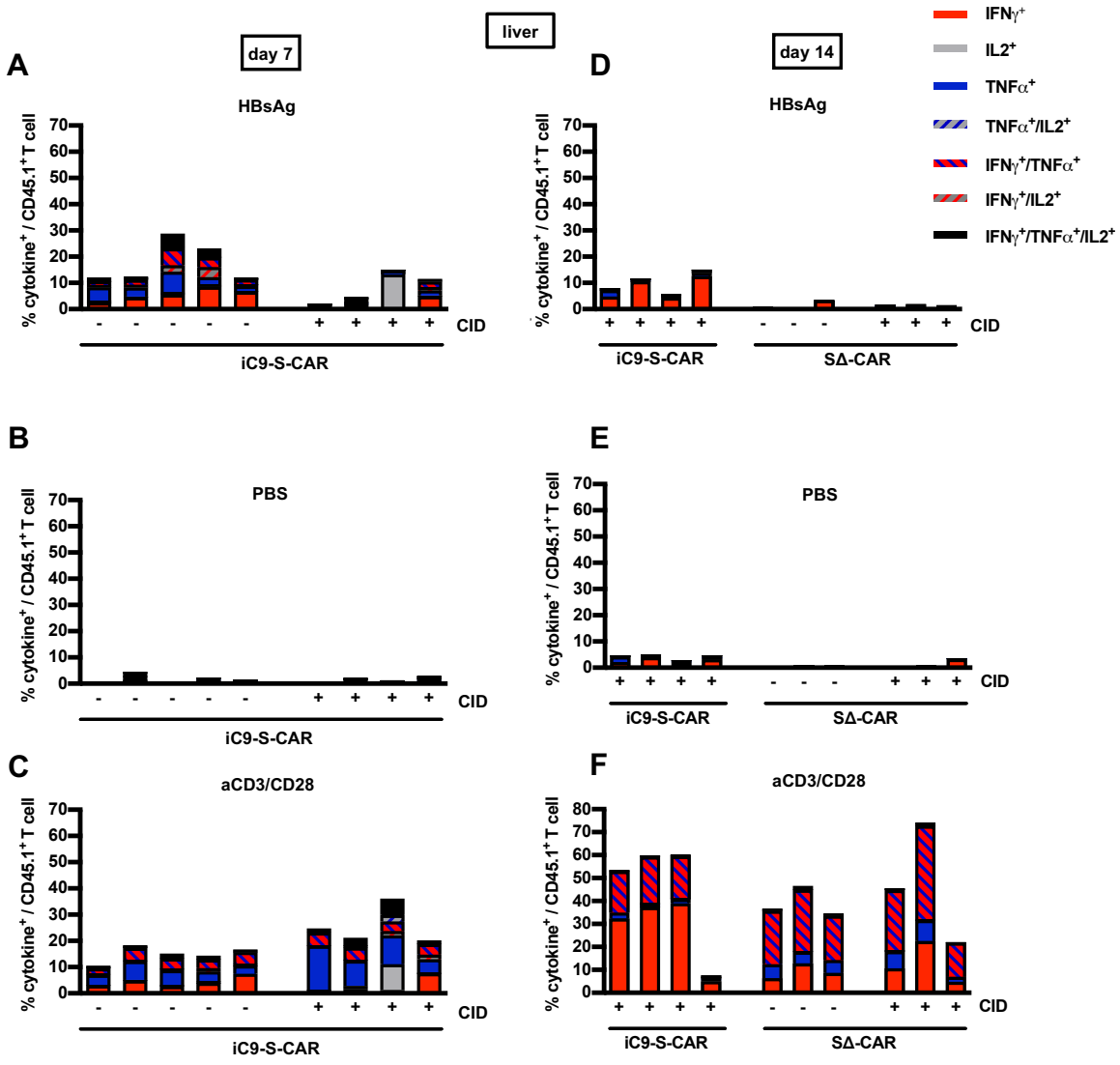

Figure 2.23 *Ex-vivo* functionality of transferred CD45.1$^+$ T cells in the liver

Isolated LALs on day seven or day 14 were cultured overnight on plate-bound HBsAg, anti-CD3/anti-CD28-antibodies or PBS for *ex-vivo* functionality assessment. On the next day, intracellular cytokine expression (IFN-γ, TNF-α and IL-2) of the cultured cells was determined by flow cytometry. **(A-F)** Intracellular cytokine expression (IFN-γ, TNF-α and IL-2) of the cultured liver-derived T cells as determined by flow cytometry analysis. Each column represents an individual animal. Figure was adapted from Klopp et al., (Klopp et al. 2021).

In the previous figures we showed that iC9 induction led to an efficient depletion of transferred T cells and that this went along with a reduction of hepatotoxicity and cytokine secretion. Based on these findings, we wondered to which extent iC9 induction would thus hamper the therapeutic, antiviral effect of adoptive T-cell therapy. Immunohistochemical HBcAg staining of liver tissue showed that in mice which received CID, immune cells no longer accumulated near the central veins (Figure 2.24A). At the same time, the number of HBcAg$^+$ hepatocytes was similar to the control groups (Figure 2.24A, B). Immunohistochemical HBsAg staining of liver tissue appeared to very diffuse and blurry so no reliable quantification of HBsAg$^+$ hepatocytes could be made. However, similar to the HBcAg stainigs, immunohistochemical HBsAg stainings of liver sections revealed a reduced accumulation of T cells in proximity of the central vein after CID injection (Figure 2.24C). Furthemore, the measurement of HBsAg over the course of the experiment showed that induction of the safeguard mechanism completely stopped the effect of S-CAR T cells on circulating HBsAg between day four and day seven (Figure 2.24D). However, the remaining S-CAR T cells that had not been depleted upon the first CID injection still led to a reduction of HBsAg by 50% between day seven and day 14 (Figure 2.24D). HBeAg levels did not change over the course of the experiment in the different groups (Figure 2.24F).

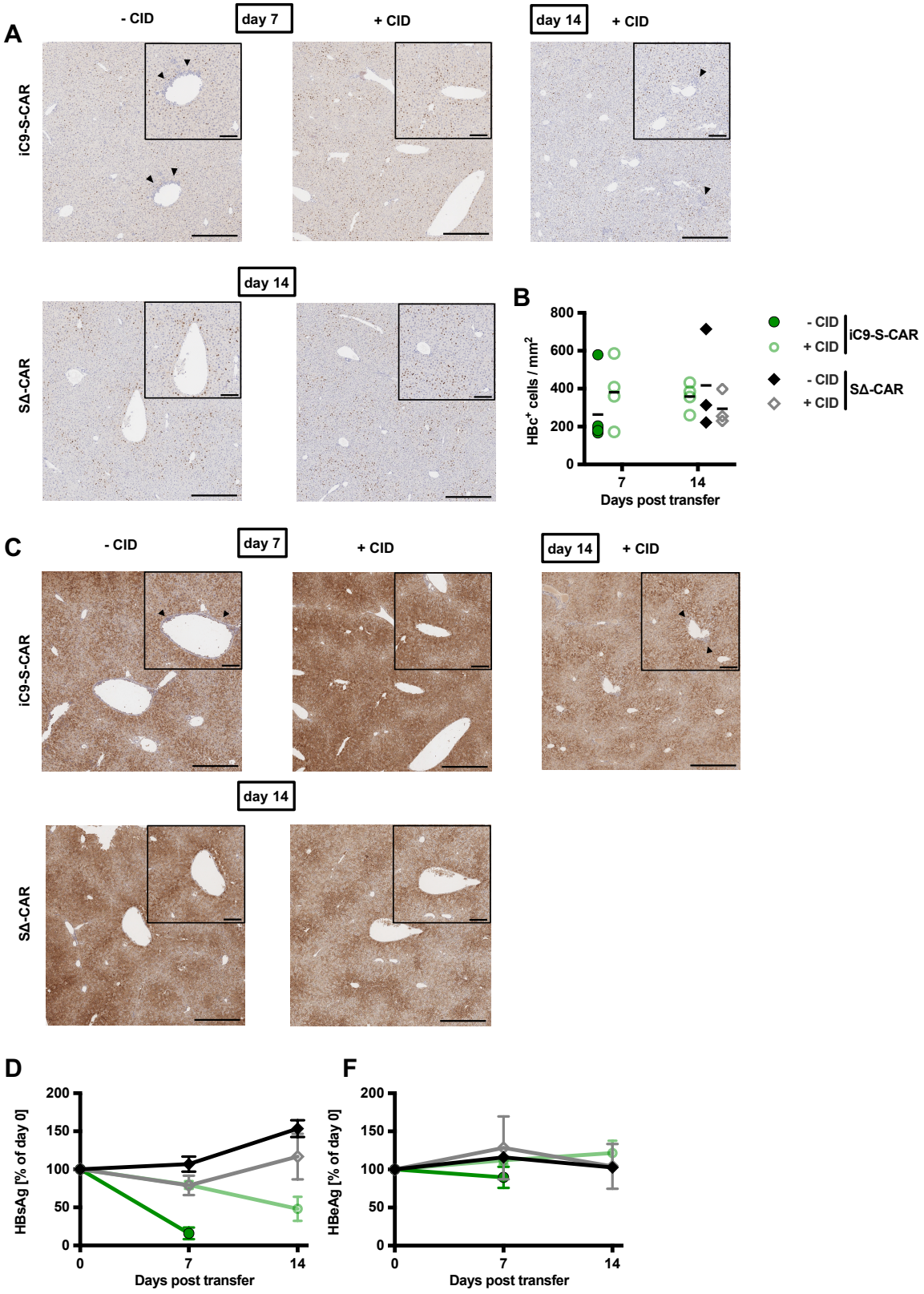

Figure 2.24 Antiviral effect of iC9 expressing S-CAR T cells in immunodeficient mice

(A) Representative (1 mouse per group) immunohistochemical HBcAg stainings of liver sections. Scale bars indicate 200 µm in the overview and 80 µm in the inlay of the central vein. Arrows point on lymphocyte infiltrates. **(B)** Quantification of $HBcAg^+$ cells per mm^2 including all the mice from all the different groups. **(C)** Representative (1 mouse per group) immunohistochemical HBsAg stainings of liver

sections. Scale bars indicate 200 µm in the overview and 80 µm in the inlay of the central vein. Arrows point on lymphocyte infiltrates. **(D, F)** Sera of the mice were analyzed for HBsAg, HBeAg by diagnostic assays on day zero, seven and 14 after T-cell transfer. (B) Data points represent individual animals and mean values are indicated. (D, F) Data are given as mean values +/- SD. (iC9-S-CAR + CID n=4 and iC9-S-CAR - CID n=5 on day seven, iC9-S-CAR + CID n=4 on day 14, SΔ-CAR n=3 per group). Figure was adapted from Klopp et al., (Klopp et al. 2021).

Taken all these findings together, we concluded that iC9 induction in immunocompromised mice led to a very strong yet not complete depletion of iC9-S-CAR T cells and thus prevented excessive hepatotoxicity and inflammatory cytokine production. All this came at the cost of the therapeutic, antiviral effect of iC9-S-CAR T cells.

2.2.3 Kinetics of depletion via iC9 in an immunocompromised mouse model

In vitro, we saw that killing by iC9-expressing HBV-specific T cells could be stopped within one hour after CID administration. We next wanted to investigate if induction of iC9 would also be that quick *in vivo.* To this end, an HBV infection was first established in $Rag2^{-/-}$IL-$2Rgc^{-/-}$ mice. Ten weeks after the infection, murine $CD45.1^{+}$ T cells co-expressing iC9 and the S-CAR were injected. CID was administered between day six and day seven and mice were sacrificed 1 hour, 6 hours or 16 hours after the CID injection. A control group received no CID (Figure 2.25).

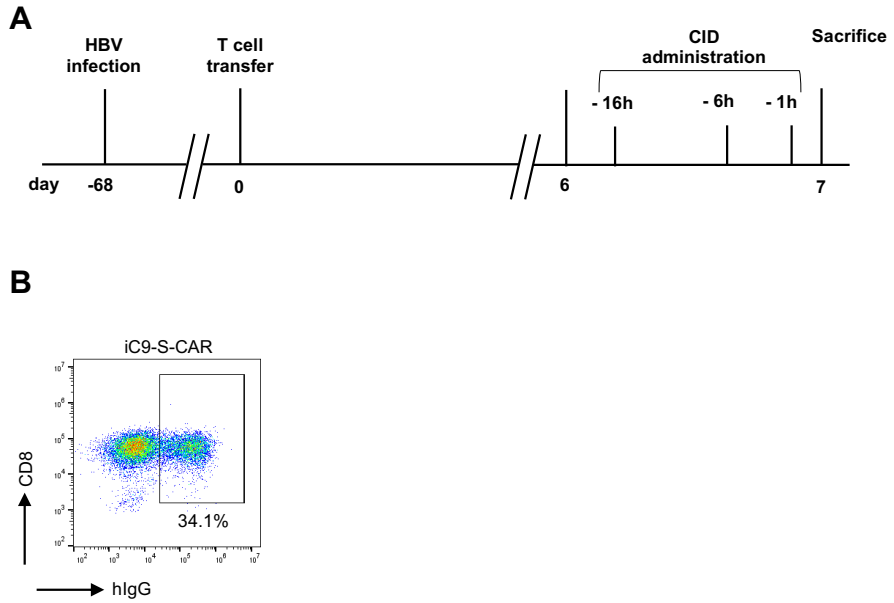

Figure 2.25 Kinetics of S-CAR T-cell depletion via iC9 in immunodeficient mice

(A) Scheme of the experimental procedure. HBV infection of Rag2$^{-/-}$IL-2Rgc$^{-/-}$ mice was established using an AAV-HBV vector. 1 x 10^{10} viral particles for male and 3 x 10^{10} viral particles for female mice were injected intravenously per mouse. After ten weeks (day zero) 2 x 10^{6} CD45.1^{+} iC9-S-CAR T cells (n=14) were transferred per mouse. Between day six and seven, CID (n=10) or a negative control (n=4) (identical preparation to the respective substance but without the active molecule) was injected intraperitoneally. The mice were sacrificed on day seven but at different timepoints after CID administration [1 hour (n = 3), 6 hours (n = 3) and 16 hours (n = 4)]. **(B)** Flow cytometry analysis showing the receptor expression of the retrovirally transduced T cells injected on day zero. Figure was adapted from Klopp et al., (Klopp et al. 2021).

Quantification of transferred cell numbers in blood revealed that already one hour after CID administration transferred cells had been reduced by 1log$_{10}$. This reduction was comparable to the one observed six and 16 hours after iC9 induction (Figure 2.26A). In the spleen and the liver however a strong reduction of transferred cells was only observed six and 16 hours after iC9 induction. One hour after iC9 induction the depletion rate in both organs was only around 50% compared to the ones observed six and 16 hours after iC9 induction (Figure 2.26B, C). Functionality assessment of the transferred T cells isolated from the spleen showed that already one hour after iC9 induction, transferred T cells could efficiently be reduced from 30 % to 5 % of cytokine secreting cells (Figure 2.26D). The same held true for the liver, where one hour after iC9 induction, the rate of cytokine secreting cells was reduced from 40 % to 10 % (Figure 2.26E). Interestingly when iC9 was induced 16 hours before sacrifice the rate of cytokine secreting cells in the liver was higher than when iC9 was induced one or six hours before sacrifice (Figure 2.26E). A possible reason could be that the T cells that had not been depleted upon CID administration started to expand again. In fact the cell cycle of activated T cells is around six hours (Yoon et al. 2010) and might thus have had an impact on the retrieved

T-cell numbers. Based on these findings we concluded that, similar to the *in vitro* results, T-cell depletion via *iC9* was very fast and happened within one hour.

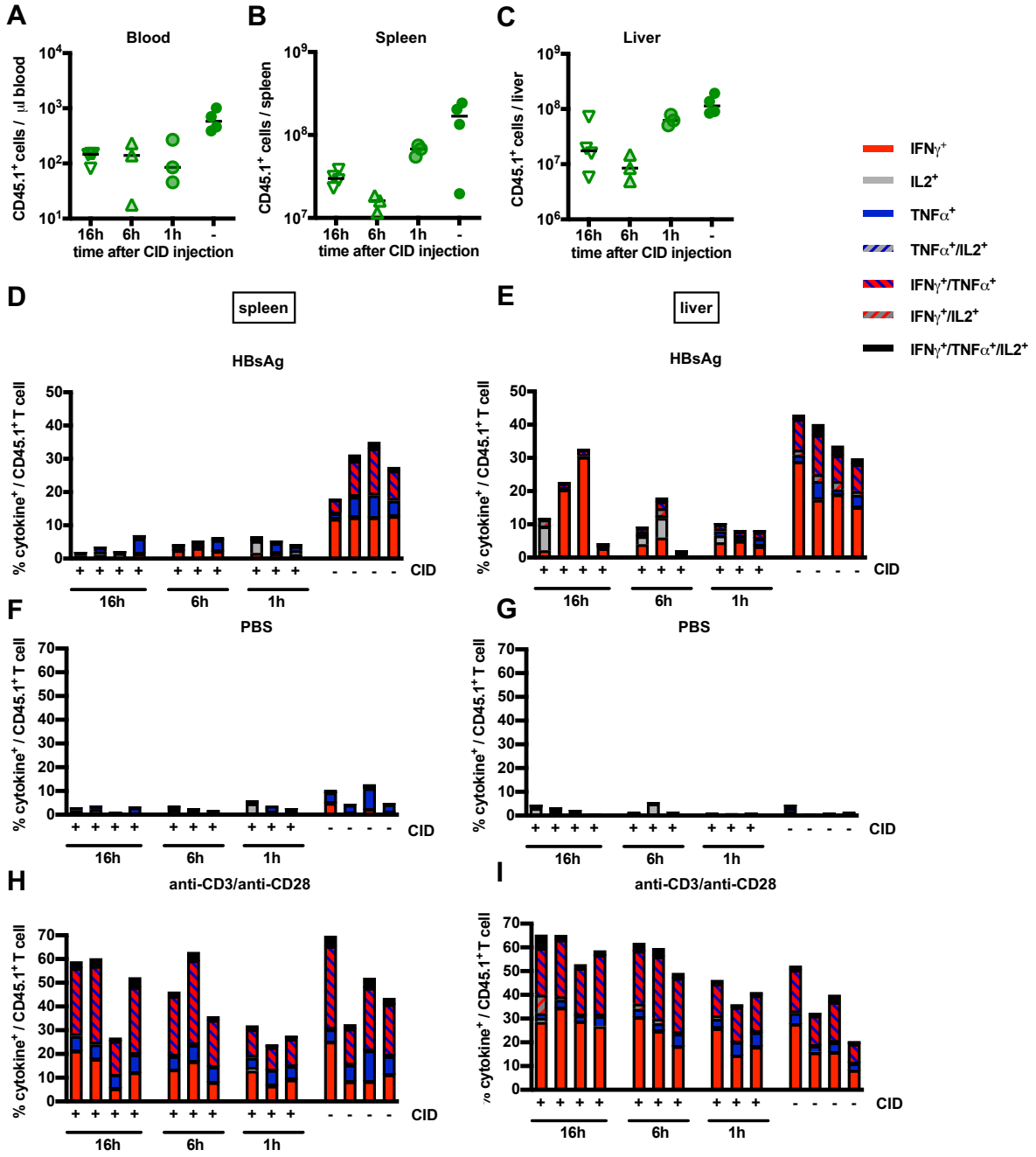

Figure 2.26 Efficiency of iC9-mediated T-cell depletion at different timepoints after CID administration

(A, B, C) Count of transferred CD45.1$^+$ T cells isolated from the blood, the spleen and the liver on different timepoints after CID administration. Absolute cell counting was accomplished by adding counting beads to the respective flow cytometric sample and the result was extrapolated to the concentration in blood or to the whole organ considering the proportion that was used to isolate splenocytes or LALs. **(D-I)** To determine their *ex-vivo* functionality, transferred CD45.1$^+$ T cells isolated at different timepoints from the spleen and the liver on day seven were cultured overnight on plate-bound HBsAg for specific restimulation, plate-bound anti-CD3/anti-CD28-antibodies for unspecific restimulation and on PBS as negative control. On the next day, intracellular cytokine expression (IFN-γ, TNF-α and IL-2) of the cultured cells was determined by flow. Each column represents an individual

animal. (A, B, C) Data points represent individual animals and mean values are indicated. (D-I) Each column represents an individual animal. (1 hour n = 3, 6 hours n = 3, 16 hours n = 4, no CID n =4). Figure was adapted from Klopp et al., (Klopp et al. 2021).

In the previous mouse experiment, we saw that S-CAR T-cell depletion via iC9 prevented excessive liver damage and cytokine production within three days. As it is very important to counteract side effects as quickly as possible and given the successful T cell depletion via iC9 within hours (Figure 2.26), we next asked how quickly iC9 induction could prevent toxicity from S-CAR T cells. To this end, ALT levels were measured on day zero (day of T-cell transfer) and then shortly before CID administration and at the time of sacrifice (i.e. one, six or 16 hours after CID administration). A significant difference between ALT levels measured before and after CID injection was not observed (Figure 2.27A). Considering the cytokine production of transferred T cells, only IFNγ was reduced by 1.5x in the mice that were sacrificed one hour after iC9 induction (Figure 2.27B). However, in this particular group, cytokine levels of TNFα, IL-6 and MCP were even higher after CID injection than before (Figure 2.27C, D, E). A possible reason could be the stress caused to the animals by the injection procedure leading to release of inflammatory cytokines. In the other groups a significant difference between cytokine production measured before and after CID injection was not observed (Figure 2.27B-E).

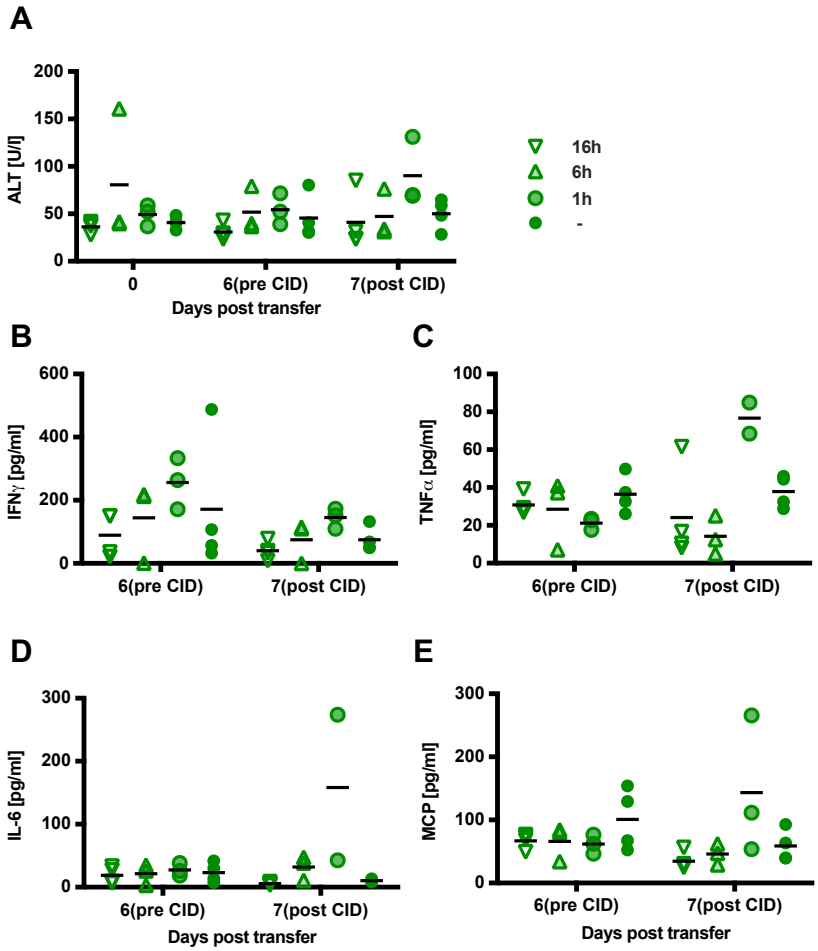

Figure 2.27 Effect of iC9 induction on adverse effects of adoptive T-cell therapy at different timepoints after CID administration

(A) Sera of the mice were analyzed for ALT just before CID administration and at different timepoints after CID administration **(B-E)** Sera of the mice were analyzed for cytokines by cytometric bead array and flow cytometry just before CID administration and at different timepoints after CID administration (A) Data points represent individual animals and mean values are indicated. (D-I) Data points represent individual animals and mean values are indicated. (1 hour n = 3, 6 hours n = 3, 16 hours n = 4, no CID n =4) Figure was adapted from Klopp et al., (Klopp et al. 2021).

2.2.4 Conclusion

In vitro, HBV-specific T cells co-expressing HSV-TK or iC9 showed promising results, showing efficient killing of HBV^+ target cells and the killing by these being reduced or stopped in presence of the CID or GCV, respectively. *In vivo*, induction of cell death via iC9 led to a strong and fast but not complete depletion of transduced T cells. It prevented cytotoxicity but on the costs of the antiviral effect. Considering the generated *in vitro* and in *vivo* data, we think that co-expressing iC9 in HBV-specific T cells is a very interesting and promising means to reverse possible side effects of adoptive T cell therapy for CHB and could give supplementary assurance to both the physician and the patient in a clinical setting.

3 Discussion

3.1 Safeguard mechanisms in HBV-specific T cells

Even though adoptive T-cell therapy has experienced great success in recent years, possible side effects are very concerning and still limit their use. They include several on and off-target effects as well as side effects related to the excessive secretion of cytokines like the cytokine release syndrome or the immune effector cell-Associated Neurotoxicity Syndrome (see section 1.2.4.). Based on these concerns, several strategies have been developed to increase the safety of adoptive T-cell therapy, for example the inclusion of suicides genes which allow the selective elimination of adoptively transferred cells (Jones et al. 2014).

In this thesis, the effectiveness of different safeguard molecules was investigated in HBV-specific T cells. To do so, the safeguard molecules were first cloned into a retroviral vector encoding for HBV-specific receptors. Retroviral vectors allow a stable integration of the transgene in the genome of the host cell. However, this integration only takes place in dividing cells and in random positions of the genome (Trono 2003), increasing the risk of insertional mutagenesis and thus the oncogenic transformation of the cell (Li et al. 2002, Davé et al. 2004). Another possibility of transducing T cells, is the use of lentiviral vectors, allowing the transduction of non-dividing cells and at a lower risk of insertional mutagenesis. Cattoglio et al. have in fact demonstrated that recurrent insertion sites of retroviruses are very often located in proto-oncogenes or growth-controlling genes while this was not observed for lentiviral vectors (Cattoglio et al. 2007). The production of HBV-specific T cells using lentiviral vectors is currently being investigated in our lab and showed promising first results (Antje Malo, unpublished data). In our study, the newly cloned retroviral vectors contained one of three safeguard molecules linked via a 2A peptide, which should guarantee equimolar expression of both proteins, either to the S-CAR, TCR 4G (S-specific) or TCR 6K (core-specific). Co-expression of the safeguard molecule partly reduced receptor expression. The slight diminished receptor expression could be explained to the decreased protein expression of a protein on the second gene position (after the 2A sequence) on a bi-cistronic vector (Liu et al. 2017). The expression rate of the safeguard molecules was not determined but one can assume it to be at least as high as the expression rate of the receptors because their sequence is placed prior to the 2A- and receptor sequence.

The most commonly used and scientifically examined safeguard mechanisms currently used for adoptive T-cell therapy in a clinical setting are iC9 (Straathof et al. 2005, Gargett et al. 2014), HSV-TK (Bonini et al. 1997, Greco et al. 2015) and the antibody-based, truncated EGFR (EGFRt) (Wang et al. 2011). New safeguard mechanisms are constantly being developed, for example RQR8 which combines both epitopes from CD20 and from CD34. This allows, on one hand the selection and tracking of RQR8-transduced T cells with an anti-CD34 antibody and on the other hand the specific deletion of the T cells after rituximab administration (Philip et al. 2014). In this thesis, we aimed to select the most convenient safeguard mechanisms in context of adoptive T-cell therapy against chronic hepatitis B. As Hattoum et al. showed that expression of EGFR occurred on regenerative clusters of hepatocytes, we excluded EGFRt as possible safeguard mechanism and selected iC9, RQR8 and HSV-TK for further evaluation.

3.2 Comparison of safeguard mechanisms *in vitro*

To determine the most suitable safeguard mechanism in the context of an HBV-specific T-cell therapy, several *in vitro* experiments were performed. These included functionality assessments of both the HBV-specific receptors and the safeguard molecules in *in vitro* co-culture experiments. The retrovirally transduced T cells were co-cultured with HBV^+ Hep G2.2.15 or S-protein expressing Huh7S target cells and the viability of the target cell line was measured using real-time cytotoxicity assays. The constant monitoring of the viability of the target cells via the real-time cytotoxicity assays allowed us to exactly induce the different safeguard mechanisms when the desired amount of target cells (i.e. 40%) was killed and thus made the comparison of the safeguard mechanisms more equal.

In vitro, the functionality of HBV-specific T cells was not altered when a safeguard mechanism was co-expressed. Interestingly, target cells were more efficiently killed by T cells expressing an HBV-specific TCR (4G or 6K) than by those expressing an S-CAR. Very efficient killing by S-CAR expressing T cells was mostly observed on Huh7S target cells. This cell line expresses the S protein from a transgene and has a higher density of S protein on the cell surface than HepG2.2.15 cells (Antje Malo, personal communication), HBV-infected cells (HepG2NTCP) or physiologically infected hepatocytes in a clinical situation (Lily Zhao, unpublished data). The difference between the killing efficiency of S-CAR T cells in comparison to TCR-expressing T cells could be explained by the difference of the sensitivity of both receptors. Although, the physiological affinity range of TCRs (10^4 -10^6 M^{-1}) is lower than the one of a CAR (10^6 – 10^9 M^{-1}), TCRs are more sensitive (Harris et al. 2016). This increased sensitivity despite the lower

affinity is believed to be partly due to serial triggering of TCRs. In fact, due to the fast off-rate of TCRs (i.e., lower affinity), a single MHC molecule presenting a certain peptide can bind serially to many TCRs allowing the activation of the T cell by just one single antigen (Valitutti et al. 1995, Huang et al. 2013).

3.2.1 RQR8

RQR8 being an antibody-based safeguard mechanism, it was the most difficult one to reliably test *in vitro* as it induces cell-death via CDC or ADCC which is technically very difficult to realize. Also, CDC and ADCC were tested separately which only partly mimics the clinical setting in patients where CDC and ADCC work simultaneously. While in our *in vitro* setting the induction of RQR8 through ADCC led to a two-fold reduction of IFN-γ secretion by HBV-specific T cells, CDC was not initiated. Due to the complexity and costs of the assay, the assessment was only done exemplarily with RQR8-S-CAR T cells and just performed once. As the way of action and thus the technical set up for the *in vitro* assessment of RQR8 was very different from the one used to test HSV-TK or iC9, a direct comparison of RQR8 with the two other safeguard mechanism was not realizable. Beside the technical difficulties, rituximab used to induce RQR8 leads to on-target effects as CD20 is also expressed on B cells. This could be very problematic for patients that are infected with hepatitis B virus as B cells are known to play an important role in the control of HBV (Burton et al. 2018) which prompted us to set our focus on HSV-TK or iC9, respectively.

3.2.2 HSV-TK

In the performed *in vitro* experiments, killing by HBV-specific T cells was efficiently stopped within one hour after HSV-TK had been induced, thus being comparable to the induction of iC9. This however was in contrast with other studies where induction of HSV-TK took longer than of iC9 (Marin et al. 2012). A possible reason why in our setting the time of induction of HSV-TK and iC9 was comparable, is that transduced T cells were co-cultured with HBV^+ target cells and were thus in a very activate state making them more sensitive to GCV-incorporation into the DNA. Despite proving to be very effective in our *in vitro* experiments, HSV-TK is described as being immunogenic and thus limiting the persistence of $HSV\text{-}TK^+$ T cells *(Berger et al. 2006)*. Furthermore, several side and bystander effects of HSV-TK have been described (Matsumoto et al. 2015) and the fact that GCV is also used for the treatment of cytomegalovirus restricts its use in patients with a cytomegalovirus infection that had received HSV-TK modified T cells. Also, in a first *in vivo* experiment destined to compare the different safeguard mechanisms, the injection of the very alkaline GCV solution proved to be technically difficult

and caused distress to the animals. Considering all these described concerns we decided against a further in-depth evaluation of HSV-TK *in vivo*.

3.2.3 iC9

Similar to HSV-TK, suicide of HBV-specific T cells via iC9 *in vitro* halted cytotoxicity within less than one hour. Even though, several studies showed that iC9-induction led to a strong but not complete elimination of the engineered T cells (Hoyos et al. 2010, Budde et al. 2013, Warda et al. 2019) the cytotoxic effect of HBV-specific T cells was halted during the entire co-culture experiments. A possible reason could be that iC9 is known to be most effective in activated T cells and that the remaining T-cells that had not been depleted via iC9 were mostly inactive and thus had no cytotoxic effect (Budde et al. 2013). The clear advantage of iC9 in comparison to HSV-TK is that it only contains human-derived domains making it much less immunogenic. Furthermore, its activation being independent of the cell cycle, iC9 has proven to be highly effective and very fast in both preclinical and clinical studies (Tey et al. 2007, Di Stasi et al. 2011). Also, CID used to induce iC9 is very safe (Iuliucci et al. 2001) and biologically inert. All this prompted us to furth evaluate iC9 in different *in vivo* models.

3.3 *in vivo* assessment of iC9

The fist *in vivo* experiment with the idea of comparing the different safeguard mechanisms was performed in an immunocompetent mouse model. Previous experiments in our lab showed that a major reason for the transient antiviral effect in HBV-infected mice, was an immune response against the human-derived domains of the S-CAR molecule (Festag et al. 2019). Also, we assumed that this immune response could even be enhanced by the human-derived domains of the safeguard molecules and thus decided to first tolerize the mice against the allogenic domains of the S-CAR and the safeguard mechanisms similar to previous experiments performed in our lab (Festag et al. 2019). Due to the complexity of this mouse model and the fact that based on the previous in vitro and in vivo experiments we selected iC9 (working independently of the endogenous immune system) as most convenient safeguard system, an immunodeficient mouse model was chosen for further evaluation of iC9 *in vivo*. In this mouse model, all mice which received S-CAR T cells, but no CID died between day eight and 14. Previous experiments in our lab showed that the transfer of S-CAR T cells into HBV-infected mice only led to mild and transient hepatotoxicity while steadily mitigating the viral load. Here however the mouse model was optimized in order to allow a more excessive S-CAR T cell activation making the testing of iC9 easier. In fact, the transferred T cells carried a codon-optimized S-CAR with a natural IgG1-spacer which can bind to Fc-receptors of other

cells and thus lead to unwanted off-target effects in contrast to S-CAR with an immune-silenced IgG1-spacer (Hombach et al. 2010). Also, compared to the non-codon optimized S-CAR, the S-CAR used here shows a higher expression rate and leads to a much stronger T-cell activation (unpublished data). Due to the high-titer HBV infection of the mice together with the above-mentioned elements, the transferred T cells rapidly expanded, leading to a very high number of strongly and systemically activated T cells, which probably caused the death of these animals. On the other side however, these high numbers of T cells allowed us to better quantify the effect that iC9 induction had on the absolute T-cell numbers. In fact, iC9 expressing S-CAR-T cells were reduced by up to $3\log_{10}$ after injection of CID at day four in comparison to mice in which suicide of HBV-specific T cells had not been induced. Liver damage and excessive inflammatory cytokine production could be prevented but at cost of the antiviral effect. Although the induction of iC9 led to a strong elimination of engineered T cells (90% in the blood and spleen, 99% in the liver), the elimination was not complete. This was in line with other studies performed in mice (Hoyos et al. 2010, Budde et al. 2013, Warda et al. 2019), macaques (Barese et al. 2015) and men (Zhou et al. 2015, Zhang et al. 2019). Budde et al. showed for example that iC9 needs to be expressed above a certain threshold level to be efficient (Budde et al. 2013). They furthermore showed that in T cells that were not activated, iC9 was less effective, suggesting that activation of the respective cell had a positive impact on the transgene expression. This would also explain why in our setting T-cell depletion was most effective in the liver, where the S-CAR T cells faced their target. Similar results were observed by Di Stasi et al. who could however show that the cells that survived the iC9 mediated deletion *in vivo*, could be reactivated *in vitro* and be deleted after a new exposure to the CID (Di Stasi et al. 2011, Zhang et al. 2019). Another possible reason for the incomplete elimination of iC9-expressing T cells was postulated by Zhou et al. who saw an elevated resistance of virus-specific T cells to apoptotic signals generated by iC9 (Zhou et al. 2015). In this context, the co-administration of CID with an anti-apoptotic small molecule inhibitor led to a much stronger depletion of iC9-expressing cells (Minagawa et al. 2016). Especially the anti-apoptotic molecule B-cell lymphoma 2 (Bcl-2) seemed to be upregulated in iC9 resistant cells (Barese et al. 2015). Schuch et al. found that HBV polymerase-specific T cells express far less Bcl-2 than HBV core-specific T cells (Schuch et al. 2019). Based on these findings one could assume that in our setting polymerase-specific T cells were predominantly active in the liver as they were more sensitive towards CID than core-specific T cells with higher Bcl-2 expression that due to circulating HBeAg were predominantly to be found in the blood and the spleen. Other studies have demonstrated that although iC9 induction did not lead to complete elimination of transferred T cells, the remaining cells did not continue to proliferate and remained at low levels (Hoyos et al. 2010, Diaconu et al. 2017). In our experiment however, iC9-S-CAR T cells still seemed to be active after the first CID injection as a HBsAg drop was

observed between day seven and day 14 as well as loss of body weight and an increased production of inflammatory cytokines. Furthermore, we observed that the number of S-CAR T-cells in the spleen and the liver was superior when CID was administered 16 hours before sacrifice compared to when it was administered six hours before sacrifice. Probably by using a syngeneic mouse model in which the injected murine T cells are in constant interaction with the murine tissue, the remaining T cells started proliferating again. This is in contrast to other studies using xenograft mouse models where iC9-expressing T cells lacked of stimulus after being depleted and thus remained at low levels (Hoyos et al. 2010).

3.4 S-CAR T-cell therapy and its limiting factors

Considering the antiviral effect of the adoptively transferred S-CAR T cells in HBV-infected mice, in all our *in vivo* experiments we observed a decrease of serum HBsAg while serum HBeAg remained stable. The reason for this fast drop of HBsAg in comparison to HBeAg, could be that soluble HBsAg can be found in the serum of infected mice and that this circulating HBsAg can be bound by S-CAR T cells leading to a decrease of free, measurable HBsAg. Previous experiments in our lab showed that a decline of HBeAg in AAV-HBV-infected $Rag2^{-/-}$IL-$2Rgc^{-/-}$ can be detected ten days after adoptive T cell transfer of S-CAR T cells (Julia Hasreiter, unpublished data). As $Rag2^{-/-}$IL-$2Rgc^{-/-}$ mice lack B cells, the decline of HBeAg is a strong indicator for the direct antiviral effect of adoptively transferred S-CAR T cells, as it cannot be explained by the intervention of neutralizing antibodies masking the serum antigen. However, although S-CAR T cells were present in very high numbers in the blood, spleen and the liver, HBV^{+} hepatocytes could still be detected in the liver displaying that S-CAR T cell therapy failed to cure the HBV infection. One possible reason could be the short time period of seven days between transfer of the cells and sacrifice of the mice. However, a similar experiment showed that HBV^{+} hepatocytes remained even after 140 days of treatment (Marvin Festag, unpublished data). Another possible reason could be the inhibition of local immune cell activity through immune checkpoints. In fact, several studies showed an improved CAR activation when simultaneously targeting immune checkpoints (John et al. 2013, Moon et al. 2014). Experiments in our lab however with PD-1- or IL-10-deficient mice showed no influence of both immuno-regulatory mechanisms on the function of S-CAR T cells (Marvin Festag, unpublished data). The implication of further inhibitory checkpoint molecules or other mechanisms limiting the therapeutic effect of S-CAR T cells still needs to be determined. As previously mentioned, CARs are less sensitive than TCRs thus needing a higher antigen density to be activated. The S-expression on the hepatocytes of AAV-HBV infected mice might not be sufficient to lead to an activation of S-CAR T cells and thus limiting the antiviral effect. Another factor impacting the sensitivity of the S-CAR is the binding affinity of its C8 scFv

component to the S-protein which differs between the different HBV geno- and serotypes. Results from our lab showed that the affinity of C8 scFv is lower for Genotype D, serotype ayw than for other variants (Antje Malo, unpublished data), still this genotype is used in our AAV-HBV mouse model.

By using a syngeneic mouse model where the injected murine T cells are in constant interaction with the murine tissue of the host, we developed a mouse model which to a certain degree mimics the clinical setting encountered in human beings. However, the mice we used were lacking T, B, and NK cells and thus we were not able to investigate the interaction between the transferred T cells with the endogenous immune system which often plays a key role in the clinical manifestation of T-cell therapy related side effects such as a cytokine release syndrome (Lee et al. 2014).

3.5 Safety of T-cell therapy: current and upcoming approaches

While the specific deletion of adoptively transferred T cells co-expressing safeguard molecules has shown promising results in preclinical and clinical studies, other strategies have been developed the safety of adoptively transferred T cells. For example, a concern of adoptive T-cell therapy is that some antigens that are targeted by adoptively transferred T cells, are also being expressed on healthy tissues leading to on target, off tumor effects. Subviral HBV particles for example also bind to non-infected hepatocytes (Glebe et al. 2005), which could lead to killing of healthy cells by S-CAR T cells and thus induce severe liver damage. T cells can be genetically engineered to recognize two or more tumor antigens in order to better discriminate healthy tissues from tumor tissues. One example is the transduction of T cells with two CARs with distinct specificities and either an activation or co-stimulation endodomain. These T cells are only being activated when both antigens are being bound by the two CARs (Wilkie et al. 2012, Kloss et al. 2013). Another approach includes TanCARs which express two variable domains capable of recognizing two different antigens on the same cell, thus increasing its specificity (Hegde et al. 2016). Fedorov et al. have developed PD-1- and CTLA-4-based antigen specific inhibitory CARs (iCARS) to protect the off-target issue (Fedorov et al. 2013). Another way to counteract unwanted side effects in immunotherapy with CAR T cells is the tyrosine kinase inhibitor dasatinib which was shown to reversibly inhibit CAR-mediated T cell activation (Mestermann et al. 2019).

Currently, acute toxicities are mostly addressed with pharmacological immunosuppression. This includes the administration of the interleukin-6 receptor-blocking antibody tocilizumab. IL-6, mostly being produced by monocytes (Norelli et al. 2018), is believed to play a key role in

the development of T cell mediated cytokine release syndrome (CRS) and the blocking of its receptor with an appropriate antibody has shown a quick reversal of CRS symptomology (Grupp et al. 2013, Maude et al. 2014). However, the effect of tocilizumab regarding the neurological toxicities remains unknown and it does not have a direct on CAR T-cell proliferation, persistence and the antitumor effect (Bonifant et al. 2016). IL-6, playing a crucial role in the development of HBV infection, might interfere in both ways, positively or negatively, with the usual HBV treatment (Lan et al. 2015). Another therapeutic option is the administration of corticosteroids that have strong immunosuppressive properties. They have shown to be effective in the management of CRS that occurred after T cell therapy (Lee et al. 2014, Maude et al. 2014, Brudno et al. 2016). Nonetheless, the long-term use of systemic corticosteroids has been shown to negatively impact the persistence and the efficacy of CAR T cells (Davila et al. 2014). Other side effects of the prolonged use of corticosteroids are numerous and explain that its use is only considered when the toxicities are refractory to anti-IL-6-therapy (Neelapu et al. 2018). Furthermore, immune suppressive treatments including corticosteroids can lead to a reactivation of HBV infection or enhance the viral replication (KIM et al. 2010) and are thus contra-indicated in the treatment of CHB. At the end, the only tool which would allow a specific depletion of adoptively transferred T cells, not only in case of side effects but also after having fulfilled their therapeutic objective, is the integration of a safeguard mechanism. In our hands, iC9, by its fast and efficient T-cell depletion, represents a safe and efficient mean to prevent or manage possible side effects in the context of adoptive T-cell therapy against CHB.

4 Materials and Methods

4.1 Materials

4.1.1 Devices

Product	Supplier
Accu-jet pro	Brand Tech
Architect™	Abbott
Centrifuge 5920R	Eppendorf
CytoFLEX S	Beckman Coulter
DiluPhotometer OD600	Implen
ELISA-Reader infinite F200	Tecan
Freezing cell container	Nalgene / BioCision
Fusion Fx7	Peqlab
Gel chambers (agarose gel electrophoresis)	Peqlab
Incubator Heracell 150	Heraeus
Macs separator MultiStand	Miltenyi
NanoDrop One	Thermo Scientific
Neubauer improved hemocytometer	Brand
Nucleocounter NC-250	Chemometec
Pipettes	Eppendorf
Radiation Source	Buchler
Reflotron Reflovet Plus	Roche Diagnostics
Shaker and incubator for bacteria	INFORS AG; Heraeus
Sterile hood HERA safe	Thermo Scientific
T professional Trio Thermocytometer	Analytik Jena
Table-top centrifuge 5417R	Eppendorf
Thermo Mixer F1.5	Eppendorf
xCELLigence RTCA Single Plate / Multiplate	ACEA Biosciences

4.1.2 Consumables

Product	Supplier
Butterfly canula	Sarstedt
Cell culture flasks, dishes, plates	TPP
Cell strainer 70 / 100 μm	Falcon
Cryo vials	Greiner Bio One
ELISA 96-well plates Nunc MaxiSorb	Thermo Scientific
E-Plate 96	ACEA Biosciences
FACS 96-well V-bottom plates	Roth
Falcon tubes 15ml/50ml	Greiner Bio One
Filcons, sterile, 30 μm	SLG
Filter tips	Greiner Bio One / Corning
Macs separation columns (MS, LS)	Miltenyi
Microvette 1.1 ml Z-Gel	Sarstedt
Microvette 500 LH-Gel	Sarstedt
Needles	Braun
Non-tissue cultured treated plates (24-well)	Falcon
PCR tubes	Thermo Fisher Scientific
Pipette tips 10 μl – 1 ml	Biozym / Greiner Bio One / Gilson
Pipettes (disposable) 2, 5, 10, 25, 50ml	Greiner Bio One
Reaction tubes 1.5 ml, 2 ml	Greiner Bio One, Eppendorf
Reagent reservoirs, sterile	Corning
Reflotron ALT stripes	Roche Diagnostics
Sterile filters 0.45 μm and 0.2 μm	Sarstedt
Surgical disposable scalpels	Braun
Syringes	Braun

4.1.3 Chemicals, reagents and additives

Product	Supplier
Acetic acid	Roth
Agarose	Roth
Ammonium chloride	Roth

Ampicillin	Roth
B/B Homodimerizer for *in vivo* experiments	Takara, #635068
B/B Homodimerizer for *in vitro* experiments	Takara, #635059
Biocoll separating solution	Biochrom
Blasticidin	Gibco
Bovine serum albumin (BSA)	Roth
Brefeldin A (BFA)	Sigma
CD8a (Ly2) Microbeads, mouse	Miltenyi
CD56 Microbeads, human	Miltenyi
Collagen R	Serva
CountBright Absolute Counting Beads	Thermo Fisher Scientific
Cytofix/Cytoperm	BD Biosciences
Dimethyl sulfoxide (DMSO)	Sigma
DMEM	Gibco
DNA ladder 10kb	Eurogentec
EDTA	Roth
EDTA di-sodium salt (Na_2EDTA)	Roth
Ethanol	Roth
Fetal calf serum (FCS)	Gibco
Ganciclovir (GCV), 250 mg	Invivogen
Gentamicin	Ratiopharm
Heparin-Natrium 25000	Ratiopharm
Hepes 1 M	Gibco
IL-12 murine	Provided by Edgar Schmitt, Mainz
IL-2 Proleukin	Novartis
Isoflurane	Henry Schein
L-Glutamine, 200mM	Gibco
Lipofectamine 2000	Invitrogen
Non-essential amino acids (NEAA), 100x	Gibco
OptiMEM	Gibco
Paraformaldehyde (PFA), 4%	ChemCruz
PEG 400	Sigma-Aldrich
Penicillin, 100x	Gibco
Percoll density gradient media	GE Healthcare
Perm/Wash	BD Biosciences

Phosphate-buffered saline (PBS), 10x	Gibco
Poly-L-lysine	Sigma-Aldrich
Potassium bicarbonate ($KHCO_3$)	Roth
Propidiumiodide (PI)	Roth
Protamine sulfate	LEO Pharma
RetroNectin 1 μg/μl	Takara
RNA*later* RNA Stabilization Reagent	Qiagen
Roti-Safe GelStain	Roth
RPMI 1640	Gibco
RPMI 1640 Dutch modified	Gibco
SOC medium	Sigma-Aldrich
Sodium chloride	Roth
Sodium pyruvate, 10x	Gibco
Cell counting Solution 18	Chemometec
Streptomycin, 100x	Thermo Fisher Scientific
Tissue-Tek O.C.T.	Sakura
TMB solution	Thermo Fisher Scientific
Tris	Roth
Trypan blue	Gibco
Trypsin-EDTA	Gibco
Tween 20	Roth
Versene	Gibco
Williams Medium E	Gibco
β-Mercaptoethanol, 50 mM	Gibco

4.1.4 Buffers

Buffer	**Ingredients**
50x TAE buffer	2M Tris 2M acetic acid 50mM EDTA pH 8.0 in H_2O
	150 mM NH_4Cl 10 mM $KHCO_3$

ACK lysis buffer	0.1 mM Na_2EDTA pH 7.2 – 7.4 in H_2O
ELISA assay diluent	1% BSA in PBS
FACS buffer	0.1% BSA in PBS
MACS buffer	0.5 % BSA 2 mm EDTA pH 7.2 in PBS

4.1.5 Kits

Product	Supplier
ARCHITECT HBeAg Reagent Kit	Abbott
ARCHITECT HBsAg Reagent Kit	Abbott
CD8a (Ly2) MicroBeads, mouse	Miltenyi
CD56 MicroBeads, human	Miltenyi
Cell Proliferation Kit II (XTT)	Roche
Cytofix/Cytoperm (+ Perm/Wash Buffer)	BD Biosciences
GeneJET Plasmid Miniprep Kit	Thermo Fisher Scientific
Human IFN-γ uncoated ELISA	Invitrogen
Mouse IFN-γ uncoated ELISA	Invitrogen
NucleoSpin Tissue DNA and RNA	Macherey-Nagel
Phusion Hot Start Flex 2x Master Mix	New England Biolabs
Plasmid *Plus*Midi Kit	Qiagen
QIAquick Gel Extraction Kit	Qiagen

4.1.6 Cell lines and bacteria

Cell line	Description	Source
HepG2	Human hepatoma cell line	AG Protzer

HepG2.2.15	Stable HBV-producing human hepatoma cell line (derived from HepG2)	AG Protzer
Huh7	Human hepatoma cell line	AG Protzer
Huh7s	Human hepatoma cell line with transgenic CMV-driven expression of S protein	AG Protzer
PlatE	Retroviral packaging cell line to transduce murine cells	AG Protzer
RD114	Retroviral packaging cell line to transduce human cells	AG Protzer/Biovec Pharma
E. coli STBL3	Chemical competent *Escherichia coli* cells	Invitrogen

4.1.7 Antibodies

Antibody	Dilution	Article number	Supplier
hCD4-APC	1 :200	17-0048-42	eBioscience
hCD4-PE-Cy7	1 :200	317414	Biolegend
hCD8-APC-Cy7	1 :200	47-0088-42	eBioscience
hCD8-Pb	1 :200	PB984	Dako
hIgG-FITC	1 :200	SLBG4031	Sigma
hIgG-PE	1 :200	12-4998-82	eBioscience
mCD28 (for stimulation)		Clone : 37N	AG Feederle, HMGU
mCD3 (for stimulation)		Clone : 2C11H	AG Feederle, HMGU
mCD19-PerCp-Cy5.5	1 :200	561113	BD Biosciences
mCD45.1-BV660	1 :200	563754	BD Biosciences
mCD45.1-APC	1 :200	47-0453-82	eBioscience
mCD45.2-PB	1 :200	109819	BioLegend
mCD4-APC	1 :200	17-0041-83	eBioscience
mCD4-PE-Cy7	1 :200	25-0042-82	eBioscience
mCD4-V500	1 :200	560782	BD Biosciences
mCD8a-Pb	1 :200	558106	BD Biosciences

mIFN-γ-FITC	1 :300	554411	BD Biosciences
mTNF-α-PE-Cy7	1 :200	557644	BD Biosciences
mIL2-APC	1 :300	554429	BD Biosciences

4.1.8 Enzymes

Product	Supplier
Collagenase IV	Sigma-Aldrich
FastAP	Thermo Fisher Scientific
FastDigest restriction enzymes (& buffers)	Thermo Fisher Scientific
T4 DNA Ligase	Thermo Fischer Scientific
T5 exonuclease	New England Biolabs

4.1.9 Primers

Primers were purchased from Microsynth AG.

Primer name	Sequence (5' -> 3')	Application
SCAR_ClaI_revAKL2	ATATATATCGATTTAGCGAGG	Cloning
SCARkor_ClaIrevAK	ATATCGATTTAGCGAGGGGGCAGG	Cloning
SCARco_NCOI_fw_AK	CTGCCATGGATTTCGAGGT	Cloning
SCARco_Mlu_rev_AK	ATACGCGTGAATTCCCGGATCTCTCGAG	Cloning
6K_2Aovrlap_fwAKL	TCCCGGCCCTATGGGACCTCAGCTGCTGG	Cloning
4G_2Aovrlap_fwAKL	TCCCGGCCCTATGGGCAGCAGACTGCTGTG	Cloning
2A_6Kovrlap_rvAKL	AGGTCCCATAGGGCCGGGATTTTCCT	Cloning
6K4G_MluI_rev_AKL	ATATATACGCGTTCAGCTGGACCACAGCCG	Cloning
TCR4G_2Aovrlap_fw	CCAGGCCCCATGGGCAGCAGACTGCTGTG	Cloning
2A_TCR4Govrlap_rv	GCTGCCCATGGGGCCTGGGTTCTCCT	Cloning
TCR6K_2Aovrlap_fw	CCAGGCCCCATGGGACTCAGCTGCTGG	Cloning
iCSPSCARco_NotIfw	TTTTTTGCGGCCGCATGCTGGAGGGCGTGC	Cloning
iCSPSCARcoEcoRIrv	GGGGGGGAATTCTCGAGGATCATCTGGGGG	Cloning
icasp9_AgeI_fw	TGGACCGACCGGTGGTAC	Cloning

4.1.10 Plasmids

Plasmid	Transgene product(s)	Source
HSVTK-2A-CD34	HSVTK - 2A - CD34	AG Pulé
iCASP9-2A-aGD2	iCASP9 - 2A - aGD2	AG Pulé
RQR8-2A-aGD2	RQR8 - 2A – aGD2	AG Pulé
pMP71_hC8 S-CAR	Codon optimized S-CAR	K. Wisskirchen
pMP71_TCR-4G	Codon optimized TCR 4G	K. Metzger/ K. Wisskirchen
pMP71_TCR-6K	Codon optimized TCR 6K	K. Metzger/ K. Wisskirchen
HSVTK-2A-S-CAR	HSVTK and codon optimized S-CAR	Alexandre Klopp
HSVTK-2A-4G	HSVTK and codon optimized TCR 4G	Alexandre Klopp
HSVTK-2A-6K	HSVTK and codon optimized TCR 6K	Alexandre Klopp
iCASP9-2A-S-CAR	iCASP9 and codon optimized S-CAR	Alexandre Klopp
iCASP9-2A-4G	iCASP9 and codon optimized TCR 4G	Alexandre Klopp
iCASP9-2A-6K	iCASP9 and codon optimized TCR 6K	Alexandre Klopp
RQR8-2A-S-CAR	RQR8 and codon optimized S-CAR	Alexandre Klopp
RQR8-2A-4G	RQR8 and codon optimized TCR 4G	Alexandre Klopp
RQR8-2A-6K	RQR8 and codon optimized TCR 6K	Alexandre Klopp

4.1.11 Media

Medium	Ingredients	
Collagenase medium	Williams Medium E	500 ml
	Collagenase IV	25 mg
DMEM full medium	DMEM	500 ml
	FCS	50 ml
	Pen/Strep, 10.000 U/ml	5.5 ml
	L-Glutamine, 200 mM	5.5 ml
	NEAA, 100x	5.5 ml
	Sodium pyruvate, 100 mM	5.5 ml
Freezing medium	DMEM	90 %
	DMSO	10%
HepG2 Diff medium	DMEM	500 ml

	FCS	50 ml
	Pen/Strep, 10.000 U/ml	5.5 ml
	L-Glutamine, 200 mM	5.5 ml
	NEAA, 100x	5.5 ml
	Sodium pyruvate, 100 mM	5.5 ml
	DMSO	10.5 ml
Human T-cell medium (hTCM)	RPMI 1640	500 ml
	FCS	50 ml
	Pen/Strep, 10.000 U/ml	5.5 ml
	L-Glutamine, 200 mM	5.5 ml
	NEAA, 100x	5.5 ml
	Sodium pyruvate, 100 mM	5.5 ml
	HEPES	10.5 ml
	Gentamicin	208 ul
LB medium pH7	Tryptone	10 g
	Yeast extract	5 g
	NaCl	10 g
	In 1 liter H_2O	
Murine T-cell medium (mTCM)	RPMI Dutch modified	500 ml
	FCS	50 ml
	Pen/Strep, 10.000 U/ml	5.5 ml
	L-Glutamine, 200 mM	5.5 ml
	NEAA, 100x	5.5 ml
	Sodium pyruvate, 100 mM	5.5 ml
	β-Mercaptoethanol	10.5 ml
RPMI full medium	RPMI 1640	500 ml
	FCS	50 ml
	Pen/Strep, 10.000 U/ml	5.5 ml
	L-Glutamine, 200 mM	5.5 ml
	NEAA, 100x	5.5 ml
	Sodium pyruvate, 100 mM	5.5 ml
Transfection medium	DMEM	500 ml
	FCS	50 ml
	L-Glutamine, 200 mM	5.5 ml
	NEAA, 100x	5.5 ml
	Sodium pyruvate, 100 mM	5.5 ml

Wash medium	RPMI 1640	500 ml
	Pen/Strep, 10.000 U/ml	5.5 ml

4.1.12 Mouse strains

Mouse strain	Description	Source
C57Bl/6J	Wildtype C57Bl/6J	Charles River or JANVIER LABS
C57Bl/6J-CD45.1	C57Bl/6J expressing congenic marker CD45.1	In house breeding
C57Bl/6J-CD45.2	C57Bl/6J expressing congenic marker CD45.2	In house breeding
C57Bl/6J-CD45.1/CD45.2	C57Bl/6J expressing congenic markers CD45.1 and CD45.2	In house breeding
$Rag2^{-/-}\ \gamma c^{-/-}$	C57Bl/6J, homozygous deficiency in Rag2 and IL-2Rγ locus; no B-, T- and NK-cell development	In house breeding

4.1.13 Viral vectors

Viral vector	Description	Source
AAV-HBV	AAV genome serotype 2 containing the 1.2 overlength genome of HBV genotype D packed into AAV capside serotype 8	Plateforme de thérapie génique (Nantes, France)

4.1.14 Proteins

Protein	Source
HBsAg, serotype ayw, CHO	Roche

4.1.15 Softwares

Software	Application	Supplier
FlowJo, version 10.4	Flow cytometry analysis	BD Biosciences
Prism 5.01	Graph design, ELISA calculations, statistical analyzes	GraphPad Software Inc.
RTCA Software 2.0	xCELLigence viability analysis	ACEA Biosciences
Serial cloner	DNA and protein sequence anlaysis	SerialBasics
Windowa 7/8/10, MS Office	Word, Excel, Powerpoint	Windows

4.2 Methods

4.2.1 Molecular biological methods

4.2.1.1 Polymerase chain reaction (PCR)

PCRs for molecular cloning were performed with the Phusion Hot Start Flex 2x Master Mix according to the manufacturer's instructions. 2,5 µl of each primer in a concentration of 10 µM and 1-10 ng of plasmid DNA were added to 25 µl of the 2x Master Mix. H2O was added to a total reaction volume of 50 µl. The amplification of the gene of interest was then performed using the following PCR program:

	Temperature [°C]	Time [sec]	Cycles
Denaturation	98	30	1
Denaturation	98	10	30
Annealing	55-65 (depending on primers)	20	
Elongation	72	30 per 1kb	
Elongation	72	600	1
Cooling	4		1

To fuse two PCR fragments equimolar fragments (total of 300 ng) with an overlap of ~ 18 bp were used. The first PCR run using the PCR program of above was conducted without primers for 15 cycles. After addition of the primers 15 additional cycles were performed. The annealing temperature could differ between the two PCR steps.

The annealing temperatures of the primers were determined using the online Tm calculator from New England Biolabs.

4.2.1.2 Restriction enzyme digestion

In order to analyze plasmids and to obtain fragments for molecular cloning restriction digests using restrictions enzymes were performed. For this, plasmid DNA or PCR fragments were added to 2 µl of FastDigest Green Buffer (10x) and 1 µL of the needed enzymes not exceeding 10% (volume/volume) of the total volume. H2O was added to keep a total reaction volume of 20 µl followed by a 30 – 60 min incubation at 37 °C in a heat block.

4.2.1.3 DNA gel electrophoresis and gel extraction

Agarose gels were prepared using TAE, 1% agarose and 6 µL of Roti gel stain per 100 mL of total volume. A DNA latter was run together with the samples at 80-150 mV to determine the size of the desired samples. The extraction of the bands was achieved using a scalpel and keeping the ultraviolet light exposure as low as possible. The DNA was then extracted using the QIAquick Gel Extraction Kit according to the manufacturer's instructions.

4.2.1.4 Ligation and bacterial transformation

For ligation, 100 ng of the backbone was ligated in a molar ratio of 1:3 with the insert in a total volume of 20 µL with 2 µL T4 ligase buffer, and 1 µL T4 Ligase. H2O was added to keep a total reaction volume of 20 µL followed by a 30 min incubation at room temperature. Exact calculations regarding the molar ratio were performed using following website: http://molbiol.edu.ru/eng/scripts/01_07.html. E.coli STBL3 were used for bacterial transformation. They were thawed on ice and 5 µL of the ligation were added to 50 µL bacteria. After 30 min of incubation on ice, a heat shock was performed for 90 sec at 42 °C and bacteria were chilled on ice for another 2-3 min. 500 µL SOC-Medium was then added to the bacteria followed by an incubation period of 1h at 37 °C. Finally, the bacteria were plated on ampicillin-resistant plates and incubated overnight at 37 °C.

4.2.1.5 Amplification and isolation of plasmid DNA

After picking the bacterial colonies on the plates, the bacteria were inoculated and amplified in overnight cultures in LB medium supplemented with 100 µg/mL ampicillin at 37 °C, 185 rpm. On the next day, bacteria were harvested by centrifugation (3400 g, 10 min, 4 °C) and isolated with GeneJET Plasmid Miniprep Kit or the Plasmid *Plus*Midi Kit, respectively, following the manufacturer's instructions.

4.2.1.6 Sequencing

Sequencing was performed at Eurofins using 20 μL per primer (10 μM) and 30-100 ng/μL of the plasmid template. Sequencing results were downloaded on their website and analyzed using Serial Cloner.

4.2.1.7 Cloning strategy for safeguard mechanism integration

The HBV-specific receptors were cloned from an pMP71 retroviral vector into SFG vectors (kindly provided by Martin Pulé), which encode the different safeguard mechanisms. Initially, new restriction sites were introduced into the receptor sequences through PCR, using specific primers (primer sequences are provided in section 4.1.9). Different restriction sites were utilized for the cloning process, depending on the specific inserts. The exact PCR setup is detailed in section 4.2.1.

To clone into the SFG vector, the PCR products were first verified by agarose gel electrophoresis to confirm the expected length. The desired bands were excised and purified (see section 4.2.1.3). The purified PCR inserts and the target vectors were then digested with the appropriate restriction enzymes (see section 4.2.1.2).

The digested products were subsequently purified using a Qiagen kit and ligated using T4 ligase, following the manufacturer's instructions. The molar ratio of insert to vector was maintained at 3:1 (insert to vector) (see section 4.2.1.4). The ligation mix was then transformed into chemically competent E. coli STBL3 bacteria, which were subsequently plated on ampicillin-containing plates (see section 4.2.1.4).

Amplification and isolation of the newly constructed plasmids were carried out as described in section 4.2.1.5. To confirm successful cloning, the plasmids were sequenced by Eurofins, and the results were analyzed using Serial Cloner (see section 4.2.1.6).

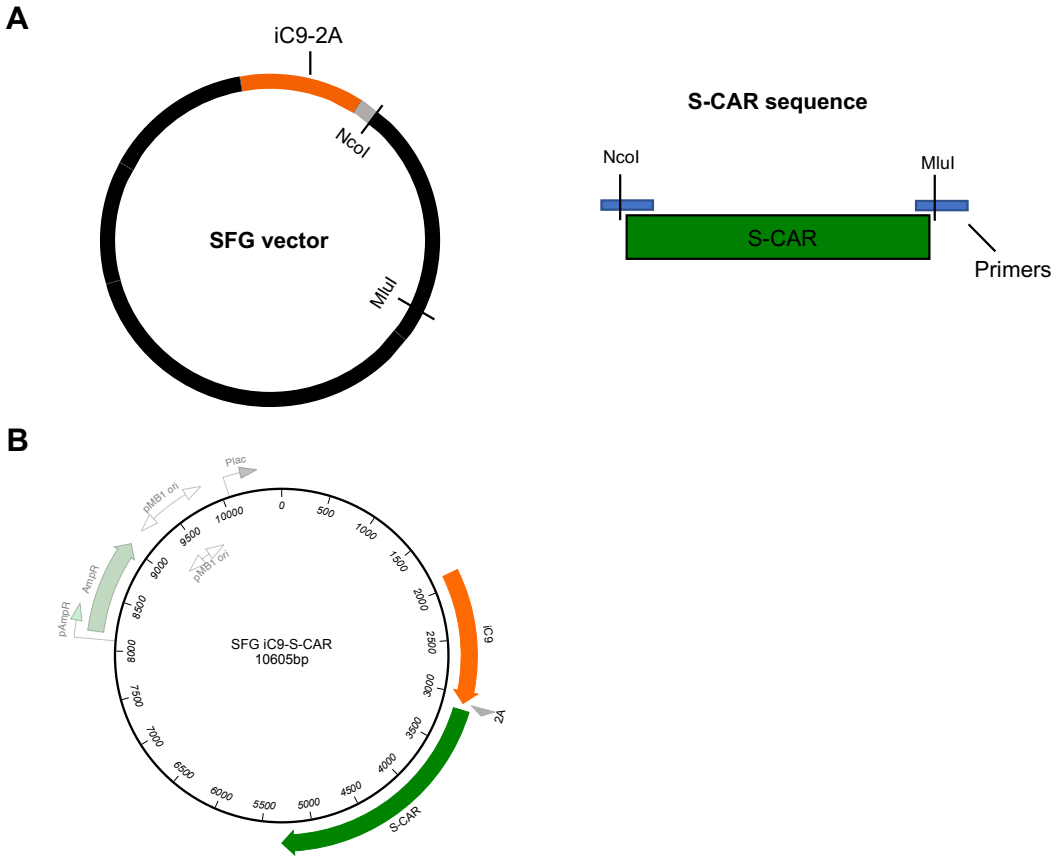

Figure 4.1 Exemplary Cloning Scheme for iC9 and S-CAR
(A) S-CAR was cloned into a SFG vector, which encodes iC9-2A, using the restriction sites NcoI and MluI. **(B)** Plasmid map of SFG iC9-2A-S-CAR. Plasmid map was generated with Serial Cloner.

4.2.2 General cell culture methods

All cell-culture experiments were performed under sterile conditions. The cells were incubated at 37 °C, 5% CO2 and 95% humidity. Adherent cells were cultured in DMEM full medium and were passaged 1:5 or 1:10 every three to four days depending on their confluency. For the differentiation of HepG2-derived cells, culture flasks or plates were coated with collagen (1:10 in H2O, 30 min, 37 °C) and washed twice with PBS before seeding the cells.
Cells were counted using a Neubauer improved hemocytometer. For this, cells were harvested and suspended in order to obtain a single-cell suspension. 10 µL of the cell suspension was then diluted 1:2 with trypan blue and cells were counted by eye under the microscope. Alternatively, cells were counted using a Nucleocounter NC-250. Here, 1 µL of Solution 18 was added to 20 µL of the cell suspension and automated counting was performed.

For freezing, cells were centrifugated (350 g, 5 min, 4°C), the cell pellet was resuspended in 1ml of freezing medium per cryo vial and the vials were transferred to a freezing device and stored immediately at -80 °C or in liquid nitrogen.
To thaw cells, 1 mL of prewarmed medium was added to the frozen cryo vial and slowly transferred forth and back until the solution was thawed. The cells were then transferred into a 15 mL falcon with 4 mL of prewarmed medium. Cells were centrifugated (350 g, 5 min, RT) and seeded with respective cell medium in appropriate cell culture flask.

4.2.3 Transfection of cells and production of retroviral supernatants

Retroviral supernatants that allow the transduction and thus the transgenic expression of TCR- or CAR-constructs on T cells were obtained from transiently transfected or stably transduced producer cell lines RD114 or PlatE. While the retroviral supernatant produced from RD114 cells was used to transduce human T cells, murine T cells were transduced using the supernatant of PlatE cells. For transient production of retrovirus, the producer cell lines were transfected with the desired plasmids. Cells were seeded on 6-well plates at least one day prior transfection in order to achieve a confluency of 60-70% at the day of transfection. 4 μg of plasmid DNA was diluted in Opti-MEM to a total volume of 125 μl. In a separate tube, 10 μl of Lipofectamine 2000 was diluted with 115 μl of Opti-MEM. After 5 minutes of incubation at RT, the diluted DNA was added to the Lipofectamine 2000 mix, carefully mixed by resuspending and incubated for 20 minutes at RT. During the incubation period, medium of cells was changed to 1.5 mL transfection medium. The DNA/Lipofectamine 2000 mix was then added to the cells and incubated for two days in the incubator. After two days, the supernatant was collected and filtered through a 0.45 μm filter. Fresh medium was added to the cells and the step was repeated on day three. To generate stably transduced producer cell lines, RD114 or PlatE cells were first transiently transfected with the desired plasmid as described above. After two days, the supernatant was filtered with a 0.45 μM filter and added to RD114 or PlatE cells that had previously been plated on a 12-well plate. This step was repeated on the next day. When the transduced cells reached confluency, they were first transferred to a 6-well plate and afterwards to a T75 cell culture flask. Transduced cells expressing the transgene were then sorted by flow cytometry. The sorted cells were then expanded in a T75 cell culture flask until 80% confluency. They were then supplied with fresh medium and the supernatant containing the virus was collected after 24 and 48 h and subsequently used for retroviral transduction of T cells or stored at – 80 °C until further use.

4.2.4 Isolation of primary immune cells

4.2.4.1 Isolation of murine splenocytes

For the isolation of murine splenocytes, spleens were collected from C57BL/6 donor mice. Spleens were then mashed through a 100 μm cell strainer into a 6-well plate using the plunger of a 2 ml syringe and 3 mL of mouse T cell medium (mTCM). The cell strainer was cleaned with another 2 ml of mTCM and the cells were collected in a 50 mL falcon tube. These steps were repeated 2 times and the collected splenocytes were pelleted (350g, 5min, 4 °C).
The pellet was resuspended in 2 mL of ACK lysis buffer and incubated for 2 min at RT to induce lysis of erythrocytes. After the reaction was ceased by adding 48 mL of mTCM and the splenocytes were pelleted (350 g, 5 min, 4°C) and resuspended in the appropriate medium and volume.

4.2.4.2 Isolation of liver-associated lymphocytes

To isolate liver-associated lymphocytes, livers were first perfused with PBS to remove non-liver associated lymphocytes. The livers were then mashed through a 100 μm cell strainer with the plunger of a 5 ml syringe. The cell strainer was repeatedly cleaned with wash medium followed by additional mashing steps. The flow through was collected with a 20 G canula and passed through a new 100 μm cell strainer in order to assure a single-cell suspension. Cells were then pelleted (350 g , 5 min, 4 °C), resuspended in 12.5 mL collagenase medium (4500 U collagenase type 4 in Williams Medium E supplemented with 8.75 μL $CaCl_2$) and digested at 37 °C for 20 min with repeated shaking. After filling up to 30 mL with wash medium, the cells were pelleted and resuspended in 4 ml PBS-buffered 40% Percoll solution. This solution was carefully layered onto 4 mL PBS-buffered 80% Percoll in a 15ml falcon tube and centrifuged at 1400 g for 20 min at RT without breaks. The LAL fraction between the Percoll layers was collected into a new 15 ml tube, washed twice with wash medium and resuspended in the appropriate medium and volume.

4.2.4.3 Isolation of murine PBMCs

15 μl of heparinized whole blood from Microvette 500 LH-Gel tubes were mixed with 230 μl PBS in a 96-well-V-bottom plate. After centrifugation (450g, 2min, 4°C), erythrocytes were lysed after addition of 250 μl ACK buffer and incubation of 2 min at RT. Cells were then pelted and washed once with 200 μl of FACS buffer. Staining for flow cytometry analyses was then started.

4.2.4.4 Isolation of human PBMCs

Human PBMCs were collected from healthy donors using a syringe containing heparin. The blood was then diluted 1:2 with wash medium. 30 mL of the diluted blood was then layered on top of 15 mL Bicoll separating solution and centrifuged for 20 min with 1200 g at RT without breaks. The lymphocyte ring was then transferred into a new 50 mL falcon and washed twice with wash medium (350 g, 5 min, RT). Cells were then resuspended in human T-cell medium (hTCM) and counted.

4.2.5 Retroviral transduction of T cells

4.2.5.1 Transduction of murine splenocytes

Two different protocols were used for the transduction of murine splenocytes. The IL-2 transduction protocol allowed the retroviral transduction of $CD8^+$ and $CD4^+$ T cells, whereas only $CD8^+$ T cells were transduced with the IL12-transduction protocol. The IL-2 transduction protocol was used for the tolerization process of the mice in the first mouse experiment as for the tolerization process no pure CD8 T-cell population was needed. For the other steps of the experiments and for all the other mouse experiments, the IL-12 transduction protocol was used, allowing us to generate a homogenous, transduced $CD8^+$ T-cell population.

Transduction with IL-2 stimulation

For the transduction with IL-2, freshly isolated murine splenocytes were adjusted to 3 x 10^6 cells per mL of mouse T cell medium (mTCM) supplemented with 300 U/mL IL-2, 2 μg/mL anti-mCD3 and 0,1 μg/ml anti-mCD28 antibodies. Cells were incubated overnight at 37 °C. Before transduction, non-tissue 6- or 24-well-plates were coated with 250μl or 1000 μl retronectin (20 μg/ml in PBS) and incubated for two hours at RT. Retronectin was then collected and stored at 4°C for re-use on the following day. Plates were blocked using 2% BSA in PBS for 30 minutes at 37°C and then washed twice with PBS. Next, 1 ml or 5 ml of the filtered retrovirus supernatant was added per well and the plates were centrifuged (2000 g, 2 h, 32 °C). The splenocytes were counted, washed and adjusted to 1 x 10^6 cells per mL fresh mTCM supplemented with 300 U/mL IL-2. After centrifugation 1 ml or 5 ml of the cell suspension was added to the plates containing the supernatant. The supernatant in the wells was also supplemented with 30 U/mL IL-2. The plates were centrifuged once again (1000g, 10min, 32 °C) and incubated at 37 °C overnight. On the next day, a second transduction round similar to the first round was performed. For this round, the splenocytes were transferred well-by-well to the new plates without refreshing their medium. The following day, the transduction rate was determined by FACS. The cells were counted, washed and resuspended in PBS for adoptive transfer experiments.

Transduction with IL-12 stimulation

For the transduction with IL-12, 24-well tissue-plates were coated with anti-mCD3 and anti-mCD28 antibodies (each 10 μg/ml in PBS, 250 μl/well). After an incubation of 2 h at 37 °C, the plates were blocked for 30 min at 37 °C with 2 % BSA in PBS. Freshly isolated murine splenocytes were sorted for $CD8^+$ T cells by positive selection with CD8a (Ly2) Microbeads using MS columns on a OctoMACS Separator according to manufacturer's instructions. They were then counted, washed and adjusted to 0.8 x1 0^6 cells per 1.5 mL mTCM supplemented with 5 ng/mL IL-12. 1.5 ml of the cell suspension per well was then seeded on the antibody-coated 24-well plate and the plate was incubated at 37 °C overnight. The next day, the retroviral supernatant from transiently transfected or stably transduced PlatE cells was collected, filtered and protaminsulfate was added (2 μg/mL) to the supernatnats and the activated $CD8^+$ T cells. 1 mL of supernatant was removed and collected from every well of the plates containing the T cells and stored at 37 °C. The remaining 1.5 ml of retroviral supernatant was then added to the wells and the plates were centrifuged (2500 rpm, 90 min, 32 °C). After centrifugation, 2 μg/ml protaminsulfate was added to the stored supernatant. 500 μl was removed from every well of the plates and 1 ml of the old supernatant was added to the cells. Cells were incubated overnight at 37 °C. On the next day, a second transduction round similar to the first round was performed. Here, 2 mL of supernatant was removed and collected from the plates and re-added after the centrifugation step and supplied of 2 μg/ml protaminsulfate. On day four, the transduction rate was determined by flow cytometry analysis. The cells were counted, washed and resuspended in PBS for adoptive transfer experiments.

4.2.5.2 Transduction of human PBMCs

For the transduction of human PBMCs, 24-well non-tissue plates were coated with human anti-CD3 (5 μg/ml) and anti-CD28 (0.05 μg/ml) antibodies (250 μL/well, 2 h, 37 °C). The plates were blocked for 30 minutes at 37 °C with 2% BSA in PBS and then washed twice with PBS. Freshly isolated or thawed human PBMCs were counted and adjusted to 0.6-0.8x10^6 cells/mL hTCM supplemented with 300 U/mL IL-2 and 1.5 mL of the cell suspension was seeded per well (day one). Cells were incubated for 48 hours at 37 °C. After incubation, two transduction rounds on two consecutive days (day three and four), identical to the IL-2 transduction of murine splenocytes (see section 4.2.5.1), were performed. On day five and six, the T cells were collected, washed and counted. They were adjusted to 0.5 x 10^6 cells/mL and supplemented with 180 U/mL IL-2 for expansion. The transduction rate of the T cells was then determined by FACS on day ten and they were directly used for functional assessment or stored at – 80 °C until further use.

4.2.6 T-cell stimulation and co-culture experiments

4.2.6.1 T-cell stimulation on plate-bound HBsAg or anti-CD3/anti CD28 antibodies

Flat-bottom 96-well tissue-plates were coated with 100 µl HBsAg of the indicated concentration diluted in PBS and incubated for two hours at 37 °C. For unspecific T-cell stimulation, wells were coated with 100 µl of anti-CD3 and anti-CD28 antibodies in a concentration of 10 µg/mL followed by two hours of incubation at 37 °C. Volumes were scaled up accordingly to the well format. After incubation, the wells were washed twice with PBS and transduced T cells, freshly isolated splenocytes or LALs were added in 200 µl of medium and appropriate number ($2x10^5$ cells/well) to the plate. Cells were then incubated for the indicated time at 37 °C. For the analysis of intracellular cytokine expression by ICS, Brefeldin A (1 µg/ml) was added to cells 2 hours after start of stimulation and cells were incubated for additional 14 hours at 37 °C.

4.2.6.2 Co-culture experiments

For functional assessment of the transduced T cells, they were co-cultured with different target cells. The viability of target cells as well as the activation of T cells were assessed. In general, unless otherwise indicated, 5 x 10^4 target cells in 200 µl DMEM full medium (HepG2-derived cells or Huh7/Huh7-S cells) were seeded seven to ten days prior start of the co-culture on a collagen-coated (Collagen R 1:10 in H_2O for 30 min at 37 °C) 96-well plate (xCELLigence plate or flat-bottom 96-well tissue-plates). The following day, medium was changed to Diff medium (DMEM full medium + 2,5 % DMSO), allowing the target cells to differentiate and to express higher concentration of HBsAg. Medium was changed every three days until start of the co-culture. On the day of the co-culture, transduced T cells that were either directly taken from an expansion culture or thawed one day prior start of the co-culture and cultured at 1 x 10^6 /mL hTCM supplemented with 30 U/mL IL-2, were washed and resuspended in appropriate amount of fresh hTCM not supplemented with IL-2. On the plates with the target cells, medium was exchanged to 100 µl/well of appropriate co-culture medium (DMEM full medium with 2% DMSO). Transduced T cells were added to the wells in different E:T ratios in 100 µl/well of DMEM full medium.

XTT assay

End-point viability of target cells was determined using an XTT assay. XTT is a tetrazolium derivate that is reduced to the orange-colored formazan by mitochondrial enzymes. Those enzymes are inactivated shortly after cell-death. Thus, the amount of formazan produced is in direct relation to the number of metabolic active cells and can be photometrically quantified at

450nm. In a 96-well plate, 100 µl DMEM, 25 µl of XTT labeling reagent and 0.5 µl of electron coupling reagent were added per well. After two hours of incubation at 37 °C conversion to formazan was determined by measurement of OD_{450} subtracted by OD_{650} on an ELISA-Reader infinite F200.

xCELLigence assay

To determine real-time viability of target cells in co-culture experiments an xCELLigence SP Real-Time Cell Analyzer was used. Through the measurement of electrical impedance from viable, adherent target cells, the xCELLigence system allows a continuous (every 15 min) quantification of the viability of target cells. For this assay, appropriate target cells were seeded on electronic microtiter plates containing interdigitated gold microelectrodes for the measurement of the impedance. Co-cultures were performed as indicated under 4.2.6.2. Impedance measurement was usually started a few days before start of the co-culture and continued for the indicated time frame. The electrical impedance displayed as cell index (CI) and determining the target cell viability was normalized to the start of the co-culture.

4.2.7 Mouse experiments

4.2.7.1 Injections

For AAV-HBV infection, virus stock solution was diluted in the indicated volume of PBS and 1 x 10^{10} - 3 x 10^{10} viral genomes (depending on experiment and gender of the mice) in 100 µl PBS were injected intravenously in the tail vein. For T-cell transfer, freshly transduced murine T cells were resuspended in the indicated volume of PBS and 1.5 x 10^6 – 3 x 10^6 transduced T cells (depending on experiment) in 200 µl PBS were injected intraperitoneally per mouse. The virus stock solution and the T cells were kept on ice until shortly before injection. CID was prepared according to the manufacturer's recommendation with the prepared stock solution (lyophilized CID in 100 % ethanol), PEG-400 (100 %) and Tween (2 %). It was injected intraperitoneally within 30 min after preparation in a dosage of 10 mg/kg and was kept on ice until shortly before injection. Murine IgG2a rituximab was isolated from K562 cells that had been transduced with the vectors coding for the antibody (cell line was kindly provided from M. Pulé). 285 µg (corresponding to approximately 375 mg/m^2) were administered by tail-vein injection. GCV was reconstituted according to the manufacturer's recommendation using distilled water and adjusting its pH to 11 using NaOH 1M and HCL 1M respectively. It was injected in a concentration of 10 mg/kg intravenously.

4.2.7.2 Bleeding

Blood collection on living mice was performed using a single-use lancet for puncture of the submandibular vein. After sacrifice of mice, blood was obtained by cardiac puncture. Blood was collected in either 500 LH-Gel tubes if analyses of whole blood and serum were necessary or in Microvette 1,5 ml Z-Gel tubes if only the serum needed to be analyzed. Serum was obtained by centrifuging the tubes for 5 min at 1000 g at RT and transferred to a new collection tube.

4.2.7.3 Serum analyses

Serum was gained as described under 4.2.7.2. For measurement of ALT levels, serum was diluted 1:4 with PBS and the Reflotron ALT test was used. HBs- and HBe-antigen levels were quantified on an Architect™ platform using the quantitative HBsAg test and the HBeAg Reagent Kit.

4.2.7.4 Final analysis

For final analysis, mice were sacrificed with CO_2 and dissected to access the internal organs. To remove non-liver associated lymphocytes, the liver was perfused with PBS through the portal vein. Lung, kidney, a piece of the liver, the spleen and the heart were fixed in 4% paraformaldehyde (PFA) for 24 hours and then transferred into PBS until paraffin embedding for histological analyses. The other lung and kidney as well as another piece of the liver, the spleen and the heart were first immerged in 15% sucrose and then transferred into 30% sucrose after 6 hours. On the following day, the organs were embed using tissue-tek and stored at – 80 °C. Further liver pieces were stored at -20 °C in T1 buffer and RNA extraction buffer for the extraction of DNA or RNA at a later time point. The rest of the liver and the spleen were used for the extraction of liver-associated lymphocytes (LALs) or splenocytes respectively as described under section 4.2.4. Liver and spleen were weight before and after pieces were removed for quantification of cell numbers.

4.2.7.5 Immunohistochemistry

Tissue pieces were fixed in 4 % paraformaldehyde (PFA) for 24 hours and then transferred into PBS until paraffin embedding for histological analyses. Liver tissues were stained with primary antibody against rabbit anti-HBcAg or anti-HBsAg (after antigen retrieval at 100 °C for 30 min with EDTA and appropriate horseradish peroxide-coupled secondary antibodies. Immunohistochemistry was performed using a Leica Bond MAX system. Slides were scanned using an Aperio AT2 slide scanner.

Quantification of HBcAg-positive hepatocytes was performed considering the localization, intensity and distributon of the signal in 10 random view fields (20x magnification). The mean numbers of HBcAg-positive hepatocytes were quantified per mm^2.

4.2.7.6 Ex vivo antigen stimulation

Isolated LALs and splenocytes were seeded on a flat-bottom 96-well non-tissue plate coated with HBsAg or anti-murine anti-CD3 and anti-CD28 antibodies as described under section 4.2.6.1. After two hours, BFA was added (1 mg/mL) and cells were incubated for another 14 hours at 37 °C before processing to the intracellular cytokine staining (ICS).

4.2.8 Enzyme-linked immunosorbent assay (ELISA)

4.2.8.1 IFN-γ ELISA

The concentration of human or murine IFN-γ in the supernatant to assess the activation of T cells was determined using commercially available ELISA kits. Experiments were performed according to manufacturer's instructions on MaxiSorb ELISA 96-well plates. The conversion of TMB substrate was determined by measurement of OD_{450} subtracted by OD_{560} on an ELISA-Reader infinite F200.

4.2.9 Flow cytometry

4.2.9.1 Surface staining

For the staining of surface proteins, cells were transferred to a V-bottom 96-well plate and centrifuged for 2 min at 450 g, 4 °C. The cells were then washed once with 200 µl of FACS buffer. Cells were then resuspended in 50 µl/well of FACS buffer with the respective antibodies and incubated for 30 min on ice and in the dark. Viability of the cells was determined using a LIVE/DEAD marker. After incubation, cells were washed three times with FACS buffer and finally resuspended in 150 – 180 µl of FACS buffer. If a CAR-expression was determined together with other surface proteins, stainings were performed sequentially. In the first instance the CAR was stained with an anti-human IgG antibody for 30 minutes. After 2 washing steps, the other surface proteins were stained with the respective antibody. The samples were then analyzed on CytoFLEX S flow cytometer. The obtained data was evalutated with FlowJo.

4.2.9.2 Intracellular cytokine staining

To identify cytokine-secreting cells, an intracellular staining was performed. One hour after start of the stimulation or the co-culture, BFA was added to the cells in order to prevent cytokine secretion and thus enhance the signal of the staining. After surface and LIVE/DEAD staining, cells were permeabilized by resuspension in 100 µl Cytofix/Cytoperm followed by a 20 min long incubation on ice and in the dark. The subsequent two washing steps were realized using Perm/Wash buffer. Finally, intracellular cytokines were stained according to the surface staining, but the respective antibodies were diluted in Perm/Wash buffer. After three further washing steps with Perm/Wash buffer, the cells were resuspended in 150 – 180 µl FACS buffer and the samples were analyzed on the CytoFLEX S flow cytometer.

4.2.9.3 Determination of absolute cell count by flow cytometry

In order to determine the absolute cell count by flow cytometry, 10 µl CountBright™ Absolute Counting Beads were added to the cell suspension shortly before measurement. The absolute input cell number was determined using the following formula:

$$\text{input cells} = \text{measured cells} \times \frac{\text{input beads}}{\text{measured beads}}$$

The obtained value was extrapolated to the concentration in blood or the whole organ considering the proportion of the organ that was used to isolate splenocytes or LALs

4.2.10 Statistical analyses

Statistical analyses were perfomed using Prism 8 software. Statistical differences were calculated using the Mann-Whitney test and P-values < 0.05 were considered significant.

5 Table of figures

6 References

Andersen, M. H., D. Schrama, P. thor Straten and J. C. Becker (2006). "Cytotoxic T cells." Journal of Investigative Dermatology **126**(1): 32-41.
Ando, M., Y. Takahashi, T. Yamashita, M. Fujimoto, M. Nishikawa, Y. Watanabe and Y. Takakura (2014). "Prevention of adverse events of interferon γ gene therapy by gene delivery of interferon γ-heparin-binding domain fusion protein in mice." Molecular Therapy-Methods & Clinical Development **1**: 14023.
Asabe, S., S. F. Wieland, P. K. Chattopadhyay, M. Roederer, R. E. Engle, R. H. Purcell and F. V. Chisari (2009). "The size of the viral inoculum contributes to the outcome of hepatitis B virus infection." Journal of virology **83**(19): 9652-9662.
Barese, C. N., T. C. Felizardo, S. E. Sellers, K. Keyvanfar, A. Di Stasi, M. E. Metzger, A. E. Krouse, R. E. Donahue, D. M. Spencer and C. E. Dunbar (2015). "Regulated Apoptosis of Genetically Modified Hematopoietic Stem and Progenitor Cells Via an Inducible C aspase-9 Suicide Gene in R hesus M acaques." Stem Cells **33**(1): 91-100.
Berger, C., M. E. Flowers, E. H. Warren and S. R. Riddell (2006). "Analysis of transgene-specific immune responses that limit the in vivo persistence of adoptively transferred HSV-TK–modified donor T cells after allogeneic hematopoietic cell transplantation." Blood **107**(6): 2294-2302.
Bertoletti, A., A. Sette, F. V. Chisari, A. Penna, M. Levrero, M. De Carli, F. Fiaccadori and C. Ferrari (1994). "Natural variants of cytotoxic epitopes are T-cell receptor antagonists for antiviral cytotoxic T cells." Nature **369**(6479): 407-410.
Bohne, F., M. Chmielewski, G. Ebert, K. Wiegmann, T. Kürschner, A. Schulze, S. Urban, M. Krönke, H. Abken and U. Protzer (2008). "T cells redirected against hepatitis B virus surface proteins eliminate infected hepatocytes." Gastroenterology **134**(1): 239-247.
Boni, C., P. Fisicaro, C. Valdatta, B. Amadei, P. Di Vincenzo, T. Giuberti, D. Laccabue, A. Zerbini, A. Cavalli and G. Missale (2007). "Characterization of hepatitis B virus (HBV)-specific T-cell dysfunction in chronic HBV infection." Journal of virology **81**(8): 4215-4225.
Bonifant, C. L., H. J. Jackson, R. J. Brentjens and K. J. Curran (2016). "Toxicity and management in CAR T-cell therapy." Molecular Therapy-Oncolytics **3**: 16011.
Bonini, C., G. Ferrari, S. Verzeletti, P. Servida, E. Zappone, L. Ruggieri, M. Ponzoni, S. Rossini, F. Mavilio and C. Traversari (1997). "HSV-TK gene transfer into donor lymphocytes for control of allogeneic graft-versus-leukemia." Science **276**(5319): 1719-1724.
Brudno, J. N. and J. N. Kochenderfer (2016). "Toxicities of chimeric antigen receptor T cells: recognition and management." Blood, The Journal of the American Society of Hematology **127**(26): 3321-3330.
Budde, L. E., C. Berger, Y. Lin, J. Wang, X. Lin, S. E. Frayo, S. A. Brouns, D. M. Spencer, B. G. Till and M. C. Jensen (2013). "Combining a CD20 chimeric antigen receptor and an inducible caspase 9 suicide switch to improve the efficacy and safety of T cell adoptive immunotherapy for lymphoma." PloS one **8**(12).
Buechner, J., S. A. Grupp, S. L. Maude, M. Boyer, H. Bittencourt, T. W. Laetsch, P. Bader, M. R. Verneris, H. Stefanski and G. D. Myers (2017). "Global registration trial of efficacy and safety of CTL019 in pediatric and young adult patients with relapsed/refractory (R/R) acute lymphoblastic leukemia (ALL): update to the interim analysis." Clinical Lymphoma, Myeloma and Leukemia **17**: S263-S264.

Burton, A. R., L. J. Pallett, L. E. McCoy, K. Suveizdyte, O. E. Amin, L. Swadling, E. Alberts, B. R. Davidson, P. T. Kennedy and U. S. Gill (2018). "Circulating and intrahepatic antiviral B cells are defective in hepatitis B." The Journal of clinical investigation **128**(10): 4588-4603.
Cattoglio, C., G. Facchini, D. Sartori, A. Antonelli, A. Miccio, B. Cassani, M. Schmidt, C. Von Kalle, S. Howe and A. J. Thrasher (2007). "Hot spots of retroviral integration in human CD34+ hematopoietic cells." Blood, The Journal of the American Society of Hematology **110**(6): 1770-1778.
Chandran, S. S., R. P. Somerville, J. C. Yang, R. M. Sherry, C. A. Klebanoff, S. L. Goff, J. R. Wunderlich, D. N. Danforth, D. Zlott and B. C. Paria (2017). "Treatment of metastatic uveal melanoma with adoptive transfer of tumour-infiltrating lymphocytes: a single-centre, two-stage, single-arm, phase 2 study." The Lancet Oncology **18**(6): 792-802.
Chu, C. and Y. Liaw (1995). "Membrane staining for hepatitis B surface antigen on hepatocytes: a sensitive and specific marker of active viral replication in hepatitis B." Journal of clinical pathology **48**(5): 470-473.
Ciceri, F., C. Bonini, M. T. L. Stanghellini, A. Bondanza, C. Traversari, M. Salomoni, L. Turchetto, S. Colombi, M. Bernardi and J. Peccatori (2009). "Infusion of suicide-gene-engineered donor lymphocytes after family haploidentical haemopoietic stem-cell transplantation for leukaemia (the TK007 trial): a non-randomised phase I–II study." The lancet oncology **10**(5): 489-500.
Clemente, C. G., M. C. Mihm Jr, R. Bufalino, S. Zurrida, P. Collini and N. Cascinelli (1996). "Prognostic value of tumor infiltrating lymphocytes in the vertical growth phase of primary cutaneous melanoma." Cancer: Interdisciplinary International Journal of the American Cancer Society **77**(7): 1303-1310.
Cooksley, W. G. (2004). Treatment with interferons (including pegylated interferons) in patients with hepatitis B. Seminars in liver disease, Copyright© 2004 by Thieme Medical Publishers, Inc., 333 Seventh Avenue, New ….
Dandri, M. and S. Locarnini (2012). "New insight in the pathobiology of hepatitis B virus infection." Gut **61**(Suppl 1): i6-i17.
Dane, D., C. Cameron and M. Briggs (1970). "Virus-like particles in serum of patients with Australia-antigen-associated hepatitis." The lancet **295**(7649): 695-698.
Davé, U. P., N. A. Jenkins and N. G. Copeland (2004). "Gene therapy insertional mutagenesis insights." Science **303**(5656): 333-333.
Davila, M. L., I. Riviere, X. Wang, S. Bartido, J. Park, K. Curran, S. S. Chung, J. Stefanski, O. Borquez-Ojeda and M. Olszewska (2014). "Efficacy and toxicity management of 19-28z CAR T cell therapy in B cell acute lymphoblastic leukemia." Science translational medicine **6**(224): 224ra225-224ra225.
Di Stasi, A., S.-K. Tey, G. Dotti, Y. Fujita, A. Kennedy-Nasser, C. Martinez, K. Straathof, E. Liu, A. G. Durett and B. Grilley (2011). "Inducible apoptosis as a safety switch for adoptive cell therapy." New England Journal of Medicine **365**(18): 1673-1683.
Diaconu, I., B. Ballard, M. Zhang, Y. Chen, J. West, G. Dotti and B. Savoldo (2017). "Inducible caspase-9 selectively modulates the toxicities of CD19-specific chimeric antigen receptor-modified T cells." Molecular Therapy **25**(3): 580-592.
Dong, C., L. Qu, H. Wang, L. Wei, Y. Dong and S. Xiong (2015). "Targeting hepatitis B virus cccDNA by CRISPR/Cas9 nuclease efficiently inhibits viral replication." Antiviral research **118**: 110-117.
Doudna, J. A. and E. Charpentier (2014). "The new frontier of genome engineering with CRISPR-Cas9." Science **346**(6213): 1258096.

Dudley, M. E., J. R. Wunderlich, T. E. Shelton, J. Even and S. A. Rosenberg (2003). "Generation of tumor-infiltrating lymphocyte cultures for use in adoptive transfer therapy for melanoma patients." Journal of immunotherapy (Hagerstown, Md.: 1997) **26**(4): 332.
El-Samaligy, M. S., Y. Rojanasakul, J. F. Charlton, G. W. Weinstein and J. K. Lim (1996). "Ocular disposition of nanoencapsulated acyclovir and ganciclovir via intravitreal injection in rabbit's eye." Drug Delivery **3**(2): 93-97.
Eshhar, Z., T. Waks, G. Gross and D. G. Schindler (1993). "Specific activation and targeting of cytotoxic lymphocytes through chimeric single chains consisting of antibody-binding domains and the gamma or zeta subunits of the immunoglobulin and T-cell receptors." Proceedings of the National Academy of Sciences **90**(2): 720-724.
Fedorov, V. D., M. Themeli and M. Sadelain (2013). "PD-1–and CTLA-4–based inhibitory chimeric antigen receptors (iCARs) divert off-target immunotherapy responses." Science translational medicine **5**(215): 215ra172-215ra172.
Festag, M. M., J. Festag, S. P. Fräßle, T. Asen, J. Sacherl, S. Schreiber, M. A. Mück-Häusl, D. H. Busch, K. Wisskirchen and U. Protzer (2019). "Evaluation of a fully human, hepatitis B virus-specific chimeric antigen receptor in an immunocompetent mouse model." Molecular Therapy **27**(5): 947-959.
Fung, J., C.-L. Lai, W.-K. Seto and M.-F. Yuen (2011). "Nucleoside/nucleotide analogues in the treatment of chronic hepatitis B." Journal of antimicrobial chemotherapy **66**(12): 2715-2725.
Gargett, T. and M. P. Brown (2014). "The inducible caspase-9 suicide gene system as a “safety switch” to limit on-target, off-tumor toxicities of chimeric antigen receptor T cells." Frontiers in pharmacology **5**: 235.
Gehring, A. J., S.-A. Xue, Z. Z. Ho, D. Teoh, C. Ruedl, A. Chia, S. Koh, S. G. Lim, M. K. Maini and H. Stauss (2011). "Engineering virus-specific T cells that target HBV infected hepatocytes and hepatocellular carcinoma cell lines." Journal of hepatology **55**(1): 103-110.
Glebe, D., S. Urban, E. V. Knoop, N. Çağ, P. Krass, S. Grün, A. Bulavaite, K. Sasnauskas and W. H. Gerlich (2005). "Mapping of the hepatitis B virus attachment site by use of infection-inhibiting preS1 lipopeptides and tupaia hepatocytes." Gastroenterology **129**(1): 234-245.
Greco, R., G. Oliveira, M. T. L. Stanghellini, L. Vago, A. Bondanza, J. Peccatori, N. Cieri, S. Marktel, S. Mastaglio and C. Bordignon (2015). "Improving the safety of cell therapy with the TK-suicide gene." Frontiers in pharmacology **6**: 95.
Grupp, S. A., M. Kalos, D. Barrett, R. Aplenc, D. L. Porter, S. R. Rheingold, D. T. Teachey, A. Chew, B. Hauck and J. F. Wright (2013). "Chimeric antigen receptor–modified T cells for acute lymphoid leukemia." New England Journal of Medicine **368**(16): 1509-1518.
Hakami, A., A. Ali and A. Hakami (2013). "Effects of hepatitis B virus mutations on its replication and liver disease severity." The open virology journal **7**: 12.
Han, D., Z. Xu, Y. Zhuang, Z. Ye and Q. Qian (2021). "Current progress in CAR-T cell therapy for hematological malignancies." Journal of Cancer **12**(2): 326.
Harris, D. T. and D. M. Kranz (2016). "Adoptive T cell therapies: a comparison of T cell receptors and chimeric antigen receptors." Trends in pharmacological sciences **37**(3): 220-230.
Hegde, M., M. Mukherjee, Z. Grada, A. Pignata, D. Landi, S. A. Navai, A. Wakefield, K. Fousek, K. Bielamowicz and K. K. Chow (2016). "Tandem CAR T cells targeting HER2 and IL13Rα2 mitigate tumor antigen escape." The Journal of clinical investigation **126**(8): 3036-3052.

Heymach, J., L. Krilov, A. Alberg, N. Baxter, S. M. Chang, R. B. Corcoran, W. Dale, A. DeMichele, C. S. Magid Diefenbach and R. Dreicer (2018). "Clinical cancer advances 2018: annual report on progress against cancer from the American Society of Clinical Oncology." Journal of Clinical Oncology **36**(10): 1020-1044.
Hombach, A., A. Hombach and H. Abken (2010). "Adoptive immunotherapy with genetically engineered T cells: modification of the IgG1 Fc 'spacer'domain in the extracellular moiety of chimeric antigen receptors avoids 'off-target'activation and unintended initiation of an innate immune response." Gene therapy **17**(10): 1206-1213.
Hoyos, V., B. Savoldo, C. Quintarelli, A. Mahendravada, M. Zhang, J. Vera, H. E. Heslop, C. M. Rooney, M. K. Brenner and G. Dotti (2010). "Engineering CD19-specific T lymphocytes with interleukin-15 and a suicide gene to enhance their anti-lymphoma/leukemia effects and safety." Leukemia **24**(6): 1160-1170.
Hu, J. and K. Liu (2017). "Complete and incomplete hepatitis B virus particles: formation, function, and application." Viruses **9**(3): 56.
Huang, J., M. Brameshuber, X. Zeng, J. Xie, Q.-j. Li, Y.-h. Chien, S. Valitutti and M. M. Davis (2013). "A single peptide-major histocompatibility complex ligand triggers digital cytokine secretion in CD4+ T cells." Immunity **39**(5): 846-857.
Hwu, P., J. Yang, R. Cowherd, J. Treisman, G. Shafer, Z. Eshhar and S. Rosenberg (1995). "In vivo antitumor activity of T cells redirected with chimeric antibody/T-cell receptor genes." Cancer research **55**(15): 3369-3373.
Ilan, Y., A. Nagler, R. Adler, E. Naparstek, R. Or, S. Slavin, C. Brautba and D. Shouva (1993). "Adoptive transfer of immunity to hepatitis B virus after T cell–depleted allogeneic bone marrow transplantation." Hepatology **18**(2): 246-252.
Introna, M., A. M. Barbui, F. Bambacioni, C. Casati, G. Gaipa, G. Borleri, S. Bernasconi, T. Barbui, J. Golay and A. Biondi (2000). "Genetic modification of human T cells with CD20: a strategy to purify and lyse transduced cells with anti-CD20 antibodies." Human gene therapy **11**(4): 611-620.
Iuliucci, J. D., S. D. Oliver, S. Morley, C. Ward, J. Ward, D. Dalgarno, T. Clackson and H. J. Berger (2001). "Intravenous safety and pharmacokinetics of a novel dimerizer drug, AP1903, in healthy volunteers." The Journal of Clinical Pharmacology **41**(8): 870-879.
Jacques, P., G. Moens, I. Desombere, J. Dewijngaert, G. Leroux-Roels, M. Wettendorff and S. Thoelen (2002). "The immunogenicity and reactogenicity profile of a candidate hepatitis B vaccine in an adult vaccine non-responder population." Vaccine **20**(31-32): 3644-3649.
Janas, M. L., P. Groves, N. Kienzle and A. Kelso (2005). "IL-2 regulates perforin and granzyme gene expression in CD8+ T cells independently of its effects on survival and proliferation." The Journal of Immunology **175**(12): 8003-8010.
Jiang, M., R. Broering, M. Trippler, L. Poggenpohl, M. Fiedler, G. Gerken, M. Lu and J. Schlaak (2014). "Toll-like receptor-mediated immune responses are attenuated in the presence of high levels of hepatitis B virus surface antigen." Journal of viral hepatitis **21**(12): 860-872.
John, L. B., C. Devaud, C. P. Duong, C. S. Yong, P. A. Beavis, N. M. Haynes, M. T. Chow, M. J. Smyth, M. H. Kershaw and P. K. Darcy (2013). "Anti-PD-1 antibody therapy potently enhances the eradication of established tumors by gene-modified T cells." Clinical cancer research **19**(20): 5636-5646.
Jones, B. S., L. S. Lamb, F. Goldman and A. Di Stasi (2014). "Improving the safety of cell therapy products by suicide gene transfer." Frontiers in pharmacology **5**: 254.
Kageyama, S., H. Ikeda, Y. Miyahara, N. Imai, M. Ishihara, K. Saito, S. Sugino, S. Ueda, T. Ishikawa and S. Kokura (2015). "Adoptive transfer of MAGE-A4 T-cell

receptor gene-transduced lymphocytes in patients with recurrent esophageal cancer." Clinical Cancer Research **21**(10): 2268-2277.
Kah, J., S. Koh, T. Volz, E. Ceccarello, L. Allweiss, M. Lütgehetmann, A. Bertoletti and M. Dandri (2017). "Lymphocytes transiently expressing virus-specific T cell receptors reduce hepatitis B virus infection." The Journal of clinical investigation **127**(8): 3177-3188.
Kieback, E., J. Charo, D. Sommermeyer, T. Blankenstein and W. Uckert (2008). "A safeguard eliminates T cell receptor gene-modified autoreactive T cells after adoptive transfer." Proceedings of the National Academy of Sciences **105**(2): 623-628.
KIM, T. W., M. N. KIM, J. W. KWON, K. M. KIM, S. H. KIM, W. Kim, H. W. PARK, Y. S. CHANG, S. H. CHO and K. U. MIN (2010). "Risk of hepatitis B virus reactivation in patients with asthma or chronic obstructive pulmonary disease treated with corticosteroids." Respirology **15**(7): 1092-1097.
Klopp, A., S. Schreiber, A. D. Kosinska, M. Pulé, U. Protzer and K. Wisskirchen (2021). "Depletion of T cells via Inducible Caspase 9 Increases Safety of Adoptive T-Cell Therapy Against Chronic Hepatitis B." Frontiers in Immunology **12**(4118).
Kloss, C. C., M. Condomines, M. Cartellieri, M. Bachmann and M. Sadelain (2013). "Combinatorial antigen recognition with balanced signaling promotes selective tumor eradication by engineered T cells." Nature biotechnology **31**(1): 71.
Ko, C., T. Michler and U. Protzer (2017). "Novel viral and host targets to cure hepatitis B." Current opinion in virology **24**: 38-45.
Korenman, J., B. Baker, J. Waggoner, J. E. Everhart, A. M. Di Bisceglie and J. H. Hoofnagle (1991). "Long-term remission of chronic hepatitis B after alpha-interferon therapy." Annals of internal medicine **114**(8): 629-634.
Kosinska, A. D., T. Bauer and U. Protzer (2017). "Therapeutic vaccination for chronic hepatitis B." Current opinion in virology **23**: 75-81.
Kowolik, C. M., M. S. Topp, S. Gonzalez, T. Pfeiffer, S. Olivares, N. Gonzalez, D. D. Smith, S. J. Forman, M. C. Jensen and L. J. Cooper (2006). "CD28 costimulation provided through a CD19-specific chimeric antigen receptor enhances in vivo persistence and antitumor efficacy of adoptively transferred T cells." Cancer research **66**(22): 10995-11004.
Krebs, K., N. Böttinger, L. R. Huang, M. Chmielewski, S. Arzberger, G. Gasteiger, C. Jäger, E. Schmitt, F. Bohne and M. Aichler (2013). "T cells expressing a chimeric antigen receptor that binds hepatitis B virus envelope proteins control virus replication in mice." Gastroenterology **145**(2): 456-465.
Kuball, J., M. L. Dossett, M. Wolfl, W. Y. Ho, R.-H. Voss, C. Fowler and P. D. Greenberg (2007). "Facilitating matched pairing and expression of TCR chains introduced into human T cells." Blood **109**(6): 2331-2338.
Lan, T., L. Chang, L. Wu and Y.-F. Yuan (2015). "IL-6 plays a crucial role in HBV infection." Journal of clinical and translational hepatology **3**(4): 271.
Lau, G., A. Lok, R. Liang, C. L. Lai, E. Chiu, Y. L. Lau and S. K. Lam (1997). "Clearance of hepatitis B surface antigen after bone marrow transplantation: role of adoptive immunity transfer." Hepatology **25**(6): 1497-1501.
Lee, D. W., R. Gardner, D. L. Porter, C. U. Louis, N. Ahmed, M. Jensen, S. A. Grupp and C. L. Mackall (2014). "Current concepts in the diagnosis and management of cytokine release syndrome." Blood, The Journal of the American Society of Hematology **124**(2): 188-195.
Li, W., J. Han and H. Wu (2016). "Regulatory T-cells promote hepatitis B virus infection and hepatocellular carcinoma progression." Chronic diseases and translational medicine **2**(2): 67-80.

Li, X., H. Kong, L. Tian, Q. Zhu, Y. Wang, Y. Dong, Q. Ni and Y. Chen (2014). "Changes of costimulatory molecule CD28 on circulating CD8+ T cells correlate with disease pathogenesis of chronic hepatitis B." BioMed research international **2014**.
Li, Z., J. Düllmann, B. Schiedlmeier, M. Schmidt, C. von Kalle, J. Meyer, M. Forster, C. Stocking, A. Wahlers and O. Frank (2002). "Murine leukemia induced by retroviral gene marking." Science **296**(5567): 497-497.
Linette, G. P., E. A. Stadtmauer, M. V. Maus, A. P. Rapoport, B. L. Levine, L. Emery, L. Litzky, A. Bagg, B. M. Carreno and P. J. Cimino (2013). "Cardiovascular toxicity and titin cross-reactivity of affinity-enhanced T cells in myeloma and melanoma." Blood, The Journal of the American Society of Hematology **122**(6): 863-871.
Liu, Z., O. Chen, J. B. J. Wall, M. Zheng, Y. Zhou, L. Wang, H. R. Vaseghi, L. Qian and J. Liu (2017). "Systematic comparison of 2A peptides for cloning multi-genes in a polycistronic vector." Scientific reports **7**(1): 1-9.
Locke, F. L., A. Ghobadi, C. A. Jacobson, D. B. Miklos, L. J. Lekakis, O. O. Oluwole, Y. Lin, I. Braunschweig, B. T. Hill and J. M. Timmerman (2019). "Long-term safety and activity of axicabtagene ciloleucel in refractory large B-cell lymphoma (ZUMA-1): a single-arm, multicentre, phase 1–2 trial." The lancet oncology **20**(1): 31-42.
Lucifora, J., Y. Xia, F. Reisinger, K. Zhang, D. Stadler, X. Cheng, M. F. Sprinzl, H. Koppensteiner, Z. Makowska and T. Volz (2014). "Specific and nonhepatotoxic degradation of nuclear hepatitis B virus cccDNA." Science **343**(6176): 1221-1228.
Maini, M. K., C. Boni, G. S. Ogg, A. S. King, S. Reignat, C. K. Lee, J. R. Larrubia, G. J. Webster, A. J. McMichael and C. Ferrari (1999). "Direct ex vivo analysis of hepatitis B virus-specific CD8+ T cells associated with the control of infection." Gastroenterology **117**(6): 1386-1396.
Maraninchi, D., D. Blaise, B. Rio, V. Leblond, F. Dreyfus, E. Gluckman, D. Guyotat, J. Pico, M. Michallet and N. Ifrah (1987). "Impact of T-cell depletion on outcome of allogeneic bone-marrow transplantation for standard-risk leukaemias." The lancet **330**(8552): 175-178.
Marin, V., E. Cribioli, B. Philip, S. Tettamanti, I. Pizzitola, A. Biondi, E. Biagi and M. Pule (2012). "Comparison of different suicide-gene strategies for the safety improvement of genetically manipulated T cells." Human gene therapy methods **23**(6): 376-386.
Matsumoto, K., A. Shigemi, K. Ikawa, N. Kanazawa, Y. Fujisaki, N. Morikawa and Y. Takeda (2015). "Risk factors for ganciclovir-induced thrombocytopenia and leukopenia." Biological and Pharmaceutical Bulletin **38**(2): 235-238.
Maude, S. L., D. Barrett, D. T. Teachey and S. A. Grupp (2014). "Managing cytokine release syndrome associated with novel T cell-engaging therapies." Cancer journal (Sudbury, Mass.) **20**(2): 119.
Maude, S. L., N. Frey, P. A. Shaw, R. Aplenc, D. M. Barrett, N. J. Bunin, A. Chew, V. E. Gonzalez, Z. Zheng and S. F. Lacey (2014). "Chimeric antigen receptor T cells for sustained remissions in leukemia." New England Journal of Medicine **371**(16): 1507-1517.
Maude, S. L., T. W. Laetsch, J. Buechner, S. Rives, M. Boyer, H. Bittencourt, P. Bader, M. R. Verneris, H. E. Stefanski and G. D. Myers (2018). "Tisagenlecleucel in children and young adults with B-cell lymphoblastic leukemia." New England Journal of Medicine **378**(5): 439-448.
Mestermann, K., T. Giavridis, J. Weber, J. Rydzek, S. Frenz, T. Nerreter, A. Mades, M. Sadelain, H. Einsele and M. Hudecek (2019). "The tyrosine kinase inhibitor dasatinib acts as a pharmacologic on/off switch for CAR T cells." Science translational medicine **11**(499).

Minagawa, K., M. O. Jamil, M. Al-Obaidi, L. Pereboeva, D. Salzman, H. P. Erba, L. S. Lamb, R. Bhatia, S. Mineishi and A. Di Stasi (2016). "In vitro pre-clinical validation of suicide gene modified anti-CD33 redirected chimeric antigen receptor T-cells for acute myeloid leukemia." PLoS One **11**(12): e0166891.
Monjezi, R., C. Miskey, T. Gogishvili, M. Schleef, M. Schmeer, H. Einsele, Z. Ivics and M. Hudecek (2017). "Enhanced CAR T-cell engineering using non-viral Sleeping Beauty transposition from minicircle vectors." Leukemia **31**(1): 186-194.
Moon, E. K., L.-C. Wang, D. V. Dolfi, C. B. Wilson, R. Ranganathan, J. Sun, V. Kapoor, J. Scholler, E. Puré and M. C. Milone (2014). "Multifactorial T-cell hypofunction that is reversible can limit the efficacy of chimeric antigen receptor–transduced human T cells in solid tumors." Clinical Cancer Research **20**(16): 4262-4273.
Morgan, R. A., M. E. Dudley, J. R. Wunderlich, M. S. Hughes, J. C. Yang, R. M. Sherry, R. E. Royal, S. L. Topalian, U. S. Kammula and N. P. Restifo (2006). "Cancer regression in patients after transfer of genetically engineered lymphocytes." Science **314**(5796): 126-129.
Morgan, R. A., J. C. Yang, M. Kitano, M. E. Dudley, C. M. Laurencot and S. A. Rosenberg (2010). "Case report of a serious adverse event following the administration of T cells transduced with a chimeric antigen receptor recognizing ERBB2." Molecular Therapy **18**(4): 843-851.
Munshi, N. C., L. D. Anderson Jr, N. Shah, D. Madduri, J. Berdeja, S. Lonial, N. Raje, Y. Lin, D. Siegel and A. Oriol (2021). "Idecabtagene vicleucel in relapsed and refractory multiple myeloma." New England Journal of Medicine **384**(8): 705-716.
Nassal, M. (2015). "HBV cccDNA: viral persistence reservoir and key obstacle for a cure of chronic hepatitis B." Gut **64**(12): 1972-1984.
Neelapu, S. S., J. M. Rossi, C. A. Jacobson, F. L. Locke, D. B. Miklos, P. M. Reagan, S. J. Rodig, L. J. Lekakis, I. W. Flinn and L. Zheng (2019). "CD19-loss with preservation of other B cell lineage features in patients with large B cell lymphoma who relapsed post-axi-cel." Blood **134**: 203.
Neelapu, S. S., S. Tummala, P. Kebriaei, W. Wierda, C. Gutierrez, F. L. Locke, K. V. Komanduri, Y. Lin, N. Jain and N. Daver (2018). "Chimeric antigen receptor T-cell therapy—assessment and management of toxicities." Nature reviews Clinical oncology **15**(1): 47.
Niederau, C., T. Heintges, S. Lange, G. Goldmann, C. M. Niederau, L. Mohr and D. Häussinger (1996). "Long-term follow-up of HBeAg-positive patients treated with interferon alfa for chronic hepatitis B." New England Journal of Medicine **334**(22): 1422-1427.
Norelli, M., B. Camisa, G. Barbiera, L. Falcone, A. Purevdorj, M. Genua, F. Sanvito, M. Ponzoni, C. Doglioni and P. Cristofori (2018). "Monocyte-derived IL-1 and IL-6 are differentially required for cytokine-release syndrome and neurotoxicity due to CAR T cells." Nature medicine **24**(6): 739-748.
Parkhurst, M. R., J. C. Yang, R. C. Langan, M. E. Dudley, D.-A. N. Nathan, S. A. Feldman, J. L. Davis, R. A. Morgan, M. J. Merino and R. M. Sherry (2011). "T cells targeting carcinoembryonic antigen can mediate regression of metastatic colorectal cancer but induce severe transient colitis." Molecular Therapy **19**(3): 620-626.
Peeridogaheh, H., Z. Meshkat, S. Habibzadeh, M. Arzanlou, J. M. Shahi, S. Rostami, S. Gerayli and R. Teimourpour (2018). "Current concepts on immunopathogenesis of hepatitis B virus infection." Virus research **245**: 29-43.
Perica, K., J. C. Varela, M. Oelke and J. Schneck (2015). "Adoptive T cell immunotherapy for cancer." Rambam Maimonides medical journal **6**(1).

Philip, B., E. Kokalaki, L. Mekkaoui, S. Thomas, K. Straathof, B. Flutter, V. Marin, T. Marafioti, R. Chakraverty and D. Linch (2014). "A highly compact epitope-based marker/suicide gene for easier and safer T-cell therapy." Blood, The Journal of the American Society of Hematology **124**(8): 1277-1287.
Pol, S. and P. Lampertico (2012). "First-line treatment of chronic hepatitis B with entecavir or tenofovir in 'real-life'settings: from clinical trials to clinical practice." Journal of viral hepatitis **19**(6): 377-386.
Publicover, J., A. Gaggar, J. M. Jespersen, U. Halac, A. J. Johnson, A. Goodsell, L. Avanesyan, S. L. Nishimura, M. Holdorf and K. G. Mansfield (2018). "An OX40/OX40L interaction directs successful immunity to hepatitis B virus." Science translational medicine **10**(433): eaah5766.
Qasim, W., M. Brunetto, A. J. Gehring, S.-A. Xue, A. Schurich, A. Khakpoor, H. Zhan, P. Ciccorossi, K. Gilmour and D. Cavallone (2015). "Immunotherapy of HCC metastases with autologous T cell receptor redirected T cells, targeting HBsAg in a liver transplant patient." Journal of hepatology **62**(2): 486-491.
Rehermann, B., P. Fowler, J. Sidney, J. Person, A. Redeker, M. Brown, B. Moss, A. Sette and F. V. Chisari (1995). "The cytotoxic T lymphocyte response to multiple hepatitis B virus polymerase epitopes during and after acute viral hepatitis." The Journal of experimental medicine **181**(3): 1047-1058.
Ringelhan, M., T. O'Connor, U. Protzer and M. Heikenwalder (2015). "The direct and indirect roles of HBV in liver cancer: prospective markers for HCC screening and potential therapeutic targets." The Journal of pathology **235**(2): 355-367.
Robbins, P. F., S. H. Kassim, T. L. Tran, J. S. Crystal, R. A. Morgan, S. A. Feldman, J. C. Yang, M. E. Dudley, J. R. Wunderlich and R. M. Sherry (2015). "A pilot trial using lymphocytes genetically engineered with an NY-ESO-1–reactive T-cell receptor: long-term follow-up and correlates with response." Clinical Cancer Research **21**(5): 1019-1027.
Robbins, P. F., R. A. Morgan, S. A. Feldman, J. C. Yang, R. M. Sherry, M. E. Dudley, J. R. Wunderlich, A. V. Nahvi, L. J. Helman and C. L. Mackall (2011). "Tumor regression in patients with metastatic synovial cell sarcoma and melanoma using genetically engineered lymphocytes reactive with NY-ESO-1." Journal of Clinical Oncology **29**(7): 917.
Robek, M. D., B. S. Boyd, S. F. Wieland and F. V. Chisari (2004). "Signal transduction pathways that inhibit hepatitis B virus replication." Proceedings of the National Academy of Sciences **101**(6): 1743-1747.
Rohaan, M. W., S. Wilgenhof and J. B. Haanen (2019). "Adoptive cellular therapies: the current landscape." Virchows Archiv **474**(4): 449-461.
Rosenberg, S. A., P. Spiess and R. Lafreniere (1986). "A new approach to the adoptive immunotherapy of cancer with tumor-infiltrating lymphocytes." Science **233**(4770): 1318-1321.
Ruby, J. and I. Ramshaw (1991). "The antiviral activity of immune CD8+ T cells is dependent on interferon-gamma." Lymphokine and cytokine research **10**(5): 353-358.
Sadelain, M., R. Brentjens and I. Rivière (2013). "The basic principles of chimeric antigen receptor design." Cancer discovery **3**(4): 388-398.
Santomasso, B., C. Bachier, J. Westin, K. Rezvani and E. J. Shpall (2019). "The other side of CAR T-cell therapy: cytokine release syndrome, neurologic toxicity, and financial burden." American Society of Clinical Oncology Educational Book **39**: 433-444.
Schmidt, J., H. E. Blum and R. Thimme (2013). "T-cell responses in hepatitis B and C virus infection: similarities and differences." Emerging microbes & infections **2**(1): 1-8.

Schuch, A., E. S. Alizei, K. Heim, D. Wieland, M. M. Kiraithe, J. Kemming, S. Llewellyn-Lacey, Ö. Sogukpinar, Y. Ni and S. Urban (2019). "Phenotypic and functional differences of HBV core-specific versus HBV polymerase-specific CD8+ T cells in chronically HBV-infected patients with low viral load." Gut **68**(5): 905-915.
Schurich, A., P. Khanna, A. R. Lopes, K. J. Han, D. Peppa, L. Micco, G. Nebbia, P. T. Kennedy, A. M. Geretti and G. Dusheiko (2011). "Role of the coinhibitory receptor cytotoxic T lymphocyte antigen-4 on apoptosis-Prone CD8 T cells in persistent hepatitis B virus infection." Hepatology **53**(5): 1494-1503.
Schuster, S., M. R. Bishop, C. Tam, E. K. Waller, P. Borchmann, J. McGuirk, U. Jäger, S. Jaglowski, C. Andreadis and J. Westin (2017). "Global Pivotal Phase 2 trial of the CD19-targeted therapy CTL019 in adult patients with relapsed or refractory (R/R) diffuse large B-cell lymphoma (DLBCL)—an interim analysis." Hematological Oncology **35**: 27-27.
Seeger, C. and W. S. Mason (2015). "Molecular biology of hepatitis B virus infection." Virology **479**: 672-686.
Sheth, V. S. and J. Gauthier (2021). "Taming the beast: CRS and ICANS after CAR T-cell therapy for ALL." Bone marrow transplantation **56**(3): 552-566.
Shi, B., G. Ren, Y. Hu, S. Wang, Z. Zhang and Z. Yuan (2012). "HBsAg inhibits IFN-α production in plasmacytoid dendritic cells through TNF-α and IL-10 induction in monocytes." PloS one **7**(9).
Shimabukuro-Vornhagen, A., P. Gödel, M. Subklewe, H. J. Stemmler, H. A. Schlößer, M. Schlaak, M. Kochanek, B. Böll and M. S. von Bergwelt-Baildon (2018). "Cytokine release syndrome." Journal for immunotherapy of cancer **6**(1): 56.
Shouval, D. and O. Shibolet (2013). Immunosuppression and HBV reactivation. Seminars in liver disease, Thieme Medical Publishers.
Straathof, K. C., M. A. Pule, P. Yotnda, G. Dotti, E. F. Vanin, M. K. Brenner, H. E. Heslop, D. M. Spencer and C. M. Rooney (2005). "An inducible caspase 9 safety switch for T-cell therapy." Blood **105**(11): 4247-4254.
Tan, A. T. and S. Schreiber (2020). "Adoptive T-cell therapy for HBV-associated HCC and HBV infection." Antiviral research **176**: 104748.
Tang, H., L. Delgermaa, F. Huang, N. Oishi, L. Liu, F. He, L. Zhao and S. Murakami (2005). "The transcriptional transactivation function of HBx protein is important for its augmentation role in hepatitis B virus replication." Journal of virology **79**(9): 5548-5556.
Tang, H., N. Oishi, S. Kaneko and S. Murakami (2006). "Molecular functions and biological roles of hepatitis B virus x protein." Cancer science **97**(10): 977-983.
Tang, L. S., E. Covert, E. Wilson and S. Kottilil (2018). "Chronic hepatitis B infection: a review." Jama **319**(17): 1802-1813.
Teachey, D. T., S. R. Rheingold, S. L. Maude, G. Zugmaier, D. M. Barrett, A. E. Seif, K. E. Nichols, E. K. Suppa, M. Kalos and R. A. Berg (2013). "Cytokine release syndrome after blinatumomab treatment related to abnormal macrophage activation and ameliorated with cytokine-directed therapy." Blood, The Journal of the American Society of Hematology **121**(26): 5154-5157.
Tey, S.-K., G. Dotti, C. M. Rooney, H. E. Heslop and M. K. Brenner (2007). "Inducible caspase 9 suicide gene to improve the safety of allodepleted T cells after haploidentical stem cell transplantation." Biology of Blood and Marrow Transplantation **13**(8): 913-924.
Tey, S. K. (2014). "Adoptive T-cell therapy: adverse events and safety switches." Clinical & translational immunology **3**(6): e17.

Thimme, R., S. Wieland, C. Steiger, J. Ghrayeb, K. A. Reimann, R. H. Purcell and F. V. Chisari (2003). "CD8+ T cells mediate viral clearance and disease pathogenesis during acute hepatitis B virus infection." Journal of virology **77**(1): 68-76.
Tillmann, H. L. and K. Patel (2014). "Therapy of acute and fulminant hepatitis B." Intervirology **57**(3-4): 181-188.
Trono, D. (2003). "Picking the right spot." Science **300**(5626): 1670-1671.
Urbani, S., C. Boni, B. Amadei, P. Fisicaro, S. Cerioni, M. A. Valli, G. Missale and C. Ferrari (2005). "Acute phase HBV-specific T cell responses associated with HBV persistence after HBV/HCV coinfection." Hepatology **41**(4): 826-831.
Valitutti, S., S. Müller, M. Cella, E. Padovan and A. Lanzavecchia (1995). "Serial triggering of many T-cell receptors by a few peptide–MHC complexes." Nature **375**(6527): 148-151.
van Loenen, M. M., R. de Boer, A. L. Amir, R. S. Hagedoorn, G. L. Volbeda, R. Willemze, J. J. van Rood, J. F. Falkenburg and M. H. Heemskerk (2010). "Mixed T cell receptor dimers harbor potentially harmful neoreactivity." Proceedings of the National Academy of Sciences **107**(24): 10972-10977.
Visvanathan, K., N. A. Skinner, A. J. Thompson, S. M. Riordan, V. Sozzi, R. Edwards, S. Rodgers, J. Kurtovic, J. Chang and S. Lewin (2007). "Regulation of Toll-like receptor-2 expression in chronic hepatitis B by the precore protein." Hepatology **45**(1): 102-110.
Wang, H., H. Luo, X. Wan, X. Fu, Q. Mao, X. Xiang, Y. Zhou, W. He, J. Zhang and Y. Guo (2020). "TNF-α/IFN-γ profile of HBV-specific CD4 T cells is associated with liver damage and viral clearance in chronic HBV infection." Journal of hepatology **72**(1): 45-56.
Wang, S., Z. Chen, C. Hu, F. Qian, Y. Cheng, M. Wu, B. Shi, J. Chen, Y. Hu and Z. Yuan (2013). "Hepatitis B virus surface antigen selectively inhibits TLR2 ligand–induced IL-12 production in monocytes/macrophages by interfering with JNK activation." The Journal of Immunology **190**(10): 5142-5151.
Wang, X., W.-C. Chang, C. W. Wong, D. Colcher, M. Sherman, J. R. Ostberg, S. J. Forman, S. R. Riddell and M. C. Jensen (2011). "A transgene-encoded cell surface polypeptide for selection, in vivo tracking, and ablation of engineered cells." Blood, The Journal of the American Society of Hematology **118**(5): 1255-1263.
Warda, W., F. Larosa, M. N. Da Rocha, R. Trad, E. Deconinck, Z. Fajloun, C. Faure, D. Caillot, M. Moldovan and S. Valmary-Degano (2019). "CML Hematopoietic Stem Cells Expressing IL1RAP Can Be Targeted by Chimeric Antigen Receptor–Engineered T Cells." Cancer research **79**(3): 663-675.
Wherry, E. J., J. N. Blattman, K. Murali-Krishna, R. Van Der Most and R. Ahmed (2003). "Viral persistence alters CD8 T-cell immunodominance and tissue distribution and results in distinct stages of functional impairment." Journal of virology **77**(8): 4911-4927.
Wilkie, S., M. C. van Schalkwyk, S. Hobbs, D. M. Davies, S. J. van der Stegen, A. C. P. Pereira, S. E. Burbridge, C. Box, S. A. Eccles and J. Maher (2012). "Dual targeting of ErbB2 and MUC1 in breast cancer using chimeric antigen receptors engineered to provide complementary signaling." Journal of clinical immunology **32**(5): 1059-1070.
Winkler, U., M. Jensen, O. Manzke, H. Schulz, V. Diehl and A. Engert (1999). "Cytokine-release syndrome in patients with B-cell chronic lymphocytic leukemia and high lymphocyte counts after treatment with an anti-CD20 monoclonal antibody (rituximab, IDEC-C2B8)." Blood, The Journal of the American Society of Hematology **94**(7): 2217-2224.

Wisskirchen, K., J. Kah, A. Malo, T. Asen, T. Volz, L. Allweiss, J. M. Wettengel, M. Lütgehetmann, S. Urban and T. Bauer (2019). "T cell receptor grafting allows virological control of Hepatitis B virus infection." The Journal of clinical investigation **129**(7): 2932-2945.
Wisskirchen, K., K. Metzger, S. Schreiber, T. Asen, L. Weigand, C. Dargel, K. Witter, E. Kieback, M. F. Sprinzl and W. Uckert (2017). "Isolation and functional characterization of hepatitis B virus-specific T-cell receptors as new tools for experimental and clinical use." PloS one **12**(8).
Wu, J., Z. Meng, M. Jiang, R. Pei, M. Trippler, R. Broering, A. Bucchi, J. P. Sowa, U. Dittmer and D. Yang (2009). "Hepatitis B virus suppresses toll-like receptor–mediated innate immune responses in murine parenchymal and nonparenchymal liver cells." Hepatology **49**(4): 1132-1140.
Wu, M., Y. Xu, S. Lin, X. Zhang, L. Xiang and Z. Yuan (2007). "Hepatitis B virus polymerase inhibits the interferon-inducible MyD88 promoter by blocking nuclear translocation of Stat1." Journal of General Virology **88**(12): 3260-3269.
Wudhikarn, K., M. L. Palomba, M. Pennisi, M. Garcia-Recio, J. R. Flynn, S. M. Devlin, A. Afuye, M. L. Silverberg, M. A. Maloy and G. L. Shah (2020). "Infection during the first year in patients treated with CD19 CAR T cells for diffuse large B cell lymphoma." Blood cancer journal **10**(8): 1-11.
Yan, H., G. Zhong, G. Xu, W. He, Z. Jing, Z. Gao, Y. Huang, Y. Qi, B. Peng and H. Wang (2012). "Sodium taurocholate cotransporting polypeptide is a functional receptor for human hepatitis B and D virus." elife **1**: e00049.
Yao, W., J.-c. He, Y. Yang, J.-m. Wang, Y.-w. Qian, T. Yang and L. Ji (2017). "The prognostic value of tumor-infiltrating lymphocytes in hepatocellular carcinoma: a systematic review and meta-analysis." Scientific reports **7**(1): 1-11.
Yoon, H., T. S. Kim and T. J. Braciale (2010). "The cell cycle time of CD8+ T cells responding in vivo is controlled by the type of antigenic stimulus." PloS one **5**(11): e15423.
Yuen, M.-F., D.-S. Chen, G. M. Dusheiko, H. L. Janssen, D. T. Lau, S. A. Locarnini, M. G. Peters and C.-L. Lai (2018). "Hepatitis B virus infection." Nature Reviews Disease Primers **4**(1): 1-20.
Zhang, P., J. Raju, M. A. Ullah, R. Au, A. Varelias, K. H. Gartlan, S. D. Olver, L. D. Samson, E. Sturgeon and N. Zomerdijk (2019). "Phase I trial of inducible caspase 9 T cells in adult stem cell transplant demonstrates massive clonotypic proliferative potential and long-term persistence of transgenic T cells." Clinical Cancer Research **25**(6): 1749-1755.
Zhou, X., A. Di Stasi, S.-K. Tey, R. A. Krance, C. Martinez, K. S. Leung, A. G. Durett, M.-F. Wu, H. Liu and A. M. Leen (2014). "Long-term outcome after haploidentical stem cell transplant and infusion of T cells expressing the inducible caspase 9 safety transgene." Blood, The Journal of the American Society of Hematology **123**(25): 3895-3905.
Zhou, X., G. Dotti, R. A. Krance, C. A. Martinez, S. Naik, R. T. Kamble, A. G. Durett, O. Dakhova, B. Savoldo and A. Di Stasi (2015). "Inducible caspase-9 suicide gene controls adverse effects from alloreplete T cells after haploidentical stem cell transplantation." Blood **125**(26): 4103-4113.
Zhu, A., X. Liao, S. Li, H. Zhao, L. Chen, M. Xu and X. Duan (2019). "HBV cccDNA and its potential as a therapeutic target." Journal of clinical and translational hepatology **7**(3): 258.
Zoulim, F. and D. Durantel (2015). "Antiviral therapies and prospects for a cure of chronic hepatitis B." Cold Spring Harbor perspectives in medicine **5**(4): a021501.

Publications and meetings

Klopp, A., Schreiber, S., Kosinska, A., Pulé, M., Protzer, U., Wisskirchen, K. *Depletion of T cells via inducible caspase 9 increases safety of adoptive T-cell therapy against chronic hepatitis B.* Frontiers in Immunology (October 2021)

Klopp, A., Pulé, M., Protzer, U., Wisskirchen, K. *Activation of inducible caspase 9 allows efficient depletion of adoptively transferred HBV-specific T cells.* Poster presented at the International Liver Congress (ILC) (June 2021)

Klopp, A., Philip, B., Pulé, M., Protzer, U., Wisskirchen, K. *Evaluation of strategies to increase safety of adoptively transferred HBV-specific T cells.* Poster presented at the international HBV Meeting in Melbourne (October 2019)

Klopp, A., Philip, B., Pulé, M., Protzer, U., Wisskirchen, K. *Evaluation of strategies to increase safety of adoptively transferred HBV-specific T cells.* Poster presented at the annual meeting of the German Association of the Study of the Liver (GASL) in Heidelberg (February 2019)

Acknowledgments

First of all, I would like to thank Ulrike Protzer for giving me the opportunity to work on this very interesting project. Thank you for the active support throughout the project and for giving me the chance to attend several congresses that have contributed to my personal development.

Thank you also to Angela Krackhardt who as my mentor and member of my thesis committee gave great input during my thesis committee meetings and thereby substantially contributed to my progress.

My special thanks go to my supervisor Karin Wisskirchen for the excellent supervision of my thesis even when she was on maternal leave. Her outstanding expertise and constructive ideas were the foundation of the success of this thesis. Thank you for always being available and introducing me to the scientific world. Without you, this work would not have been possible.

Finally, I want to thank my family, friends and of course Eloïse for their motivating words and their unconditional support throughout my life. Thank you!

Appenidx

Plasmid sequences

iC9-S-CAR

ATGCTGGAGGGCGTGCAGGTGGAGACCATCAGCCCAGGCGACGGCAGAACCTTCCCC
AAGAGAGGCCAGACCTGCGTGGTGCACTATACCGGCATGCTGGAGGACGGCAAGAAG
GTGGACAGCAGCCGCGACCGCAATAAGCCCTTCAAGTTCATGCTGGGCAAGCAGGAG
GTGATCAGAGGCTGGGAGGAGGGCGTGGCCCAGATGAGCGTGGGCCAGAGAGCCAA
GCTGACCATCAGCCCCGACTACGCCTATGGCGCCACCGGCCACCCCGGCATCATCCCA
CCCCACGCCACCCTGGTGTTTGATGTGGAGCTGCTGAAGCTGGAGTCCGGAGGCGGC
TCCGGCGTGGATGGCTTCGGCGACGTGGGAGCCCTGGAGAGCCTGAGAGGCAACGCC
GATCTGGCCTACATCCTGAGCATGGAGCCCTGTGGCCACTGCCTGATCATCAACAACG
TGAACTTCTGCCGGGAGAGCGGCCTGCGGACCCGGACCGGCAGCAACATCGACTGCG
AGAAGCTGAGGAGGCGCTTCTCCTCCCTGCACTTTATGGTGGAGGTGAAAGGCGATCT
GACTGCCAAGAAAATGGTGCTGGCCCTGCTGGAGCTGGCCCAGCAGGACCACGGAGC
CCTGGATTGCTGTGTGGTGGTGATCCTGTCCCACGGCTGCCAGGCCAGCCACCTGCAG
TTCCCCGGAGCCGTGTACGGCACCGACGGCTGTCCCGTGTCCGTGGAGAAGATCGTG
AACATCTTCAACGGCACCTCCTGCCCCTCCCTGGGCGGCAAGCCCAAGCTGTTCTTTAT
CCAGGCCTGTGGCGGCGAGCAGAAGGACCACGGCTTTGAGGTGGCCAGCACCTCCCC
CGAGGACGAGAGCCCAGGCAGCAACCCCGAGCCCGACGCCACCCCCTTCCAGGAGG
GCCTGCGCACCTTCGACCAGCTGGACGCCATCAGCAGCCTGCCCACCCCCAGCGACA
TCTTCGTGAGCTACAGCACCTTTCCCGGCTTCGTGAGCTGGCGCGATCCCAAGTCCGG
CTCTTGGTATGTGGAGACCCTGGACGACATCTTTGAGCAGTGGGCTCATAGCGAGGAC
CTGCAGAGCCTGCTGCTGCGCGTGGCCAATGCCGTGAGCGTGAAGGGCATCTACAAG
CAGATGCCAGGCTGCTTCAACTTCCTGCGGAAGAAGCTGTTCTTCAAGACCAGCGCCT
CCAGAGCCGAGGGCAGAGGCAGCCTGCTGACCTGCGGCGATGTGGAGGAGAACCCAG
GCCCCATGGATTTCGAGGTGCAGATCTTCAGCTTCCTGCTGATCTCCGCCAGCGTGATC
ATGAGCCGGATGGCCGAAGTGCAGCTGGTGGAATCTGGCGGCGGACTGCTGCAGCCT
GGCGGATCTCTGAGACTGAGCTGTGCCGCCAGCGGCTTCACCTTTAGCGGCTACGCCA
TGAGCTGGGTGCGCCAGGCTCCTGGCAAAGGCCTGGAATGGGTGTCCAGCATCTCTG
GCTCTGGCGGCAGCACCTACTACGCCGATAGCGTGAAGGGCCGGTTCACCATCAGCC
GGGACAACAGCAAGAACACCCTGTACCTGCAGATGAACAGCCTGCGGGCCGAGGACA
CCGCCCTGTACTATTGTGCCAAGCCCCCTGGCCGGCAGGAATATTACGGCAGCTCCAT
CTACTACTTCCCCCTGGGCAATTGGGGCCAGGGCACACTCGTGACAGTGTCCAGCGCC
AGCACCAAGGGCCCCAAGCTGGAAGAGGGCGAGTTCAGCGAAGCCAGAGTGCAGAGC
GCCCTGACACAGCCTGCCTCCGTGTCTGTGGCTCCTGGACAGACCGCCAGAATCACCT
GTGGCGGCAACAACATCGGCAGCAAGAGCGTGCACTGGTATCAGCAGAAGCCCGGCC
AGGCACCTGTGCTGGTGGTGTACGACGACAGCGACAGACCCAGCGGCATCCCCGAGA
GATTCAGCGGCAGCAACTCCGGCAATACCGCCACCCTGACCATCAGCAGAGTGGAAGC
CGGCGACGAGGCCGACTACTACTGCCAAGTGTGGGACAGCAGCAGCGACCTGGTGGT
GTTTGGCGGAGGCACCAAGCTGACAGTGCTGGGCCAGCCTAAAGCCGCCCCTAGCGT
GACCCTGTTCCCTCCTAGTTCTGCCGCCGCAGGCGATCCTGCCGAGCCTAAGAGCCCC
GACAAGACCCACACCTGTCCCCCTTGTCCTGCCCCTGAACTGCTGGGCGGACCTTCCG
TGTTCCTGTTCCCCCCAAAGCCCAAGGACACCCTGATGATCAGCCGGACCCCCGAAGT
GACCTGCGTGGTGGTGGATGTGTCCCACGAGGACCCTGAAGTGAAGTTCAATTGGTAC
GTGGACGGCGTGGAAGTGCACAACGCCAAGACCAAGCCCAGAGAGGAACAGTACAAC
TCCACCTACCGGGTGGTGTCCGTGCTGACCGTGCTGCACCAGGACTGGCTGAACGGC
AAAGAGTACAAGTGCAAGGTGTCCAACAAGGCCCTGCCTGCCCCCATCGAGAAAACCA
TCTCCAAGGCCAAGGGCCAGCCCCGCGAACCCCAGGTGTACACACTGCCCCCTAGCA
GGGACGAGCTGACCAAGAACCAGGTGTCCCTGACCTGTCTCGTGAAGGGATTCTACCC
CTCCGATATCGCCGTGGAATGGGAGAGCAACGGCCAGCCCGAGAACAACTACAAGACC

ACCCCTCCCGTGCTGGACAGCGACGGCTCATTCTTCCTGTACAGCAAACTGACCGTGG
ACAAGAGCCGGTGGCAGCAGGGCAACGTGTTCAGCTGCAGCGTGATGCACGAGGCCC
TGCACAACCACTACACCCAGAAGTCCCTGAGCCTGAGCCCTGGCAAGAAGGACCCCAA
GTTCTGGGTGCTGGTGGTCGTGGGCGGAGTGCTGGCCTGTTACAGCCTGCTCGTGAC
CGTGGCCTTCATCATCTTTTGGGTGCGCAGCAAGCGGAGCCGGCTGCTGCACTCCGAC
TACATGAACATGACCCCCAGACGGCCAGGCCCCACCAGAAAGCACTACCAGCCTTACG
CCCCTCCCAGAGACTTCGCCGCCTACAGATCCCTGCGCGTGAAGTTCTCCAGAAGCGC
CGACGCCCCTGCCTATCAGCAGGGACAGAACCAGCTGTACAACGAGCTGAACCTGGGC
AGACGGGAAGAGTACGACGTGCTGGATAAGCGGAGAGGCCGGGACCCTGAGATGGGC
GGCAAGCCTAGAAGAAAGAACCCCCAGGAAGGCCTGTATAACGAACTGCAGAAAGACA
AGATGGCCGAGGCCTACAGCGAGATCGGCATGAAGGGCGAGCGGAGAAGAGGCAAGG
GCCACGATGGCCTGTACCAGGGACTGAGCACCGCCACAAAGGACACCTATGACGCACT
GCACATGCAGGCTCTGCCCCCCAGATGA

iC9-4G TCR

ATGCTGGAGGGCGTGCAGGTGGAGACCATCAGCCCAGGCGACGGCAGAACCTTCCCC
AAGAGAGGCCAGACCTGCGTGGTGCACTATACCGGCATGCTGGAGGACGGCAAGAAG
GTGGACAGCAGCCGCGACCGCAATAAGCCCTTCAAGTTCATGCTGGGCAAGCAGGAG
GTGATCAGAGGCTGGGAGGAGGGCGTGGCCCAGATGAGCGTGGGCCAGAGAGCCAA
GCTGACCATCAGCCCCGACTACGCCTATGGCGCCACCGGCCACCCCGGCATCATCCCA
CCCCACGCCACCCTGGTGTTTGATGTGGAGCTGCTGAAGCTGGAGTCCGGAGGCGGC
TCCGGCGTGGATGGCTTCGGCGACGTGGGAGCCCTGGAGAGCCTGAGAGGCAACGCC
GATCTGGCCTACATCCTGAGCATGGAGCCCTGTGGCCACTGCCTGATCATCAACAACG
TGAACTTCTGCCGGGAGAGCGGCCTGCGGACCCGGACCGGCAGCAACATCGACTGCG
AGAAGCTGAGGAGGCGCTTCTCCTCCCTGCACTTTATGGTGGAGGTGAAAGGCGATCT
GACTGCCAAGAAAATGGTGCTGGCCCTGCTGGAGCTGGCCCAGCAGGACCACGGAGC
CCTGGATTGCTGTGTGGTGGTGATCCTGTCCCACGGCTGCCAGGCCAGCCACCTGCAG
TTCCCCGGAGCCGTGTACGGCACCGACGGCTGTCCCGTGTCCGTGGAGAAGATCGTG
AACATCTTCAACGGCACCTCCTGCCCCTCCCTGGGCGGCAAGCCCAAGCTGTTCTTTAT
CCAGGCCTGTGGCGGCGAGCAGAAGGACCACGGCTTTGAGGTGGCCAGCACCTCCCC
CGAGGACGAGAGCCCAGGCAGCAACCCCGAGCCCGACGCCACCCCCTTCCAGGAGG
GCCTGCGCACCTTCGACCAGCTGGACGCCATCAGCAGCCTGCCCACCCCCAGCGACA
TCTTCGTGAGCTACAGCACCTTTCCCGGCTTCGTGAGCTGGCGCGATCCCAAGTCCGG
CTCTTGGTATGTGGAGACCCTGGACGACATCTTTGAGCAGTGGGCTCATAGCGAGGAC
CTGCAGAGCCTGCTGCTGCGCGTGGCCAATGCCGTGAGCGTGAAGGGCATCTACAAG
CAGATGCCAGGCTGCTTCAACTTCCTGCGGAAGAAGCTGTTCTTCAAGACCAGCGCCT
CCAGAGCCGAGGGCAGAGGCAGCCTGCTGACCTGCGGCGATGTGGAGGAGAACCCAG
GCCCCATGGGCAGCAGACTGCTGTGTTGGGTGCTGCTGTGTCTGCTGGGAGCCGGAC
CTGTGAAAGCCGGCGTGACCCAGACCCCCAGATACCTGATCAAGACCAGAGGCCAGCA
AGTGACCCTGAGCTGCAGCCCCATCAGCGGCCACAGAAGCGTGTCCTGGTATCAGCAG
ACCCCAGGCCAGGGCCTGCAGTTCCTGTTCGAGTACTTCAGCGAGACACAGAGGAACA
AGGGCAACTTCCCCGGCAGATTCAGCGGCAGACAGTTCAGCAACAGCCGCAGCGAGAT
GAACGTGTCCACCCTGGAACTGGGCGACAGCGCCCTGTACCTGTGTGCCAGTTCTCAC
GGCGGAGCCTACGAGCAGTACTTCGGCCCTGGCACCAGACTGACCGTGACCGAAGAT
CTGAGGAACGTGACCCCCCCCAAGGTGTCCCTGTTCGAGCCCAGCAAGGCCGAGATC
GCCAACAAGCAGAAAGCCACCCTCGTGTGCCTGGCCAGAGGCTTCTTCCCCGACCACG
TGGAACTGTCCTGGTGGGTCAACGGCAAAGAGGTGCACAGCGGAGTCTGCACCGACC
CCCAGGCTTACAAAGAGAGCAACTACAGCTACTGCCTGTCCAGCAGACTGCGGGTGTC
CGCTACCTTCTGGCACAACCCCCGGAACCACTTCAGATGCCAGGTGCAGTTCCACGGC
CTGAGCGAAGAGGACAAGTGGCCCGAGGGCAGCCCCAAGCCCGTGACCCAGAATATC
AGCGCCGAGGCCTGGGGCAGAGCCGATTGTGGCATCACCAGCGCCAGCTACCACCAG
GGGGTGCTGAGCGCCACCATCCTGTACGAGATCCTGCTGGGCAAGGCCACCCTGTAC
GCCGTGCTGGTGTCCGGACTGGTGCTGATGGCCATGGTCAAGAAGAAGAACAGCGGC

AGCGGCGCCACCAACTTCAGCCTGCTGAAGCAGGCCGGCGACGTGGAGGAGAACCCC
GGCCCCATGGAAACCGTGCTGCAGGTGCTGCTGGGCATCCTGGGATTTCAGGCCGCC
TGGGTGTCCAGCCAGGAACTGGAACAGAGCCCCCAGAGCCTGATCGTGCAGGAAGGC
AAGAACCTGACCATCAACTGCACCAGCAGCAAGACCCTGTACGGCCTGTACTGGTACA
AGCAGAAGTACGGCGAGGGCCTGATCTTCCTGATGATGCTGCAGAAGGGCGGCGAGG
AAAAGAGCCACGAGAAGATCACCGCCAAGCTGGACGAGAAGAAGCAGCAGAGCAGCC
TGCACATCACCGCCTCCCAGCCTTCTCACGCCGGCATCTATCTGTGTGGCGCCGACAC
CAGCACCGACAAGCTGATCTTTGGCACCGGCACCAGACTGCAGGTGTTCCCCAATATC
CAGAACCCCGAGCCCGCCGTGTACCAGCTGAAGGACCCCAGAAGCCAGGACAGCACC
CTGTGTCTGTTCACCGACTTCGACAGCCAGATCAACGTGCCCAAGACCATGGAAAGCG
GCACCTTCATCACCGATAAGTGCGTGCTGGACATGAAGGCCATGGACAGCAAGAGCAA
CGGCGCCATTGCCTGGTCCAACCAGACCAGCTTCACATGCCAGGACATCTTCAAAGAG
ACAAACGCCACCTACCCTTCCAGCGACGTGCCCTGTGACGCCACCCTGACCGAGAAGT
CCTTCGAGACAGACATGAATCTGAATTTCCAGAACCTGAGCGTGATGGGCCTGCGGAT
CCTGCTGCTGAAAGTGGCCGGCTTCAACCTGCTGATGACCCTGCGGCTGTGGTCCAGC
TGA

iC9-6K TCR

ATGCTGGAGGGCGTGCAGGTGGAGACCATCAGCCCAGGCGACGGCAGAACCTTCCCC
AAGAGAGGCCAGACCTGCGTGGTGCACTATACCGGCATGCTGGAGGACGGCAAGAAG
GTGGACAGCAGCCGCGACCGCAATAAGCCCTTCAAGTTCATGCTGGGCAAGCAGGAG
GTGATCAGAGGCTGGGAGGAGGGCGTGGCCCAGATGAGCGTGGGCCAGAGAGCCAA
GCTGACCATCAGCCCCGACTACGCCTATGGCGCCACCGGCCACCCCGGCATCATCCCA
CCCCACGCCACCCTGGTGTTTGATGTGGAGCTGCTGAAGCTGGAGTCCGGAGGCGGC
TCCGGCGTGGATGGCTTCGGCGACGTGGGAGCCCTGGAGAGCCTGAGAGGCAACGCC
GATCTGGCCTACATCCTGAGCATGGAGCCCTGTGGCCACTGCCTGATCATCAACAACG
TGAACTTCTGCCGGGAGAGCGGCCTGCGGACCCGGACCGGCAGCAACATCGACTGCG
AGAAGCTGAGGAGGCGCTTCTCCTCCCTGCACTTTATGGTGGAGGTGAAAGGCGATCT
GACTGCCAAGAAAATGGTGCTGGCCCTGCTGGAGCTGGCCCAGCAGGACCACGGAGC
CCTGGATTGCTGTGTGGTGGTGATCCTGTCCCACGGCTGCCAGGCCAGCCACCTGCAG
TTCCCCGGAGCCGTGTACGGCACCGACGGCTGTCCCGTGTCCGTGGAGAAGATCGTG
AACATCTTCAACGGCACCTCCTGCCCCTCCCTGGGCGGCAAGCCCAAGCTGTTCTTTAT
CCAGGCCTGTGGCGGCGAGCAGAAGGACCACGGCTTTGAGGTGGCCAGCACCTCCCC
CGAGGACGAGAGCCCAGGCAGCAACCCCGAGCCCGACGCCACCCCCTTCCAGGAGG
GCCTGCGCACCTTCGACCAGCTGGACGCCATCAGCAGCCTGCCCACCCCCAGCGACA
TCTTCGTGAGCTACAGCACCTTTCCCGGCTTCGTGAGCTGGCGCGATCCCAAGTCCGG
CTCTTGGTATGTGGAGACCCTGGACGACATCTTTGAGCAGTGGGCTCATAGCGAGGAC
CTGCAGAGCCTGCTGCTGCGCGTGGCCAATGCCGTGAGCGTGAAGGGCATCTACAAG
CAGATGCCAGGCTGCTTCAACTTCCTGCGGAAGAAGCTGTTCTTCAAGACCAGCGCCT
CCAGAGCCGAGGGCAGAGGCAGCCTGCTGACCTGCGGCGATGTGGAGGAGAACCCAG
GCCCCATGGGACCTCAGCTGCTGGGATACGTGGTGCTGTGTCTGCTGGGAGCCGGAC
CTCTGGAAGCCCAAGTGACCCAGAACCCCAGATACCTGATCACCGTGACCGGCAAGAA
ACTGACCGTGACCTGCAGCCAGAACATGAACCACGAGTACATGAGCTGGTACAGACAG
GACCCCGGCCTGGGCCTGCGGCAGATCTACTACAGCATGAACGTGGAAGTGACCGAC
AAGGGCGACGTGCCCGAGGGCTACAAGGTGTCCCGGAAAGAGAAGCGGAACTTCCCA
CTGATCCTGGAAAGCCCCAGCCCCAACCAGACCAGCCTGTACTTCTGTGCCAGCAGCC
TGAGCATGAGCACCTACAACGAGCAGTTCTTCGGCCCTGGCACCCGGCTGACAGTGCT
GGAAGATCTGAGGAACGTGACCCCCCCCAAGGTGTCCCTGTTCGAGCCCAGCAAGGC
CGAGATCGCCAACAAGCAGAAAGCCACCCTCGTGTGCCTGGCCAGAGGCTTCTTCCCC
GACCACGTGGAACTGTCCTGGTGGGTCAACGGCAAAGAGGTGCACAGCGGAGTCTGC
ACCGACCCCCAGGCTTACAAAGAGAGCAACTACAGCTACTGCCTGTCCAGCAGACTGC
GGGTGTCCGCTACCTTCTGGCACAACCCCCGGAACCACTTCAGATGCCAGGTGCAGTT
CCACGGCCTGAGCGAAGAGGACAAGTGGCCCGAGGGCAGCCCCAAGCCCGTGACCCA

GAATATCAGCGCCGAGGCCTGGGGCAGAGCCGATTGTGGCATCACCAGCGCCAGCTA
CCACCAGGGGGTGCTGAGCGCCACCATCCTGTACGAGATCCTGCTGGGCAAGGCCAC
CCTGTACGCCGTGCTGGTGTCCGGACTGGTGCTGATGGCCATGGTCAAGAAGAAGAAC
AGCGGCAGCGGCGCCACCAACTTCAGCCTGCTGAAGCAGGCCGGCGACGTGGAGGAG
AACCCCGGCCCCATGACCAGCATCCGGGCCGTGTTCATCTTCCTGTGGCTGCAGCTGG
ACCTCGTGAACGGCGAGAACGTGGAACAGCACCCCAGCACCCTGAGCGTGCAGGAAG
GCGATAGCGCCGTGATCAAGTGCACCTACAGCGACAGCGCCAGCAACTACTTCCCCTG
GTACAAGCAGGAACTGGGCAAGCGGCCCCAGCTGATCATCGACATCAGATCCAACGTG
GGCGAGAAGAAGGACCAGCGGATCGCCGTGACCCTGAACAAGACCGCCAAGCACTTC
AGCCTGCACATCACCGAGACACAGCCCGAGGACAGCGCCGTGTACTTCTGTGCCGCCA
TCGGCTTCGGCAACGTGCTGCACTGTGGCAGCGGCACACAAGTGATCGTGCTGCCCCA
TATCCAGAACCCCGAGCCCGCCGTGTACCAGCTGAAGGACCCCAGAAGCCAGGACAG
CACCCTGTGTCTGTTCACCGACTTCGACAGCCAGATCAACGTGCCCAAGACCATGGAAA
GCGGCACCTTCATCACCGATAAGTGCGTGCTGGACATGAAGGCCATGGACAGCAAGAG
CAACGGCGCCATTGCCTGGTCCAACCAGACCAGCTTCACATGCCAGGACATCTTCAAA
GAGACAAACGCCACCTACCCTTCCAGCGACGTGCCCTGTGACGCCACCCTGACCGAGA
AGTCCTTCGAGACAGACATGAATCTGAATTTCCAGAACCTGAGCGTGATGGGCCTGCG
GATCCTGCTGCTGAAAGTGGCCGGCTTCAACCTGCTGATGACCCTGCGGCTGTGGTCC
AGCTGA

HSV-TK-S-CAR

ATGGCCAGCTACCCCTGCCACCAGCACGCCAGCGCCTTCGACCAGGCCGCCCGGAGC
CGGGGCCACAGCAACCGGCGGACCGCCCTGCGGCCCAGGAGGCAGCAGGAGGCCAC
CGAGGTGCGGCCCGAGCAGAAGATGCCCACCCTGCTGCGGGTGTACATCGACGGCCC
ACACGGCATGGGCAAGACCACCACCACCCAGCTGCTGGTGGCCCTGGGCAGCCGGGA
CGACATCGTGTACGTGCCCGAGCCCATGACCTACTGGCGGGTGCTGGGCGCCAGCGA
GACCATCGCCAACATCTACACCACCCAGCACCGGCTGGACCAGGGCGAGATCAGCGC
CGGCGACGCCGCCGTGGTGATGACCAGCGCCCAGATCACAATGGGCATGCCCTACGC
CGTGACCGACGCCGTGCTGGCCCCACACATCGGCGGCGAGGCCGGCAGCAGCCACG
CCCCACCACCCGCCCTGACCATCTTCCTGGACCGGCACCCCATCGCCTTCATGCTGTG
CTACCCCGCTGCCCGGTACCTGATGGGCAGCATGACCCCACAGGCCGTGCTGGCCTT
CGTGGCCCTGATCCCACCCACCCTGCCCGGCACCAACATCGTGCTGGGCGCCCTGCC
CGAGGACCGGCACATCGACCGGCTGGCCAAGCGGCAGCGGCCCGGCGAGCGGCTGG
ACCTGGCCATGCTGGCCGCCATCCGGCGGGTGTACGGCCTGCTGGCCAACACCGTGC
GGTACCTGCAGTGCGGCGGCAGCTGGCGGGAGGACTGGGGCCAGCTGAGCGGCACC
GCCGTGCCACCCCAGGGCGCCGAGCCCCAGAGCAACGCCGGCCCCAGACCCCACATC
GGCGACACCCTGTTCACCCTGTTCCGGGCCCCAGAGCTGCTGGCCCCAAACGGCGAC
CTGTACAACGTGTTCGCCTGGGCCCTGGACGTGCTGGCCAAGCGGCTGCGGAGCATG
CACGTGTTCATCCTGGACTACGACCAGAGCCCCGCCGGCTGCCGGGACGCCCTGCTG
CAGCTGACCAGCGGCATGGTGCAGACCCACGTGACCACCCCAGGCAGCATCCCCACC
ATCTGCGACCTGGCCCGGACCTTCGCCCGGGAGATGGGCGAGGCCAACCGCGCAGAG
GGCCGGGGCTCATTGCTGACCTGTGGAGATGTCGAGGAAAATCCCGGCCCTATGGATT
TCGAGGTGCAGATCTTCAGCTTCCTGCTGATCTCCGCCAGCGTGATCATGAGCCGGAT
GGCCGAAGTGCAGCTGGTGGAATCTGGCGGCGGACTGCTGCAGCCTGGCGGATCTCT
GAGACTGAGCTGTGCCGCCAGCGGCTTCACCTTTAGCGGCTACGCCATGAGCTGGGTG
CGCCAGGCTCCTGGCAAAGGCCTGGAATGGGTGTCCAGCATCTCTGGCTCTGGCGGC
AGCACCTACTACGCCGATAGCGTGAAGGGCCGGTTCACCATCAGCCGGGACAACAGCA
AGAACACCCTGTACCTGCAGATGAACAGCCTGCGGGCCGAGGACACCGCCCTGTACTA
TTGTGCCAAGCCCCCTGGCCGGCAGGAATATTACGGCAGCTCCATCTACTACTTCCCC
CTGGGCAATTGGGGCCAGGGCACACTCGTGACAGTGTCCAGCGCCAGCACCAAGGGC
CCCAAGCTGGAAGAGGGCGAGTTCAGCGAAGCCAGAGTGCAGAGCGCCCTGACACAG
CCTGCCTCCGTGTCTGTGGCTCCTGGACAGACCGCCAGAATCACCTGTGGCGGCAACA
ACATCGGCAGCAAGAGCGTGCACTGGTATCAGCAGAAGCCCGGCCAGGCACCTGTGC

TGGTGGTGTACGACGACAGCGACAGACCCAGCGGCATCCCCGAGAGATTCAGCGGCA
GCAACTCCGGCAATACCGCCACCCTGACCATCAGCAGAGTGGAAGCCGGCGACGAGG
CCGACTACTACTGCCAAGTGTGGGACAGCAGCAGCGACCTGGTGGTGTTTGGCGGAG
GCACCAAGCTGACAGTGCTGGGCCAGCCTAAAGCCGCCCCTAGCGTGACCCTGTTCCC
TCCTAGTTCTGCCGCCGCAGGCGATCCTGCCGAGCCTAAGAGCCCCGACAAGACCCAC
ACCTGTCCCCCTTGTCCTGCCCCTGAACTGCTGGGCGGACCTTCCGTGTTCCTGTTCC
CCCCAAAGCCCAAGGACACCCTGATGATCAGCCGGACCCCCGAAGTGACCTGCGTGGT
GGTGGATGTGTCCCACGAGGACCCTGAAGTGAAGTTCAATTGGTACGTGGACGGCGTG
GAAGTGCACAACGCCAAGACCAAGCCCAGAGAGGAACAGTACAACTCCACCTACCGGG
TGGTGTCCGTGCTGACCGTGCTGCACCAGGACTGGCTGAACGGCAAAGAGTACAAGTG
CAAGGTGTCCAACAAGGCCCTGCCTGCCCCCATCGAGAAAACCATCTCCAAGGCCAAG
GGCCAGCCCCGCGAACCCCAGGTGTACACACTGCCCCCTAGCAGGGACGAGCTGACC
AAGAACCAGGTGTCCCTGACCTGTCTCGTGAAGGGATTCTACCCCTCCGATATCGCCGT
GGAATGGGAGAGCAACGGCCAGCCCGAGAACAACTACAAGACCACCCCTCCCGTGCT
GGACAGCGACGGCTCATTCTTCCTGTACAGCAAACTGACCGTGGACAAGAGCCGGTGG
CAGCAGGGCAACGTGTTCAGCTGCAGCGTGATGCACGAGGCCCTGCACAACCACTACA
CCCAGAAGTCCCTGAGCCTGAGCCCTGGCAAGAAGGACCCCAAGTTCTGGGTGCTGGT
GGTCGTGGGCGGAGTGCTGGCCTGTTACAGCCTGCTCGTGACCGTGGCCTTCATCATC
TTTTGGGTGCGCAGCAAGCGGAGCCGGCTGCTGCACTCCGACTACATGAACATGACCC
CCAGACGGCCAGGCCCCACCAGAAAGCACTACCAGCCTTACGCCCCTCCCAGAGACTT
CGCCGCCTACAGATCCCTGCGCGTGAAGTTCTCCAGAAGCGCCGACGCCCCTGCCTAT
CAGCAGGGACAGAACCAGCTGTACAACGAGCTGAACCTGGGCAGACGGGAAGAGTAC
GACGTGCTGGATAAGCGGAGAGGCCGGGACCCTGAGATGGGCGGCAAGCCTAGAAGA
AAGAACCCCCAGGAAGGCCTGTATAACGAACTGCAGAAAGACAAGATGGCCGAGGCCT
ACAGCGAGATCGGCATGAAGGGCGAGCGGAGAAGAGGCAAGGGCCACGATGGCCTGT
ACCAGGGACTGAGCACCGCCACAAAGGACACCTATGACGCACTGCACATGCAGGCTCT
GCCCCCCAGATGA

HSV-TK-4G TCR

ATGGCCAGCTACCCCTGCCACCAGCACGCCAGCGCCTTCGACCAGGCCGCCCGGAGC
CGGGGCCACAGCAACCGGCGGACCGCCCTGCGGCCCAGGAGGCAGCAGGAGGCCAC
CGAGGTGCGGCCCGAGCAGAAGATGCCCACCCTGCTGCGGGTGTACATCGACGGCCC
ACACGGCATGGGCAAGACCACCACCACCCAGCTGCTGGTGGCCCTGGGCAGCCGGGA
CGACATCGTGTACGTGCCCGAGCCCATGACCTACTGGCGGGTGCTGGGCGCCAGCGA
GACCATCGCCAACATCTACACCACCCAGCACCGGCTGGACCAGGGCGAGATCAGCGC
CGGCGACGCCGCCGTGGTGATGACCAGCGCCCAGATCACAATGGGCATGCCCTACGC
CGTGACCGACGCCGTGCTGGCCCCACACATCGGCGGCGAGGCCGGCAGCAGCCACG
CCCCACCACCCGCCCTGACCATCTTCCTGGACCGGCACCCCATCGCCTTCATGCTGTG
CTACCCCGCTGCCCGGTACCTGATGGGCAGCATGACCCCACAGGCCGTGCTGGCCTT
CGTGGCCCTGATCCCACCCACCCTGCCCGGCACCAACATCGTGCTGGGCGCCCTGCC
CGAGGACCGGCACATCGACCGGCTGGCCAAGCGGCAGCGGCCCGGCGAGCGGCTGG
ACCTGGCCATGCTGGCCGCCATCCGGCGGGTGTACGGCCTGCTGGCCAACACCGTGC
GGTACCTGCAGTGCGGCGGCAGCTGGCGGGAGGACTGGGGCCAGCTGAGCGGCACC
GCCGTGCCACCCCAGGGCGCCGAGCCCCAGAGCAACGCCGGCCCCAGACCCCACATC
GGCGACACCCTGTTCACCCTGTTCCGGGCCCCAGAGCTGCTGGCCCCAAACGGCGAC
CTGTACAACGTGTTCGCCTGGGCCCTGGACGTGCTGGCCAAGCGGCTGCGGAGCATG
CACGTGTTCATCCTGGACTACGACCAGAGCCCCGCCGGCTGCCGGGACGCCCTGCTG
CAGCTGACCAGCGGCATGGTGCAGACCCACGTGACCACCCCAGGCAGCATCCCCACC
ATCTGCGACCTGGCCCGGACCTTCGCCCGGGAGATGGGCGAGGCCAACCGCGCAGAG
GGCCGGGGCTCATTGCTGACCTGTGGAGATGTCGAGGAAAATCCCGGCCCTATGGGC
AGCAGACTGCTGTGTTGGGTGCTGCTGTGTCTGCTGGGAGCCGGACCTGTGAAAGCCG
GCGTGACCCAGACCCCCAGATACCTGATCAAGACCAGAGGCCAGCAAGTGACCCTGAG
CTGCAGCCCCATCAGCGGCCACAGAAGCGTGTCCTGGTATCAGCAGACCCCAGGCCA

GGGCCTGCAGTTCCTGTTCGAGTACTTCAGCGAGACACAGAGGAACAAGGGCAACTTC
CCCGGCAGATTCAGCGGCAGACAGTTCAGCAACAGCCGCAGCGAGATGAACGTGTCCA
CCCTGGAACTGGGCGACAGCGCCCTGTACCTGTGTGCCAGTTCTCACGGCGGAGCCTA
CGAGCAGTACTTCGGCCCTGGCACCAGACTGACCGTGACCGAAGATCTGAGGAACGTG
ACCCCCCCCAAGGTGTCCCTGTTCGAGCCCAGCAAGGCCGAGATCGCCAACAAGCAGA
AAGCCACCCTCGTGTGCCTGGCCAGAGGCTTCTTCCCCGACCACGTGGAACTGTCCTG
GTGGGTCAACGGCAAAGAGGTGCACAGCGGAGTCTGCACCGACCCCCAGGCTTACAA
AGAGAGCAACTACAGCTACTGCCTGTCCAGCAGACTGCGGGTGTCCGCTACCTTCTGG
CACAACCCCCGGAACCACTTCAGATGCCAGGTGCAGTTCCACGGCCTGAGCGAAGAGG
ACAAGTGGCCCGAGGGCAGCCCCAAGCCCGTGACCCAGAATATCAGCGCCGAGGCCT
GGGGCAGAGCCGATTGTGGCATCACCAGCGCCAGCTACCACCAGGGGGTGCTGAGCG
CCACCATCCTGTACGAGATCCTGCTGGGCAAGGCCACCCTGTACGCCGTGCTGGTGTC
CGGACTGGTGCTGATGGCCATGGTCAAGAAGAAGAACAGCGGCAGCGGCGCCACCAA
CTTCAGCCTGCTGAAGCAGGCCGGCGACGTGGAGGAGAACCCCGGCCCCATGGAAAC
CGTGCTGCAGGTGCTGCTGGGCATCCTGGGATTTCAGGCCGCCTGGGTGTCCAGCCA
GGAACTGGAACAGAGCCCCCAGAGCCTGATCGTGCAGGAAGGCAAGAACCTGACCATC
AACTGCACCAGCAGCAAGACCCTGTACGGCCTGTACTGGTACAAGCAGAAGTACGGCG
AGGGCCTGATCTTCCTGATGATGCTGCAGAAGGGCGGCGAGGAAAAGAGCCACGAGA
AGATCACCGCCAAGCTGGACGAGAAGAAGCAGCAGAGCAGCCTGCACATCACCGCCTC
CCAGCCTTCTCACGCCGGCATCTATCTGTGTGGCGCCGACACCAGCACCGACAAGCTG
ATCTTTGGCACCGGCACCAGACTGCAGGTGTTCCCCAATATCCAGAACCCCGAGCCCG
CCGTGTACCAGCTGAAGGACCCCAGAAGCCAGGACAGCACCCTGTGTCTGTTCACCGA
CTTCGACAGCCAGATCAACGTGCCCAAGACCATGGAAAGCGGCACCTTCATCACCGAT
AAGTGCGTGCTGGACATGAAGGCCATGGACAGCAAGAGCAACGGCGCCATTGCCTGGT
CCAACCAGACCAGCTTCACATGCCAGGACATCTTCAAAGAGACAAACGCCACCTACCCT
TCCAGCGACGTGCCCTGTGACGCCACCCTGACCGAGAAGTCCTTCGAGACAGACATGA
ATCTGAATTTCCAGAACCTGAGCGTGATGGGCCTGCGGATCCTGCTGCTGAAAGTGGC
CGGCTTCAACCTGCTGATGACCCTGCGGCTGTGGTCCAGCTGA

HSV-TK-6K TCR

ATGGCCAGCTACCCCTGCCACCAGCACGCCAGCGCCTTCGACCAGGCCGCCCGGAGC
CGGGGCCACAGCAACCGGCGGACCGCCCTGCGGCCCAGGAGGCAGCAGGAGGCCAC
CGAGGTGCGGCCCGAGCAGAAGATGCCCACCCTGCTGCGGGTGTACATCGACGGCCC
ACACGGCATGGGCAAGACCACCACCACCCAGCTGCTGGTGGCCCTGGGCAGCCGGGA
CGACATCGTGTACGTGCCCGAGCCCATGACCTACTGGCGGGTGCTGGGCGCCAGCGA
GACCATCGCCAACATCTACACCACCCAGCACCGGCTGGACCAGGGCGAGATCAGCGC
CGGCGACGCCGCCGTGGTGATGACCAGCGCCCAGATCACAATGGGCATGCCCTACGC
CGTGACCGACGCCGTGCTGGCCCCACACATCGGCGGCGAGGCCGGCAGCAGCCACG
CCCCACCACCCGCCCTGACCATCTTCCTGGACCGGCACCCCATCGCCTTCATGCTGTG
CTACCCCGCTGCCCGGTACCTGATGGGCAGCATGACCCCACAGGCCGTGCTGGCCTT
CGTGGCCCTGATCCCACCCACCCTGCCCGGCACCAACATCGTGCTGGGCGCCCTGCC
CGAGGACCGGCACATCGACCGGCTGGCCAAGCGGCAGCGGCCCGGCGAGCGGCTGG
ACCTGGCCATGCTGGCCGCCATCCGGCGGGTGTACGGCCTGCTGGCCAACACCGTGC
GGTACCTGCAGTGCGGCGGCAGCTGGCGGGAGGACTGGGGCCAGCTGAGCGGCACC
GCCGTGCCACCCCAGGGCGCCGAGCCCCAGAGCAACGCCGGCCCCAGACCCCACATC
GGCGACACCCTGTTCACCCTGTTCCGGGCCCCAGAGCTGCTGGCCCCAAACGGCGAC
CTGTACAACGTGTTCGCCTGGGCCCTGGACGTGCTGGCCAAGCGGCTGCGGAGCATG
CACGTGTTCATCCTGGACTACGACCAGAGCCCCGCCGGCTGCCGGGACGCCCTGCTG
CAGCTGACCAGCGGCATGGTGCAGACCCACGTGACCACCCCAGGCAGCATCCCCACC
ATCTGCGACCTGGCCCGGACCTTCGCCCGGGAGATGGGCGAGGCCAACCGCGCAGAG
GGCCGGGGCTCATTGCTGACCTGTGGAGATGTCGAGGAAAATCCCGGCCCTATGGGA
CCTCAGCTGCTGGGATACGTGGTGCTGTGTCTGCTGGGAGCCGGACCTCTGGAAGCC
CAAGTGACCCAGAACCCCAGATACCTGATCACCGTGACCGGCAAGAAACTGACCGTGA

CCTGCAGCCAGAACATGAACCACGAGTACATGAGCTGGTACAGACAGGACCCCGGCCT
GGGCCTGCGGCAGATCTACTACAGCATGAACGTGGAAGTGACCGACAAGGGCGACGT
GCCCGAGGGCTACAAGGTGTCCCGGAAAGAGAAGCGGAACTTCCCACTGATCCTGGAA
AGCCCCAGCCCCAACCAGACCAGCCTGTACTTCTGTGCCAGCAGCCTGAGCATGAGCA
CCTACAACGAGCAGTTCTTCGGCCCTGGCACCCGGCTGACAGTGCTGGAAGATCTGAG
GAACGTGACCCCCCCCAAGGTGTCCCTGTTCGAGCCCAGCAAGGCCGAGATCGCCAA
CAAGCAGAAAGCCACCCTCGTGTGCCTGGCCAGAGGCTTCTTCCCCGACCACGTGGAA
CTGTCCTGGTGGGTCAACGGCAAAGAGGTGCACAGCGGAGTCTGCACCGACCCCCAG
GCTTACAAAGAGAGCAACTACAGCTACTGCCTGTCCAGCAGACTGCGGGTGTCCGCTA
CCTTCTGGCACAACCCCCGGAACCACTTCAGATGCCAGGTGCAGTTCCACGGCCTGAG
CGAAGAGGACAAGTGGCCCGAGGGCAGCCCCAAGCCCGTGACCCAGAATATCAGCGC
CGAGGCCTGGGGCAGAGCCGATTGTGGCATCACCAGCGCCAGCTACCACCAGGGGGT
GCTGAGCGCCACCATCCTGTACGAGATCCTGCTGGGCAAGGCCACCCTGTACGCCGTG
CTGGTGTCCGGACTGGTGCTGATGGCCATGGTCAAGAAGAAGAACAGCGGCAGCGGC
GCCACCAACTTCAGCCTGCTGAAGCAGGCCGGCGACGTGGAGGAGAACCCCGGCCCC
ATGACCAGCATCCGGGCCGTGTTCATCTTCCTGTGGCTGCAGCTGGACCTCGTGAACG
GCGAGAACGTGGAACAGCACCCCAGCACCCTGAGCGTGCAGGAAGGCGATAGCGCCG
TGATCAAGTGCACCTACAGCGACAGCGCCAGCAACTACTTCCCCTGGTACAAGCAGGA
ACTGGGCAAGCGGCCCCAGCTGATCATCGACATCAGATCCAACGTGGGCGAGAAGAAG
GACCAGCGGATCGCCGTGACCCTGAACAAGACCGCCAAGCACTTCAGCCTGCACATCA
CCGAGACACAGCCCGAGGACAGCGCCGTGTACTTCTGTGCCGCCATCGGCTTCGGCA
ACGTGCTGCACTGTGGCAGCGGCACACAAGTGATCGTGCTGCCCCATATCCAGAACCC
CGAGCCCGCCGTGTACCAGCTGAAGGACCCCAGAAGCCAGGACAGCACCCTGTGTCT
GTTCACCGACTTCGACAGCCAGATCAACGTGCCCAAGACCATGGAAAGCGGCACCTTC
ATCACCGATAAGTGCGTGCTGGACATGAAGGCCATGGACAGCAAGAGCAACGGCGCCA
TTGCCTGGTCCAACCAGACCAGCTTCACATGCCAGGACATCTTCAAAGAGACAAACGCC
ACCTACCCTTCCAGCGACGTGCCCTGTGACGCCACCCTGACCGAGAAGTCCTTCGAGA
CAGACATGAATCTGAATTTCCAGAACCTGAGCGTGATGGGCCTGCGGATCCTGCTGCT
GAAAGTGGCCGGCTTCAACCTGCTGATGACCCTGCGGCTGTGGTCCAGCTGA

RQR8-S-CAR

ATGGGCACCAGCCTGCTGTGCTGGATGGCCCTGTGCCTGCTGGGCGCCGACCACGCC
GATGCCTGCCCCTACAGCAACCCCAGCCTGTGCAGCGGAGGCGGCGGCAGCGAGCTG
CCCACCCAGGGCACCTTCTCCAACGTGTCCACCAACGTGAGCCCAGCCAAGCCCACCA
CCACCGCCTGTCCTTATTCCAATCCTTCCCTGTGTAGCGGAGGGGGAGGCAGCCCAGC
CCCCAGACCTCCCACCCCAGCCCCCACCATCGCCAGCCAGCCTCTGAGCCTGAGACC
CGAGGCCTGCCGCCCAGCCGCCGGCGGCGCCGTGCACACCAGAGGCCTGGATTTCG
CCTGCGATATCTACATCTGGGCCCCACTGGCCGGCACCTGTGGCGTGCTGCTGCTGAG
CCTGGTGATCACCCTGTACTGCAACCACCGCAACCGCAGGCGCGTGTGCAAGTGCCCC
AGGCCCGTGGTGAGAGCCGAGGGCAGAGGCAGCCTGCTGACCTGCGGCGACGTGGA
GGAGAACCCAGGCCCCATGGATTTCGAGGTGCAGATCTTCAGCTTCCTGCTGATCTCC
GCCAGCGTGATCATGAGCCGGATGGCCGAAGTGCAGCTGGTGGAATCTGGCGGCGGA
CTGCTGCAGCCTGGCGGATCTCTGAGACTGAGCTGTGCCGCCAGCGGCTTCACCTTTA
GCGGCTACGCCATGAGCTGGGTGCGCCAGGCTCCTGGCAAAGGCCTGGAATGGGTGT
CCAGCATCTCTGGCTCTGGCGGCAGCACCTACTACGCCGATAGCGTGAAGGGCCGGTT
CACCATCAGCCGGGACAACAGCAAGAACACCCTGTACCTGCAGATGAACAGCCTGCGG
GCCGAGGACACCGCCCTGTACTATTGTGCCAAGCCCCCTGGCCGGCAGGAATATTACG
GCAGCTCCATCTACTACTTCCCCCTGGGCAATTGGGGCCAGGGCACACTCGTGACAGT
GTCCAGCGCCAGCACCAAGGGCCCCAAGCTGGAAGAGGGCGAGTTCAGCGAAGCCAG
AGTGCAGAGCGCCCTGACACAGCCTGCCTCCGTGTCTGTGGCTCCTGGACAGACCGC
CAGAATCACCTGTGGCGGCAACAACATCGGCAGCAAGAGCGTGCACTGGTATCAGCAG
AAGCCCGGCCAGGCACCTGTGCTGGTGGTGTACGACGACAGCGACAGACCCAGCGGC
ATCCCCGAGAGATTCAGCGGCAGCAACTCCGGCAATACCGCCACCCTGACCATCAGCA

GAGTGGAAGCCGGCGACGAGGCCGACTACTACTGCCAAGTGTGGGACAGCAGCAGCG
ACCTGGTGGTGTTTGGCGGAGGCACCAAGCTGACAGTGCTGGGCCAGCCTAAAGCCG
CCCCTAGCGTGACCCTGTTCCCTCCTAGTTCTGCCGCCGCAGGCGATCCTGCCGAGCC
TAAGAGCCCCGACAAGACCCACACCTGTCCCCCTTGTCCTGCCCCTGAACTGCTGGGC
GGACCTTCCGTGTTCCTGTTCCCCCCAAAGCCCAAGGACACCCTGATGATCAGCCGGA
CCCCCGAAGTGACCTGCGTGGTGGTGGATGTGTCCCACGAGGACCCTGAAGTGAAGTT
CAATTGGTACGTGGACGGCGTGGAAGTGCACAACGCCAAGACCAAGCCCAGAGAGGA
ACAGTACAACTCCACCTACCGGGTGGTGTCCGTGCTGACCGTGCTGCACCAGGACTGG
CTGAACGGCAAAGAGTACAAGTGCAAGGTGTCCAACAAGGCCCTGCCTGCCCCCATCG
AGAAAACCATCTCCAAGGCCAAGGGCCAGCCCCGCGAACCCCAGGTGTACACACTGCC
CCCTAGCAGGGACGAGCTGACCAAGAACCAGGTGTCCCTGACCTGTCTCGTGAAGGGA
TTCTACCCCTCCGATATCGCCGTGGAATGGGAGAGCAACGGCCAGCCCGAGAACAACT
ACAAGACCACCCCTCCCGTGCTGGACAGCGACGGCTCATTCTTCCTGTACAGCAAACT
GACCGTGGACAAGAGCCGGTGGCAGCAGGGCAACGTGTTCAGCTGCAGCGTGATGCA
CGAGGCCCTGCACAACCACTACACCCAGAAGTCCCTGAGCCTGAGCCCTGGCAAGAAG
GACCCCAAGTTCTGGGTGCTGGTGGTCGTGGGCGGAGTGCTGGCCTGTTACAGCCTG
CTCGTGACCGTGGCCTTCATCATCTTTTGGGTGCGCAGCAAGCGGAGCCGGCTGCTGC
ACTCCGACTACATGAACATGACCCCCAGACGGCCAGGCCCCACCAGAAAGCACTACCA
GCCTTACGCCCCTCCCAGAGACTTCGCCGCCTACAGATCCCTGCGCGTGAAGTTCTCC
AGAAGCGCCGACGCCCCTGCCTATCAGCAGGGACAGAACCAGCTGTACAACGAGCTGA
ACCTGGGCAGACGGGAAGAGTACGACGTGCTGGATAAGCGGAGAGGCCGGGACCCTG
AGATGGGCGGCAAGCCTAGAAGAAAGAACCCCCAGGAAGGCCTGTATAACGAACTGCA
GAAAGACAAGATGGCCGAGGCCTACAGCGAGATCGGCATGAAGGGCGAGCGGAGAAG
AGGCAAGGGCCACGATGGCCTGTACCAGGGACTGAGCACCGCCACAAAGGACACCTA
TGACGCACTGCACATGCAGGCTCTGCCCCCCAGATGA

RQR8-4G TCR

ATGGGCACCAGCCTGCTGTGCTGGATGGCCCTGTGCCTGCTGGGCGCCGACCACGCC
GATGCCTGCCCCTACAGCAACCCCAGCCTGTGCAGCGGAGGCGGCGGCAGCGAGCTG
CCCACCCAGGGCACCTTCTCCAACGTGTCCACCAACGTGAGCCCAGCCAAGCCCACCA
CCACCGCCTGTCCTTATTCCAATCCTTCCCTGTGTAGCGGAGGGGGAGGCAGCCCAGC
CCCCAGACCTCCCACCCCAGCCCCCACCATCGCCAGCCAGCCTCTGAGCCTGAGACC
CGAGGCCTGCCGCCCAGCCGCCGGCGGCGCCGTGCACACCAGAGGCCTGGATTTCG
CCTGCGATATCTACATCTGGGCCCCACTGGCCGGCACCTGTGGCGTGCTGCTGCTGAG
CCTGGTGATCACCCTGTACTGCAACCACCGCAACCGCAGGCGCGTGTGCAAGTGCCCC
AGGCCCGTGGTGAGAGCCGAGGGCAGAGGCAGCCTGCTGACCTGCGGCGACGTGGA
GGAGAACCCAGGCCCCATGGGCAGCAGACTGCTGTGTTGGGTGCTGCTGTGTCTGCT
GGGAGCCGGACCTGTGAAAGCCGGCGTGACCCAGACCCCCAGATACCTGATCAAGAC
CAGAGGCCAGCAAGTGACCCTGAGCTGCAGCCCCATCAGCGGCCACAGAAGCGTGTC
CTGGTATCAGCAGACCCCAGGCCAGGGCCTGCAGTTCCTGTTCGAGTACTTCAGCGAG
ACACAGAGGAACAAGGGCAACTTCCCCGGCAGATTCAGCGGCAGACAGTTCAGCAACA
GCCGCAGCGAGATGAACGTGTCCACCCTGGAACTGGGCGACAGCGCCCTGTACCTGT
GTGCCAGTTCTCACGGCGGAGCCTACGAGCAGTACTTCGGCCCTGGCACCAGACTGAC
CGTGACCGAAGATCTGAGGAACGTGACCCCCCCCAAGGTGTCCCTGTTCGAGCCCAGC
AAGGCCGAGATCGCCAACAAGCAGAAAGCCACCCTCGTGTGCCTGGCCAGAGGCTTCT
TCCCCGACCACGTGGAACTGTCCTGGTGGGTCAACGGCAAAGAGGTGCACAGCGGAG
TCTGCACCGACCCCCAGGCTTACAAAGAGAGCAACTACAGCTACTGCCTGTCCAGCAG
ACTGCGGGTGTCCGCTACCTTCTGGCACAACCCCCGGAACCACTTCAGATGCCAGGTG
CAGTTCCACGGCCTGAGCGAAGAGGACAAGTGGCCCGAGGGCAGCCCCAAGCCCGTG
ACCCAGAATATCAGCGCCGAGGCCTGGGGCAGAGCCGATTGTGGCATCACCAGCGCC
AGCTACCACCAGGGGGTGCTGAGCGCCACCATCCTGTACGAGATCCTGCTGGGCAAG
GCCACCCTGTACGCCGTGCTGGTGTCCGGACTGGTGCTGATGGCCATGGTCAAGAAGA
AGAACAGCGGCAGCGGCGCCACCAACTTCAGCCTGCTGAAGCAGGCCGGCGACGTGG

AGGAGAACCCCGGCCCCATGGAAACCGTGCTGCAGGTGCTGCTGGGCATCCTGGGAT
TTCAGGCCGCCTGGGTGTCCAGCCAGGAACTGGAACAGAGCCCCCAGAGCCTGATCG
TGCAGGAAGGCAAGAACCTGACCATCAACTGCACCAGCAGCAAGACCCTGTACGGCCT
GTACTGGTACAAGCAGAAGTACGGCGAGGGCCTGATCTTCCTGATGATGCTGCAGAAG
GGCGGCGAGGAAAAGAGCCACGAGAAGATCACCGCCAAGCTGGACGAGAAGAAGCAG
CAGAGCAGCCTGCACATCACCGCCTCCCAGCCTTCTCACGCCGGCATCTATCTGTGTG
GCGCCGACACCAGCACCGACAAGCTGATCTTTGGCACCGGCACCAGACTGCAGGTGTT
CCCCAATATCCAGAACCCCGAGCCCGCCGTGTACCAGCTGAAGGACCCCAGAAGCCAG
GACAGCACCCTGTGTCTGTTCACCGACTTCGACAGCCAGATCAACGTGCCCAAGACCA
TGGAAAGCGGCACCTTCATCACCGATAAGTGCGTGCTGGACATGAAGGCCATGGACAG
CAAGAGCAACGGCGCCATTGCCTGGTCCAACCAGACCAGCTTCACATGCCAGGACATC
TTCAAAGAGACAAACGCCACCTACCCTTCCAGCGACGTGCCCTGTGACGCCACCCTGA
CCGAGAAGTCCTTCGAGACAGACATGAATCTGAATTTCCAGAACCTGAGCGTGATGGG
CCTGCGGATCCTGCTGCTGAAAGTGGCCGGCTTCAACCTGCTGATGACCCTGCGGCTG
TGGTCCAGCTGA

RQR8-6K TCR

ATGGGCACCAGCCTGCTGTGCTGGATGGCCCTGTGCCTGCTGGGCGCCGACCACGCC
GATGCCTGCCCCTACAGCAACCCCAGCCTGTGCAGCGGAGGCGGCGGCAGCGAGCTG
CCCACCCAGGGCACCTTCTCCAACGTGTCCACCAACGTGAGCCCAGCCAAGCCCACCA
CCACCGCCTGTCCTTATTCCAATCCTTCCCTGTGTAGCGGAGGGGGAGGCAGCCCAGC
CCCCAGACCTCCCACCCCAGCCCCCACCATCGCCAGCCAGCCTCTGAGCCTGAGACC
CGAGGCCTGCCGCCCAGCCGCCGGCGGCGCCGTGCACACCAGAGGCCTGGATTTCG
CCTGCGATATCTACATCTGGGCCCCACTGGCCGGCACCTGTGGCGTGCTGCTGCTGAG
CCTGGTGATCACCCTGTACTGCAACCACCGCAACCGCAGGCGCGTGTGCAAGTGCCCC
AGGCCCGTGGTGAGAGCCGAGGGCAGAGGCAGCCTGCTGACCTGCGGCGACGTGGA
GGAGAACCCAGGCCCCATGGGACCTCAGCTGCTGGGATACGTGGTGCTGTGTCTGCT
GGGAGCCGGACCTCTGGAAGCCCAAGTGACCCAGAACCCCAGATACCTGATCACCGTG
ACCGGCAAGAAACTGACCGTGACCTGCAGCCAGAACATGAACCACGAGTACATGAGCT
GGTACAGACAGGACCCCGGCCTGGGCCTGCGGCAGATCTACTACAGCATGAACGTGG
AAGTGACCGACAAGGGCGACGTGCCCGAGGGCTACAAGGTGTCCCGGAAAGAGAAGC
GGAACTTCCCACTGATCCTGGAAAGCCCCAGCCCCAACCAGACCAGCCTGTACTTCTG
TGCCAGCAGCCTGAGCATGAGCACCTACAACGAGCAGTTCTTCGGCCCTGGCACCCGG
CTGACAGTGCTGGAAGATCTGAGGAACGTGACCCCCCCCCAAGGTGTCCCTGTTCGAGC
CCAGCAAGGCCGAGATCGCCAACAAGCAGAAAGCCACCCTCGTGTGCCTGGCCAGAG
GCTTCTTCCCCGACCACGTGGAACTGTCCTGGTGGGTCAACGGCAAAGAGGTGCACAG
CGGAGTCTGCACCGACCCCCAGGCTTACAAAGAGAGCAACTACAGCTACTGCCTGTCC
AGCAGACTGCGGGTGTCCGCTACCTTCTGGCACAACCCCCGGAACCACTTCAGATGCC
AGGTGCAGTTCCACGGCCTGAGCGAAGAGGACAAGTGGCCCGAGGGCAGCCCCAAGC
CCGTGACCCAGAATATCAGCGCCGAGGCCTGGGGCAGAGCCGATTGTGGCATCACCA
GCGCCAGCTACCACCAGGGGGTGCTGAGCGCCACCATCCTGTACGAGATCCTGCTGG
GCAAGGCCACCCTGTACGCCGTGCTGGTGTCCGGACTGGTGCTGATGGCCATGGTCAA
GAAGAAGAACAGCGGCAGCGGCGCCACCAACTTCAGCCTGCTGAAGCAGGCCGGCGA
CGTGGAGGAGAACCCCGGCCCCATGACCAGCATCCGGGCCGTGTTCATCTTCCTGTGG
CTGCAGCTGGACCTCGTGAACGGCGAGAACGTGGAACAGCACCCCAGCACCCTGAGC
GTGCAGGAAGGCGATAGCGCCGTGATCAAGTGCACCTACAGCGACAGCGCCAGCAAC
TACTTCCCCTGGTACAAGCAGGAACTGGGCAAGCGGCCCCAGCTGATCATCGACATCA
GATCCAACGTGGGCGAGAAGAAGGACCAGCGGATCGCCGTGACCCTGAACAAGACCG
CCAAGCACTTCAGCCTGCACATCACCGAGACACAGCCCGAGGACAGCGCCGTGTACTT
CTGTGCCGCCATCGGCTTCGGCAACGTGCTGCACTGTGGCAGCGGCACACAAGTGATC
GTGCTGCCCCATATCCAGAACCCCGAGCCCGCCGTGTACCAGCTGAAGGACCCCAGAA
GCCAGGACAGCACCCTGTGTCTGTTCACCGACTTCGACAGCCAGATCAACGTGCCCAA
GACCATGGAAAGCGGCACCTTCATCACCGATAAGTGCGTGCTGGACATGAAGGCCATG

GACAGCAAGAGCAACGGCGCCATTGCCTGGTCCAACCAGACCAGCTTCACATGCCAGG
ACATCTTCAAAGAGACAAACGCCACCTACCCTTCCAGCGACGTGCCCTGTGACGCCAC
CCTGACCGAGAAGTCCTTCGAGACAGACATGAATCTGAATTTCCAGAACCTGAGCGTGA
TGGGCCTGCGGATCCTGCTGCTGAAAGTGGCCGGCTTCAACCTGCTGATGACCCTGCG
GCTGTGGTCCAGCTGA